NAVAL POSTGRADUATE SCHOOL

MONTEREY, CALIFORNIA

THESIS

MODELING THE IMPACTS OF INTRASEASONAL TO INTERANNUAL CLIMATE VARIATIONS ON TROPICAL CYCLONE FORMATIONS IN THE WESTERN NORTH PACIFIC

by

Stephanie A. Johnson

September 2011

Thesis Co-Advisors: Tom Murphree
David Meyer

Approved for public release; distribution is unlimited

THIS PAGE INTENTIONALLY LEFT BLANK

REPORT DOCUMENTATION PAGE			Form Approved OMB No. 0704–0188
Public reporting burden for this collection of information is estimated to average 1 hour per response, including the time for reviewing instruction, searching existing data sources, gathering and maintaining the data needed, and completing and reviewing the collection of information. Send comments regarding this burden estimate or any other aspect of this collection of information, including suggestions for reducing this burden, to Washington headquarters Services, Directorate for Information Operations and Reports, 1215 Jefferson Davis Highway, Suite 1204, Arlington, VA 22202–4302, and to the Office of Management and Budget, Paperwork Reduction Project (0704–0188) Washington DC 20503.			
1. AGENCY USE ONLY ***(Leave blank)***	**2. REPORT DATE** September 2011	**3. REPORT TYPE AND DATES COVERED** Master's Thesis	
4. TITLE AND SUBTITLE Modeling the Impacts of Intraseasonal to Interannual Climate Variations on Tropical Cyclone Formations in the Western North Pacific		**5. FUNDING NUMBERS**	
6. AUTHOR(S) Stephanie A. Johnson			
7. PERFORMING ORGANIZATION NAME(S) AND ADDRESS(ES) Naval Postgraduate School Monterey, CA 93943–5000		**8. PERFORMING ORGANIZATION REPORT NUMBER**	
9. SPONSORING /MONITORING AGENCY NAME(S) AND ADDRESS(ES) N/A		**10. SPONSORING/MONITORING AGENCY REPORT NUMBER**	
11. SUPPLEMENTARY NOTES The views expressed in this thesis are those of the author and do not reflect the official policy or position of the Department of Defense or the U.S. Government. IRB Protocol number NA.			
12a. DISTRIBUTION / AVAILABILITY STATEMENT Approved for public release; distribution is unlimited		**12b. DISTRIBUTION CODE**	

13. ABSTRACT

We have analyzed the modulation of TC formations in the western North Pacific (WNP) during July-October by El Niño (EN), La Niña (LN), and the Madden Julian Oscillation (MJO). This analysis was conducted from the perspective of several large scale environmental factors (LSEFs) that strongly influence tropical cyclone (TC) formation: sea surface temperature (SST), low level relative vorticity, vertical wind shear, and upper level divergence. We examined the variations in each LSEF associated with EN, LN, and MJO. We used composite LSEFs for EN, LN, and each of the eight MJO phases to force the Naval Postgraduate School (NPS) statistical model for calculating TC formation probabilities. We then compared the resulting probabilities to actual formations to determine how accurately the model represented ENLN and MJO related variations in TC formations. The model based probabilities provide a realistic quantitative representation of how ENLN and MJO make TC formation more and less likely in the WNP. Our results should be useful in improving the education, training, and environmental situational awareness of TC forecasters. Our results also indicate that the NPS model has the potential to improve operational forecasting of TC formations in the WNP, if forced by skillful forecasts of the LSEFs.

14. SUBJECT TERMS Tropical Cyclones, Western North Pacific, Long Range Forecasting, Large Scale Environmental Factors, El Niño, La Niña, Madden-Julian Oscillation			**15. NUMBER OF PAGES** 111
			16. PRICE CODE
17. SECURITY CLASSIFICATION OF REPORT Unclassified	**18. SECURITY CLASSIFICATION OF THIS PAGE** Unclassified	**19. SECURITY CLASSIFICATION OF ABSTRACT** Unclassified	**20. LIMITATION OF ABSTRACT** UU

NSN 7540–01–280–5500

Standard Form 298 (Rev. 8–98)
Prescribed by ANSI Std. Z39.18

THIS PAGE INTENTIONALLY LEFT BLANK

Approved for public release; distribution is unlimited

MODELING THE IMPACTS OF INTERSEASONAL TO INTERANNUAL CLIMATE VARIATIONS ON TROPICAL CYCLONE FORMATIONS IN THE WESTERN NORTH PACIFIC

Stephanie A. Johnson
Lieutenant, United States Navy
B.A., University of Washington, 2006

Submitted in partial fulfillment of the
requirements for the degree of

MASTER OF SCIENCE IN METEOROLOGY AND PHYSICAL OCEANOGRAPHY

from the

NAVAL POSTGRADUATE SCHOOL
September 2011

Author: Stephanie A. Johnson

Approved by: Tom Murphree
Thesis Co-Advisor

David W. Meyer
Thesis Co-Advisor

Wendell Nuss
Chair, Department of Meteorology

THIS PAGE INTENTIONALLY LEFT BLANK

ABSTRACT

We have analyzed the modulation of TC formations in the western North Pacific (WNP) during July–October by El Niño (EN), La Niña (LN) and the Madden Julian Oscillation (MJO). This analysis was conducted from the perspective of several large scale environmental factors (LSEFs) that strongly influence tropical cyclone (TC) formation: sea surface temperature (SST), low level relative vorticity, vertical wind shear, and upper level divergence. We examined the variations in each LSEF associated with EN, LN, and MJO. We used composite LSEFs for EN, LN, and each of the eight MJO phases to force the Naval Postgraduate School (NPS) statistical model for calculating TC formation probabilities. We then compared the resulting probabilities to actual formations to determine how accurately the model represented ENLN and MJO related variations in TC formations.

The model based probabilities provide a realistic quantitative representation of how ENLN and MJO make TC formations more and less likely in the WNP. In particular, the model accurately represents: (1) the southeastward (northwestward) shift in conditions favorable for TC formation during EN (LN); and (2) the enhancement (suppression) of formation favorable conditions to the west and east of the Philippines during phases 4–7 (1–3, 8) of the MJO. For ENLN, the LSEF variations that appear to have the most direct impacts on the TC formation probability variations are those in SST, low level relative vorticity, and the zonal component of vertical wind shear. For MJO, the LSEF variations that appear to have the most direct impacts on the TC formation probability variations are those in low level relative vorticity, the zonal component of vertical wind shear, and upper level divergence. Our results should be useful in improving the education, training, and environmental situational awareness of TC forecasters. Our results also indicate that the NPS model has the potential to improve operational forecasting of TC formations in the WNP, if forced by skillful

forecasts of the LSEFs. If so, the resulting forecasts would be useful in improving the planning of DoD and other operations in the WNP.

TABLE OF CONTENTS

LIST OF FIGURES

THIS PAGE INTENTIONALLY LEFT BLANK

LIST OF TABLES

THIS PAGE INTENTIONALLY LEFT BLANK

LIST OF ACRONYMS AND ABBREVIATIONS

ACE	Accumulated cyclone energy
AMIP-II	Atmospheric Model Intercomparison Project-II
BOM	Australian Bureau of Meteorology
CFS	Climate Forecast System
CFSR	Climate Forecast System Reanalysis
CPC	Climate Prediction Center
DoD	Department of Defense
ECMWF	European Centre for Medium-range Weather Forecasts
EKE	Eddy kinetic energy
EN	El Niño
ENLN	El Niño/La Niña
EOF	Empirical orthogonal function
GCM	Global circulation model
GPI	Genesis potential index
IDL	International dateline
IRI	International Research Institute for Climate and Society
JASO	July, August, September, and October
JTWC	Joint Typhoon Warning Center
LN	La Niña
LRF	Long range forecasting
LSEF	Large scale environmental factor
LTM	Long term mean
MEI	Multivariate ENSO Index
MJO	Madden-Julian Oscillation
NCAR	National Center for Atmospheric Research
NCEP	National Centers for Environmental Prediction
NOAA	National Oceanic and Atmospheric Administration
OI	Optimum interpolation
OLR	Outgoing longwave radiation
PC	Principal component

R1	NCEP/NCAR Reanalysis 1
R2	NCEP/DOE AMIP-II Reanalysis
RMM	Real-Time Multivariate MJO
ROC	Relative operating characteristic
SOI	Southern Oscillation Index
SST	Sea surface temperature
TC	Tropical cyclone
WNP	Western North Pacific

ACKNOWLEDGMENTS

Through this thesis process I had a great deal of help and while this is not an all inclusive list these are a few of the people I would like to highlight for making this process as smooth as possible: Bob Creasey for his help in acquiring the reanalysis data, Bruce Ford for his help in manipulating the reanalysis fields, and Prof. Pat Harr for his discussions on all things tropical. Lastly I need to thank my advisors Prof. Tom Murphree and David Meyer; Prof. Murphree for the countless hours spent working with me and reviewing my results and David for his Matlab expertise and help through the thesis process.

THIS PAGE INTENTIONALLY LEFT BLANK

I. INTRODUCTION

In 1984, Gray reported on the impacts of El Niño (EN) and other factors on tropical cyclone (TC) activity in the North Atlantic TC basin (Gray 1984a). This result contributed to the development by Gray and others of seasonal TC forecasts—that is, forecasts of TC activity valid an entire TC season (e.g., forecasts of the number of TCs during a season but without an indication of where and when during the season they will occur; Gray 1984b). Many centers now produce seasonal forecasts using statistical and/or dynamical methods. While these seasonal forecasts are informative, they do not provide the Department of Defense (DoD) with sufficient spatial or temporal resolution for operational planning. For this planning, TC forecasts with resolutions of several degrees and several days to weeks, and lead times of weeks to seasons or longer, are needed.

Intraseasonal forecasting (lead times of about 10–70 days) is relatively new and experimental, but shows promise, especially as modeling and ensembling techniques and opportunities improve (van den Dool 2007; NRC 2010). One of the key requirements for producing skillful TC forecasts at intraseasonal lead times is the ability to simulate climate variations and their impacts on TC formations.

TC formations are affected by several large scale environmental factors (LSEFs) (Gray 1975). TC formations, as well as tracks and intensities, are also impacted by climate variations such as El Niño/La Niña (ENLN) and the Madden-Julian Oscillation (MJO); (e.g., Wang and Chan 2002; Frank and Roundy 2006). However, relatively little of this research quantifies how ENLN, and especially the MJO, impact the LSEFs that influence TC formations, and how those impacts then affect TC formations. Research on this topic could be useful in improving TC formation forecasting, especially at medium and long lead times.

We focused our work in the western North Pacific (WNP) basin for three primary reasons: (1) the WNP is an important region for DoD operations; (2) the WNP is the most active TC basin in the world (e.g., highest total TC formations per year, on average; McBride 1995): and (3) the WNP is strongly affected by ENLN and the MJO.

A. LONG RANGE FORECASTING

We define long range forecasting (LRF) as forecasting with lead times of two weeks or longer. To achieve LRF skill, it is essential to understand and model the impacts of intraseasonal, interannual, and longer period climate variations. In this study, we have investigated methods for modeling the impacts of intraseasonal and interannual climate variations (MJO, ENLN) on TC formations in the WNP.

B. PRIOR RESEARCH

1. Genesis Parameters of TC Formations

Over the last 40 years, there has been extensive documentation of the influence of several LSEFs on TC formations, often described as genesis parameters (e.g., Gray 1975; McBride 1995). The genesis parameters include both dynamic and thermodynamic parameters. The dynamical parameters favorable for TC formation are: high values of low level relative vorticity, weak vertical shear, non-zero Coriolis effects, and upward vertical motion. The thermodynamic parameters favorable for TC formation are: sea surface temperatures (SST) exceeding 26°C and high mid-level humidity (McBride 1995).

These favorable LSEFs have been identified as necessary, but not necessarily sufficient, for TC formation. Frank (2006) contends “individual storms form infrequently and sporadically within large areas of favorable environmental conditions due to the effects of local flow perturbations.” This indicates that a

first step in forecasting TC formation is to accurately forecast the large scale environment conditions that affect TC formation, and then the smaller scale conditions that affect TC formation.

2. ENLN Impact on TC Formations

ENLN is one of the most studied climate variations because of its far-reaching impacts on the global climate system. ENLN impacts on TC formations have been well documented and most research agrees that EN and La Niña (LN) directly affect TCs formation points, tracks, and intensities in all TC basins (e.g., Ford 2000; Wang and Chan 2002). Hereafter, when we refer to ENLN we are referring to an interannual variation with two extreme components, EN and LN. We will use EN and LN separately when we are referring to one component of the variation.

Several mechanisms by which ENLN impact TC formations, tracks, and intensities have been explored. One mechanism that has been explored is the variation of the cross equatorial westerlies in the WNP. These westerlies are enhanced during EN years, which increases low level vorticity associated with the monsoon trough and creates more favorable conditions for TC genesis near the international dateline (IDL) in the WNP (Wang and Chan 2002). This causes the mean genesis region for TC formations to shift to the southeast of the climatological mean formation point (Wang and Chan 2002). Chan (1985) contended that changes in the Walker circulation drive the shifts in mean genesis regions during EN and LN. The North and South Pacific Highs weaken (strengthen) during EN (LN), which in turns weakens (strengthens) the equatorial easterlies, thus shifting the mean genesis region to the southeast (northwest). Regardless of the explanations for the shift in genesis regions, the results are very similar: there is a southeastward (northwestward) shift in the mean genesis region during an EN (LN).

Researchers have also explored the mechanisms behind TC intensity differences between EN and LN. ENLN variations are associated with similar numbers of TCs in the WNP, but EN (LN) is associated with higher (lower) intensity TCs (e.g., Ford 2000). This is in part due to the southeastward shift of the genesis region during EN years allowing TCs more warm ocean from which to pull energy and gain intensity as they track westward and northwestward. During a LN year, a TC reaches the cooler mid-latitudes more quickly because their mean genesis region is in the southwest portion of the WNP. This reduces the intensity and the period of TCs (Ford 2000; Wang and Chan 2002).

3. MJO Overview

The MJO is a significant intraseasonal climate variation that occurs in the tropics and has widespread impacts beyond the tropics (Madden and Julian 1994; Murphree 2010). The MJO is characterized by an eastward propagating tropical wave and convective component that originates in the Indian-west Pacific region. A typical period is 30 to 60 days. Prior research has demonstrated that the MJO has a strong influence on TC activities. The convective (subsidence) component is associated with anomalously high (low) mid-level relative humidity and high (low) low level relative vorticity (Nakazawa 1988; Liebmann et al. 1994; Madden and Julian 1994; Kim et al. 2008; Camargo et al. 2009). Because of its 30–60 day period, the MJO has the potential to be predictable in medium- and long range forecasts. However, that potential has not yet been realized, due mainly to the complexities of MJO dynamics. Skill in forecasts of MJO activity is relatively low, especially at leads greater than a week (e.g., Saha et al. 2006).

4. Wheeler and Hendon Classification of the MJO

Wheeler and Hendon (2004) developed an index to classify the MJO that is commonly used index in MJO research and forecasting. This index is based on eight MJO phases. Figure 1 shows 850 hPa wind vectors and outgoing long-wave radiation (OLR) anomalies for these eight phases. The yellow shading

indicates the subsidence component and the blue shading indicates the convective component. Note the eastward propagation of these components from phases one to eight. The MJO is in phase 1 when the convective component is located over the eastern Indian Ocean and is in phase 8 when the convective component is located east of the IDL.

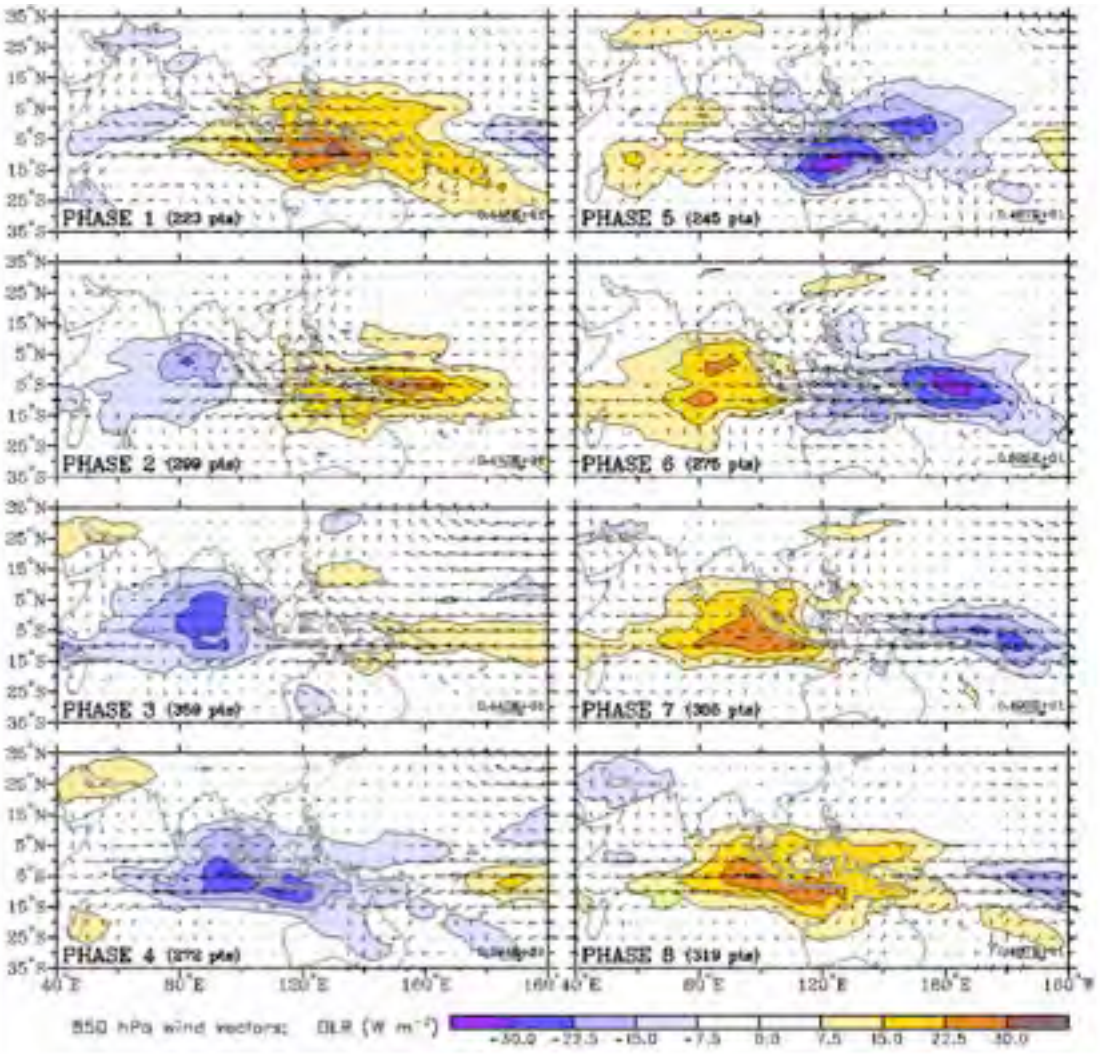

Figure 1. OLR (W m^{-2}) and 850 hPa vector winds anomalies for MJO phases 1–8 as described by Wheeler and Hendon. From http://www.bom.gov.au/bmrc/clfor/cfstaff/matw/maproom/RMM/index.htm.

The Wheeler Hendon index is based on the two leading empirical orthogonal functions (EOFs) of the normalized 200 and 850 hPa zonal winds and OLR (Wheeler and Hendon 2004). The two leading EOFs describe over 25 percent of the variance. The two leading principal components of the EOF are called real-time multivariate series 1 (RMM1) and 2 (RMM2). RMM1 and RMM2 are used to describe the phase, location, and intensity of the MJO throughout its propagation through the tropics.

5. MJO Structure

The structure of the MJO resembles the tropical atmospheric Rossby-Kelvin wave response to positive heating disturbance on the equator (Madden and Julian 1994; Murphree 2010). Figure 2 is a schematic depiction of the main MJO atmospheric anomalies. The rising (descending) motion to the west (east) is associated with upper-level anticyclones (cyclones) located poleward and westward of the convection (subsidence). The convergence of low level westerlies and easterlies just east of the convective component is associated with the eastward propagation of the MJO.

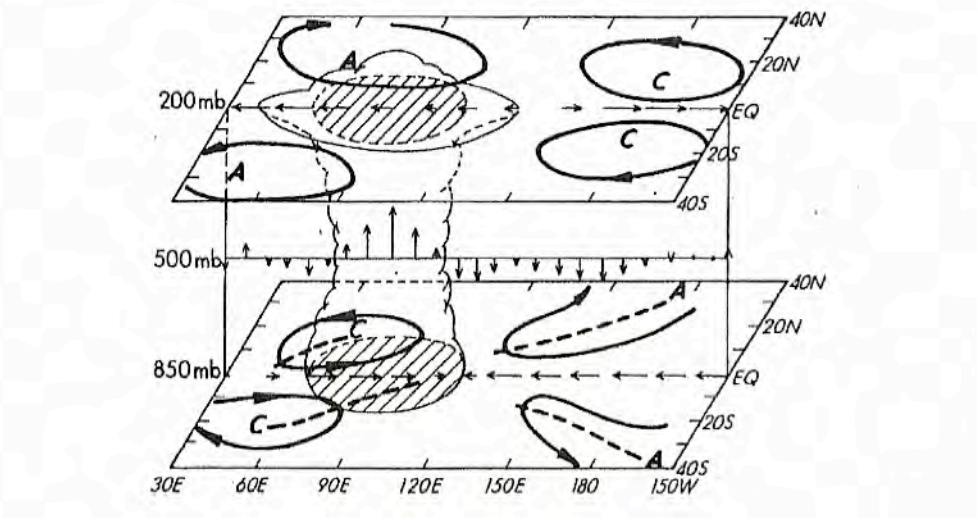

Figure 2. Schematic depiction of the three dimensional structure of the atmospheric anomalies that characterize MJOs. The cloudy (clear) region indicates the convective (subsidence) component anomalies. Arrows represent anomalous winds at 850 and 200 hPa and the vertical motions at 500 hPa. Anomalous anticyclones (cyclones) are labeled with "A" ("C"). Dashed lines mark anomalous troughs and ridges. From Rui and Wang 1990.

6. MJO Impact on TC Formations

Prior studies have shown that MJO affects TC formations, with increases (decreases) in formation associated with the convective (subsidence) phases of MJO (Chapter I.C.3). Figure 3 shows the characteristic evolution over a 31-day period of 200 hPa velocity potential anomalies associated with the MJO (color shading) and the associated TC formations. Note that there is a tendency for more (less) formations in regions where the upper level divergence anomalies are positive (negative).

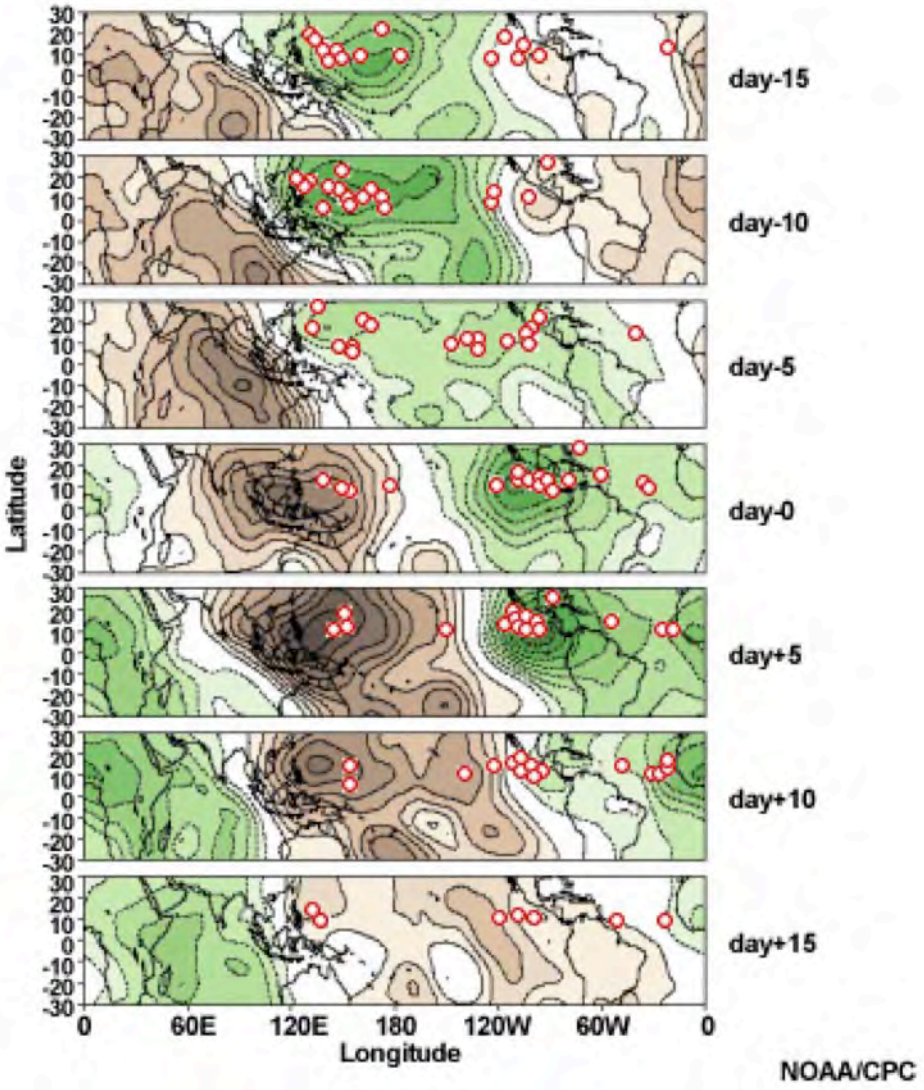

Figure 3. Composite evolution of the 200 hpa divergence anomalies (color shading, 10^5 x m^2s^{-1}) and TC formations (red circles) associated with the MJO over a 31-day period during July—September (JAS). Day 0 is roughly when the subsidence phase is over the western North Pacific. The green (brown) shading corresponds to positive (negative) divergence anomalies and regions where convection is favored (suppressed). Note the clustering of TCs over regions favorable for convection. Based on compositing velocity potential anomalies from 21 MJO events, and TC formations, during JAS 1979—1997. Contour interval is 0.5 x 10^6 m^2s^{-1} negative contours are dashed, and the zero contour is omitted for clarity. From http://www.meted.ucar.edu/climate/mjo/print.htm.

One of the first studies to investigate the mechanisms of the modulation of TCs by the MJO found that low level barotropic dynamics play a role in the process (Maloney and Hartmann 2001). The anomalous westerly 850 hPa zonal wind flow that characterizes the convective phase can increase eddy kinetic energy (EKE) due to barotropic conversion of energy from the mean low level flow. This enhances low level cyclonic circulation, surface convergence, and low level relative vorticity, which are all favorable conditions for tropical cyclogenesis. The opposite is true for the easterly 850 hPa zonal wind anomalous phase when EKE weakens (Maloney and Hartmann 2001).

Camargo et al. (2009) used a genesis potential index (GPI) to quantitatively assess the impact of the MJO on environmental factors that influence TC formations. The GPI is calculated using data on four environmental factors that are related to TC genesis. The four environmental factors—low level absolute vorticity, vertical wind shear, mid-level relative humidity, and potential intensity—are combined to produce a single index value for a given time and location. They concluded that the temporal and spatial variations of the GPI associated with MJO are approximately consistent with the variations in TC formations that are associated with MJO. They also concluded that relative humidity variations associated with MJO has a greater influence on TC genesis frequency than the three other factors used to calculate the GPI. This differs from other studies that found low level relative vorticity to be the most significant factor in determining the impacts of MJO on TC formations (e.g., Kim et al. 2008).

7. LSEF Thresholds

Several LSEF conditions are necessary for TC genesis (Chapter I.C.1). Murphree and Meyer (2011) determined thresholds for the LSEFs for the WNP. Table 1 summarizes the Murphree and Meyer LSEF threshold results, with the thresholds representing the LSEF conditions under which 95% of the WNP TCs during 1982–2006 formed. Table 1 shows that, for example, 95 percent of all

WNP TCs during 1982—2006 formed with SST of 28.1°C or greater, and with vertical wind shear magnitude of less than 20.6 ms^{-1} (see also Chapter II.D.1 discussion of wind shear units). Murphree and Meyer (2011) also found that low level relative vorticity and upper level divergence have both upper and lower bound thresholds.

LSEF	Threshold
Sea Surface Temperature	> 28.1° C
850 hPa Relative Vorticity	-3.9 $s^{-1}*10^{-6}$ < and < .62 $s^{-1}*10^{-6}$
Vertical Wind Shear (magnitude)	< 20.6 ms^{-1}
200 hPa Divergence	-4.5 $s^{-1}*10^{-6}$ < and < .22 $s^{-1}*10^{-6}$

Table 1. LSEF conditions in which 95 percent of all WNP TC formed during 1982—2006 TC formation is considered to be very unlikely even if one LSEF is outside of its threshold value or range. From Murphree and Meyer 2011. See also Chapter II.D.1 discussion of wind shear units.

8. NPS Statistical-Dynamical Model Overview

Mundhenk (2009) and Murphree and Meyer (2011) assessed the feasibility of predicting favorable regions for tropical cyclogenesis in the WNP using a statistical-dynamical forecast system. The system produces forecasts of TC formation probabilities. For our study, the statistical model component of this system is especially relevant. From here on, we refer to this statistical model for calculating TC formation probabilities as the NPS statistical model.

The NPS statistical model is a multivariate logistic regression model that uses information about the LSEFs to calculate the probability of TC formation. These calculations are made at the spatial and temporal resolution of the LSEF data used in the calculation. The LSEFs that are used in the model are SST, vertical shear of the horizontal winds between 200 hPa and 850 hPa, and divergence at 200 hPa. This set of LSEFs was selected based on extensive theoretical and statistical analyses (Mundhenk 2009). Relative and specific

humidity were not included in this set because of its close association with SST and low level relative vorticity (Mundhenk 2009).

The data used to develop the NPS statistical model came from the National Centers for Environmental Protection (NCEP) / Department of Energy (DOE) Atmospheric Model Intercomparison Project-11 (AIMP-II) Reanalysis (hereafter referred to as R2) (Kanamitsu et al. 2002) and the NCEP Optimum Interpolation (OI) SST data set (Reynolds et al. 2002) for June—November 1982—2006 (during the months of peak TC activity in the WNP). Additional information about the model development can be found in Mundhenk (2009) and Murphree and Meyer (2011).

The NPS statistical model was evaluated using zero lead cross validated hindcasts for 1982—2007 and was found to have skill, as indicated by several metrics (e.g., Brier skill score, relative operating characteristic, hit rate). For example, the hindcast hit rate was 0.89, with 671 of 759 (89 percent) of the WNP TCs during the hindcast period forming within a forecasted region (Mundhenk 2009).

The NPS statistical model was used within the overall statistical-dynamical forecast system to produce experimental forecasts for 2009—2011 (Murphree and Meyer 2011). Figure 4 shows examples of these forecasts at 90-, 60-, and 30-day leads. Verification of the 2009—2011 forecasts indicates the overall system, and the NPS statistical model, have skill (Murphree and Meyer 2011).

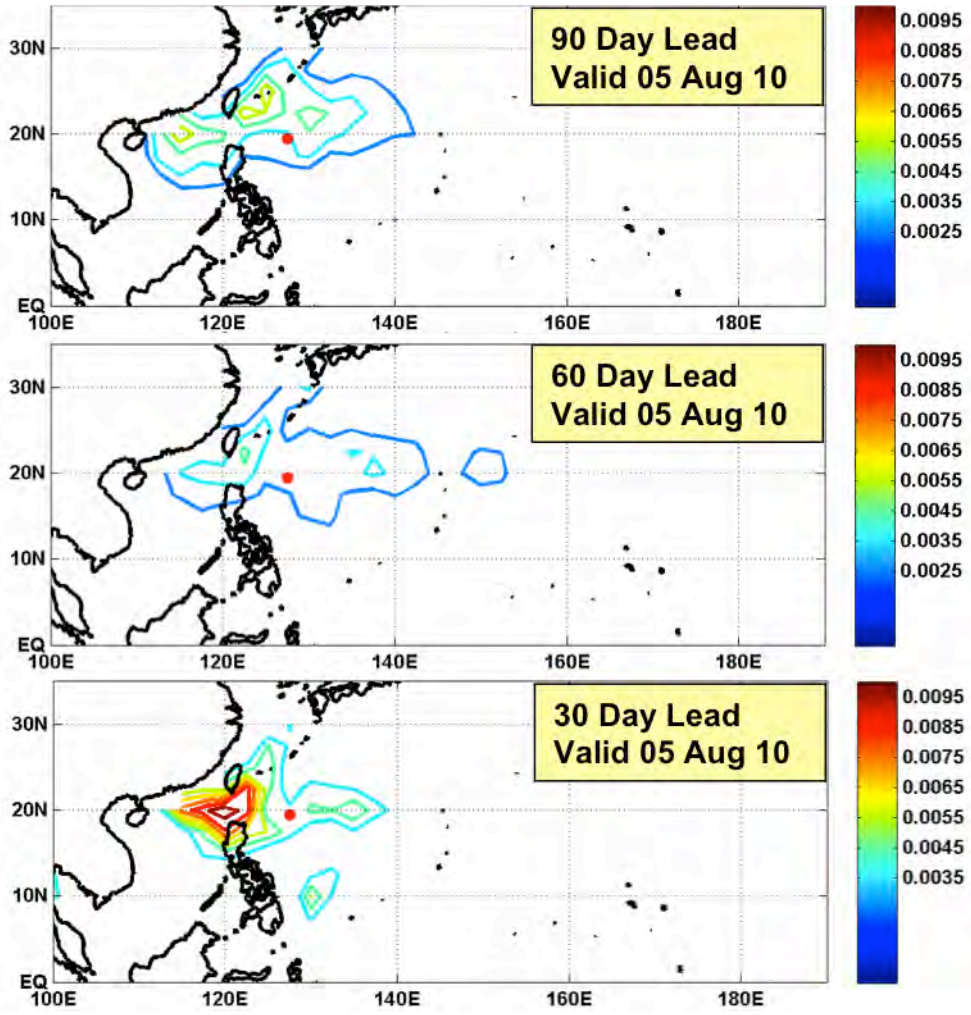

Figure 4. Examples of TC formation forecasts generated by the NPS statistical-dynamical forecast system. Contours represent ensemble mean forecasted probabilities with the contoured regions indicating areas in which TC formation is high compared to the long term mean probability. The formation of 05W (Dianmu) on the forecast valid date of 05 August 2010 is indicated by the red dot. Note the correspondence between the forecasts and the 05W formation, and the relatively high degree of consistency in the three forecasts from 90 day lead to 30 day lead. From Murphree and Meyer 2011.

C. LONG RANGE TC FORECAST PRODUCTS

1. Seasonal

Each year, several universities and operational weather centers around the world issue seasonal TC forecasts for the various TC basins. The forecasts generally characterize the upcoming season by providing information such as the likely number of formations for the season and whether he number of formations will be above-, below-, or near-normal. These forecasts are generated using statistical and/or dynamical methods, and have relatively low spatial and temporal resolution. For example: (1) the forecast valid periods tend to extend over all, or all of the main part, of the TC season, with relatively little information about when in a given season the TCs will form; and (2) relatively little information is provided about where in a given basin the TCs will form.

a. Statistical

Gray (1984a,b) describes the origins of the TC seasonal forecasts issued by Colorado State University for TC numbers in the North Atlantic basin. Colorado State University now issues their first forecast for the upcoming season in December, followed by updates in April, June, and August (Camargo et al. 2007a).

The Climate Prediction Center (CPC) of the National Oceanic and Atmospheric Administration (NOAA) collaborates with the National Hurricane Center (NHC) and the Hurricane Research Division to issue a North Atlantic hurricane seasonal outlook for the North Atlantic basin. The outlooks are based primarily on predicting climate variations that are known to impact TC activity in the region (e.g., ENLN). The outlooks indicate the likely seasonal range of named storms, hurricanes, and major hurricanes. They also forecast the probabilities for season type, above-, near-, or below-normal and the accumulated cyclone energy (ACE) (Camargo et al. 2007a). The City University of Hong Kong China issues a forecast of the annual number of storms and

typhoons in the WNP based on a statistical method using several predictors, including the Niño 3.4 index and Equatorial Southern Oscillation Index (Equatorial SOI) (Chan et al. 2001).

b. Dynamical

The European Centre for Medium-range Weather Forecasting (ECMWF) and the International Research Institute for Climate and Society (IRI) produce experimental dynamical model forecasts for several TC basins around the world. The ECMWF model uses a coupled global circulation model (GCM) to identify and track tropical cyclones, and to forecast the number of named storms, the mean genesis location, the number of hurricanes, and ACE in all of the TC basins. IRI statistical-dynamical models predict possible SST scenarios, which are then used to force an atmospheric model to generate TC-like vortices (Camargo et al. 2007).

2. Intraseasonal

Intraseasonal TC forecasting is a relatively new area of research and operational forecasting. Intraseasonal TC forecasts typically have lead times of several days to weeks, and valid periods of one week to two months. CPC issues a Global Tropical Hazards/Benefits Assessment that provides predictions of TCs that will reach tropical storm intensity at leads of approximately one to eight days and for valid periods of one week. Several weather centers and universities provide inputs to these predictions, including NPS, State University of New York Albany (SUNYA), and the Central Weather Bureau of Taiwan. Figure 5 is an example of the assessments issued 03 May 2011 and valid 04–10 May 2011 and 11–17 May 2011.

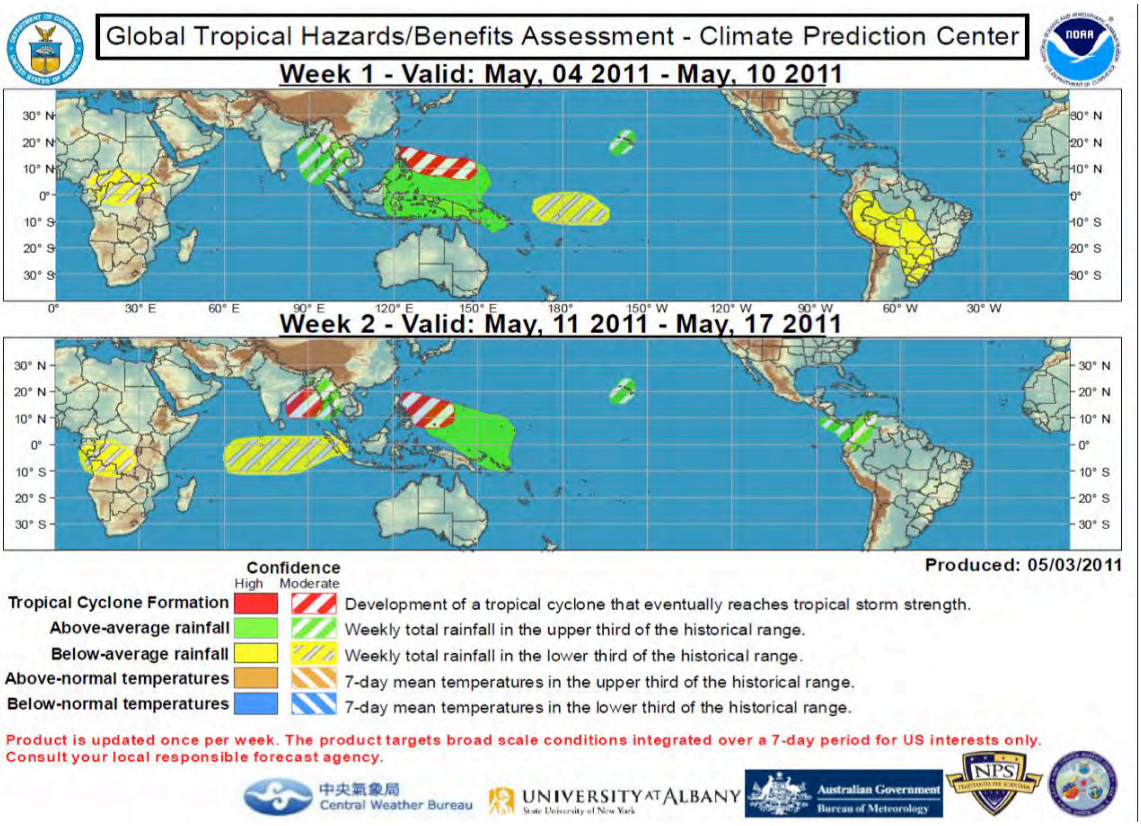

Figure 5. Example CPC Global Tropics Benefits/Hazards Assessment, issued 3 May 2011 and valid 04–10 May 2011 and 11–17 May 2011. The red and white striped regions on the figure indicate a moderate confidence in the formation of a TC that will reach tropical storm intensity in that region From http://www.cpc.ncep.noaa.gov/products/precip/CWlink/ghazards/index.php.

SUNYA has an experimental product that provides probabilities of TC occurrence associated with convectively coupled equatorial waves, ENSO, and the MJO. These 30-day outlooks are available at http://www.atmos.albany.edu/facstaff/roundy/tcforecast/tcforecast.html.

NPS issues experimental forecasts of TC formations in the WNP at leads of 4–90 days, for valid periods of one day to several weeks, and at a spatial resolution of 2.5 degrees, using the statistical-dynamical forecasting system described in the Chapter I.B.8 and Murphree and Meyer (2011). These forecasts are provided to CPC and the Joint Typhoon Warning Center (JTWC).

D. RESEARCH GOALS

1. Research Questions

The goal of this study was to develop a better understanding of how climate variations impact TC formations in a way that is useful in operational forecasting and to build a foundation for future research on the impacts of climate variations on TC tracks and intensities. To achieve our research goal, we addressed the following questions:

1) How do ENLN and the MJO affect the probabilities of TC formations in the WNP?

2) Can we quantify the impact of climate variations on TC formations in the WNP in a probabilistic sense?

3) What are the driving mechanisms behind the modulation of TC formation by ENLN and the MJO, and how do those mechanisms affect the spatial and temporal patterns of TC formation in the WNP?

2. Thesis Organization

Chapter II provides a review of our study region and period, followed by an overview of the data sets and methods. In Chapter III, we present our long term mean (LTM) results, followed by our ENLN and MJO results. In Chapter IV, we provide conclusions and recommendations for further research.

II. DATA AND METHODS

A. STUDY REGION AND PERIOD

Our study region was the WNP. We chose this region because it is of particular importance to the DoD, and because it is the most active TC basin in the world, with an average of 30 TCs occurring annually (D. W. Meyer 2011, personal communication). We define the WNP as the region bounded by 100°E–170°W and 0–30°N. This WNP region is similar to the WNP regions used in previous studies of the WNP and accounts for most TC formations in the WNP, since relatively few TCs cross these boundaries to enter the WNP.

Our study period was July to October (hereafter referred to as JASO) of 1975–2010 (a 36 year period). We focused our study on JASO because it is a peak formation period in the WNP although TC formations occur throughout the year (Figure 7). During our study period, there were 1061 TC formations in the WNP west of the IDL, with 721 (71 percent) of those formations occurring during JASO.

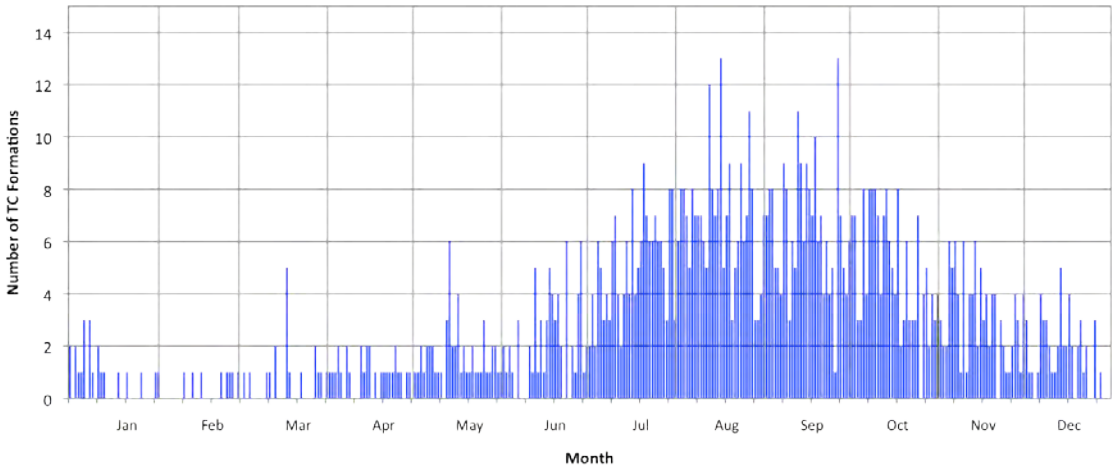

Figure 6. Number of TC formations (y-axis) for each day of the year (x-axis) for the WNP study region during 1975—2010. Constructed from JTWC best track data for the WNP west of the IDL.

We chose 1975 as the start of our study period because MJO phase and amplitude data from the Australian Bureau of Meteorology (BOM) is available starting in 1975. For some analyses, we used a shorter period, due to limited data availability, as discussed in the following sections.

B. DATA SETS AND SOURCES

1. JTWC Best Tracks

We used the best track data set as our source of TC data. We defined the TC formation time and location according to the information in the first data entry for each storm. The JTWC best track data set is not a long term retrospective analysis (reanalysis) data set. Thus, this data set may contain temporal variations in TC formations over the course of the study period that are due to variations in available observational data and in TC formation analysis procedures. Thus, the interannual variations in TC formations shown by this data set may be, to some extent, artifacts of the variations in available observational data and analysis procedures, rather than actual variations. However, we suspect that these artifacts would be relatively small (1–2 degrees and 1–2 days, or less, in the formation locations and times), based on prior assessments of real time analyses and best track analyses (D. W. Meyer 2011, personal communication). We focused our study on TC formations that occurred west of the IDL, because relatively few formations occur east of the IDL during our JASO.

2. NCEP/NCAR Reanalysis Projects Data Set

We used the NCEP and National Center for Atmospheric Research (NCAR) Reanalysis Projects data set (hereafter referred to as R1; Kalnay et al. 1996) as a primary source of LSEF data. The R1 data that we used was for SST, and 850 and 200 hPa zonal and meridional wind, which are A variables (i.e., variables that are strongly influenced by observed data and therefore

relatively reliable). The R2 data has a 2.5° horizontal resolution. We would have preferred to work with R2 data for these LSEFs, because R2 corrects several of the errors found in R1, applies improvements such as higher vertical and horizontal resolution, and was used to develop the NPS statistical model (Kanamitsu et al. 2002). However, for our use of the R1 data, the differences between R1 and R2 are probably small and unlikely to significantly affect our results (cf. Kanamitsu et al. 2002).

We also chose to work with R1 rather than R2, because R1 data was readily available for initial analysis and downloading on the web via the NOAA/OAR/ESRL PSD daily and monthly composite sites at http://www.esrl.noaa.gov/psd/. These sites allowed us to upload our own data files with specific MJO activity dates for composting (hereafter referred to as date files), so that we could readily composite a large number of nonconsecutive individual days.

3. SST Data

We used OISST (Reynolds et al. 2002) and R1 surface skin temperature to represent the SST LSEF. OISST uses in situ and satellite SSTs as well as SSTs simulated by sea ice cover. We used OISST version 2, available at weekly resolution and 1° horizontal resolution, which we interpolated to the 2.5° horizontal resolution of the R1 data for use in the NPS statistical model. We used OISST for our long term mean (LTM) and ENLN analyses. We used the R1 surface skin temperature at daily resolution for representing the SST LSEF when calculating the MJO phase composites and MJO TC formation probabilities via the NPS statistical model. This daily resolution was needed to match the daily resolution at which MJO phase and amplitude information is determined. The OISST data has a weekly resolution and so was less than ideal for use in our MJO analyses. To obtain a large number of MJO cases for our analyses, we chose to use MJO information for 1975—2010, a period for which surface skin temperature data was available, but for which OISST data was only available

from 1982 onward. Our comparisons of corresponding OISST and surface skin temperature composites (not shown) yielded relatively small differences that led to only minor differences in the associated TC formation probabilities, primarily near coastlines. The surface skin temperature was available from the ESRL site on an irregular Gaussian grid, so we interpolated the data to the 2.5° resolution grid of the other R1 data.

4. Climate Index Information

a. MEI Index

The MEI is a bimonthly index of ENLN activity based on six variables: sea-level pressure, zonal and meridional components of the surface wind, sea surface temperature, surface air temperature, and total cloudiness fraction of the sky (Wolter and Timlin 2011). The MEI is computed for each bi-monthly season (e.g., Dec/Jan, Jan/Feb). Positive (negative) MEI values exceeding 0.5 (-0.5) typically indicate EN (LN) events.

b. Wheeler and Hendon MJO Index

We used the Wheeler and Hendon (2004) RMM1/RMM2 index discussed in Chapter I.B.4 to identify and characterize MJO events. The index information is available on the web at the BOM, in text format, http://www.bom.gov.au/climate/mjo/graphics/rmm.74toRealtime.txt. Each day dating back to 01 June 1974, has both RMMI and RMM2 values, plus phase and amplitude information.

C. COMPOSITES

1. LTM

We first calculated the LTM LSEFs. This was an important step, because to analyze the impacts of ENLN and the MJO on TC formation, we needed to

understand what the typical conditions are in the WNP study region. The LTM base period we used was JASO of 1981–2010, a 30 year period.

2. ENLN Composites

To determine which years to composite for EN and LN conditions, we calculated and ranked the average MEI for Jul/Aug, Aug/Sep, and Sep/Oct from 1982–2010, the period for which OISST data was available. We then selected the eight years with the most positive MEI for the EN composites and the eight years with the most negative MEI for the LN composites. Our EN years were: 1982, 1986, 1987, 1991, 1993, 1994, 1997, and 2009. Our LN years were: 1988, 1995, 1996, 1998, 1999, 2007, 2008, and 2010.

3. MJO Composites

We used the Wheeler and Hendon (2004) MJO index to identify the dates with MJO activity, and the associated MJO phase and amplitude. We focused our analyses on dates with MJO amplitudes greater than 1.25 (see the Appendix), for reasons discussed in Chapter III. We developed composites for each MJO phase based on these dates. To obtain the 850 and 200 hPa zonal and meridional winds and surface skin temperature LSEF data for these composites, we uploaded date files for each MJO phase to the NOAA/OAR/ESRL daily mean composite site, http://www.esrl.noaa.gov/psd/data/composites/day/. At that site, we plotted daily composite means of each LSEF, and then downloaded the resulting composite LSEF data as netCDF files. As an example, the phase 1 composite files represent all phase 1 dates during JASO 1975–2010 for which the MJO amplitude was greater than 1.25, including TC formations dates. The number of dates in each phase varied with the phase, because the application of the MJO index yielded a different number of dates for each phase, as well as a different number of dates for each phase that met our amplitude criterion. Table 2 lists

the total number of days of data in each MJO phase for which the MJO amplitude was greater than 1.25 during JASO 1975—2010.

MJO Phase	Number of Days in Each Phase for Amplitudes > 1.25
1	299
2	274
3	123
4	169
5	322
6	239
7	132
8	175

Table 2. Number of days during each MJO phase when amplitude was greater than 1.25 for JASO 1975–2010. Constructed from BOM MJO phase and amplitude data. See the Appendix for a listing of all of these days.

We chose to focus on dates with MJO amplitudes greater than 1.25 to highlight the impacts of MJOs on TC formations in the WNP. Table 3 shows the number of formations in the WNP by MJO phase for all MJO amplitudes and for amplitudes greater than 1.25 for JASO 1975–2010. For all amplitudes, there is a relatively small difference between the number of formations when the subsidence component is over the WNP—phases 1–2—and when the convection is centered over the WNP—phases 5–6. However, when the amplitude is greater than 1.25, the difference Is much greater, with nearly double the amount of formations in phases 5–6 compared to phases 1–2. This suggests that during weak phase 1 and 2 periods, the subsidence component is too weak to substantially reduce the number of TC formations, and during weak phase 5 and 6 periods, the convective component is too weak to substantially increase the number of TC formations. Thus, weak (strong) MJOs have relatively small (large) impacts of TC formations in the WNP.

MJO Phase	Total Number of TC Formations in Each Phase for All Amplitudes	Total Number of TC Formations in Each Phase for Amplitudes > 1.25
1	98	27
2	84	30
3	66	13
4	96	30
5	115	66
6	105	56
7	73	23
8	61	28

Table 3. Comparison of the number of WNP TC formations for each MJO phase for all amplitudes and for amplitudes > 1.25 for JASO 1975–2010. Based on JTWC WNP best track data and BOM MJO phase and amplitude data.

Note that all the LSEF and probability composites (LTM, ENLN, and MJO composites) represent time averaged conditions (e.g., daily average conditions). Thus, the MJO phase composites are effectively adjusted for the differences in the number of days for each phase (Table 2). However, this is not the case for the TC formations during the different MJO phases, since there is no correction of the TC formations for the differing number of days in each phase.

D. CALCULATION OF LSEF VARIABLES

1. LSEF Calculations

The R1 data available at the ESRL daily and monthly composite sites does not include 850 hPa relative vorticity, 200–850 hPa vertical shear of the horizontal wind, or 200 hPa divergence. Therefore, we had to calculate these LSEFs from the R1 zonal and meridional winds at 850 and 200 hPa that were

available from the ESRL site. To calculate the relative vorticity and divergence LSEFs, we used second order centered finite differencing (cf. Mundhenk 2009). The unit of wind shear are $ms^{-1}m^{-1} = s^{-1}$. However, for our study, we chose to analyze vertical wind shear in terms of the unit of ms^{-1}, which is a common convention in TC related discussions of vertical wind shear (e.g., Knaff et al. 2004).

2. Anomaly Calculations

A common way to represent a climate variation is in terms of the difference between the value of a variable for a specific location and time and the LTM value of that variable. For example, the 200 hPa divergence anomaly for MJO phase 1 would be calculated as:

$$200\ hPa\ Div\ Anomaly_{JASO\_Phase1} = 200\ hPa\ Div_{JASO\_Phase1} - LTM\ 200\ hPa\ Div_{JASO}$$

We analyzed LSEF anomalies for EN, LN, and the MJO phases, and for TC formation probabilities to highlight how conditions during EN, LN, and MJO differ from LTM conditions.

E. NPS STATISTICAL MODEL APPLICATION

Mundhenk (2009) and Murphree and Meyer (2011) demonstrated that the NPS statistical model has skill in depicting the probability of TC formation in the WNP. Thus, we chose to use the NPS statistical model to calculate daily average TC formation probabilities for LTM, EN, LN, and MJO phase 1–8 conditions. We did so by forcing the model with daily average LTM LSEFs, and with composite LSEFs for EN, LN, and each of the eight MJO phases. We chose to analyze these model based probabilities rather than probabilities calculated from actual formations, because a 36 year time span and the rareness of TC formations does not provide enough TC formations to allow a physically realistic calculation of formation probabilities based only on actual formations. Maps of TC formation probability based on actual formations are unrealistically patchy (cf. Camargo et al. 2009; Mundhenk 2009).

F. VERIFICATION

To verify our results, we compared the resulting probabilities to actual formations to determine how accurately the model represented LTM formations, and ENLN and MJO related variations in TC formations. To accomplish this, we overlaid on maps of the modeled formation probabilities the corresponding TC formations.

For the LTM and ENLN composites, we plotted all the formations that occurred during the years used in the composites, with the number of days being equal for the EN and LN composites. However, for MJO composites, there were a different number of total days in each phase (Table 2). Thus, when verifying the MJO TC formation probabilities by overlaying the corresponding TC formations, we needed to account for the different numbers of days in each phase, so that: (a) the verification would not be skewed; and (b) so that we could make a direct and fair comparison between the phases. To do this accounting, we randomly selected an equal number of days for each phase from all the days representing that phase. The TC formations for that randomly selected set of days were the TC formations that we overlaid on the probabilities for that phase. The equal number we used was 123, because that was the number of days in the phase composite that had the fewest number of days (phase 3; see Table 2). The random selection was made using the Matlab randperm function to generate random permutations of the days in each phase.

THIS PAGE INTENTIONALLY LEFT BLANK

III. RESULTS

A major goal of this study was to analyze the modulation of TC formations in the WNP by ENLN and the MJO from the perspective of the LSEFs that influence TC formations. In order to conduct this analysis, we first analyzed the LTM TC formation in the WNP. We then calculated the LTM LSEFs and compared them to the corresponding model based TC formation probabilities. We then compared these probabilities to the LTM TC formations. Through this set of analyzes, we developed an assessment of how the LTM LSEFs are related to the LTM formations, and how well the NPS statistical model based on the LTM LSEFs represents the LTM formations. We used this assessment as a baseline for analyzing the impacts on TC formations of EN, LN, and the eight phases of MJO. The ENLN and MJO analyses followed the same process that we used for the LTM analyses.

A. LTM

1. TC Formations

Figure 8 shows the TC formations that occurred during JASO 1975—2010 in the WNP west of the IDL (see Chapter II, sections A-B). Note the general northwest-southeast trend in the distribution of the formations, consistent with the LTM position of the monsoon trough (McBride 1995).

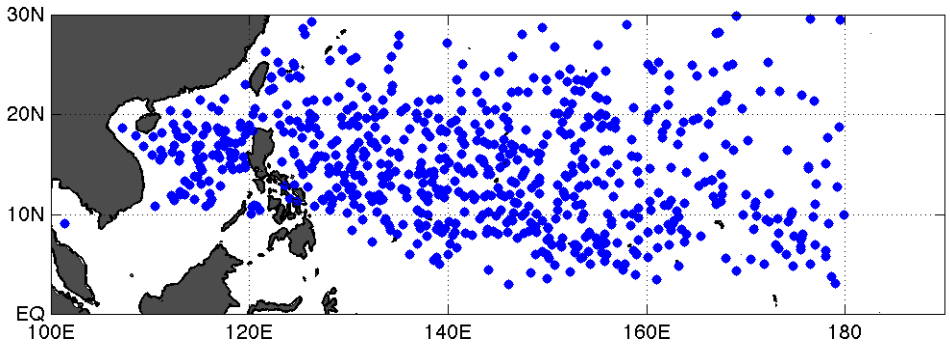

Figure 7. TC formation locations (blue dots) during JASO 1975—2010 in the WNP west of the IDL. The total number of formations depicted is 721. Based on JTWC WNP best track data.

2. LSEFs

Figure 8 shows the corresponding LTM LSEFs.

The SST shows a large region of the WNP in which the SSTs exceed 28^{o}C and are thus favorable for TC formation.

Low level relative vorticity is positive in an approximately zonal band that extends across much of the central WNP that corresponds to the monsoon trough where cross equatorial westerlies converge with easterlies in the region resulting in a low level counterclockwise circulation (McBride 1995).

Easterly zonal vertical wind shear dominates much of the southwestern portion of the region, while westerly vertical wind shear dominates the northeast region. The intervening low wind shear region has a northwest-southeast orientation across the WNP that is approximately coincident with the region of positive low level relative vorticity. The meridional vertical wind shear is weak over most of the WNP, and especially near the area of weak zonal wind shear.

Strong positive values of upper level divergence dominate the southern portion of the WNP. The monsoon trough region has positive values, especially in the South China Sea.

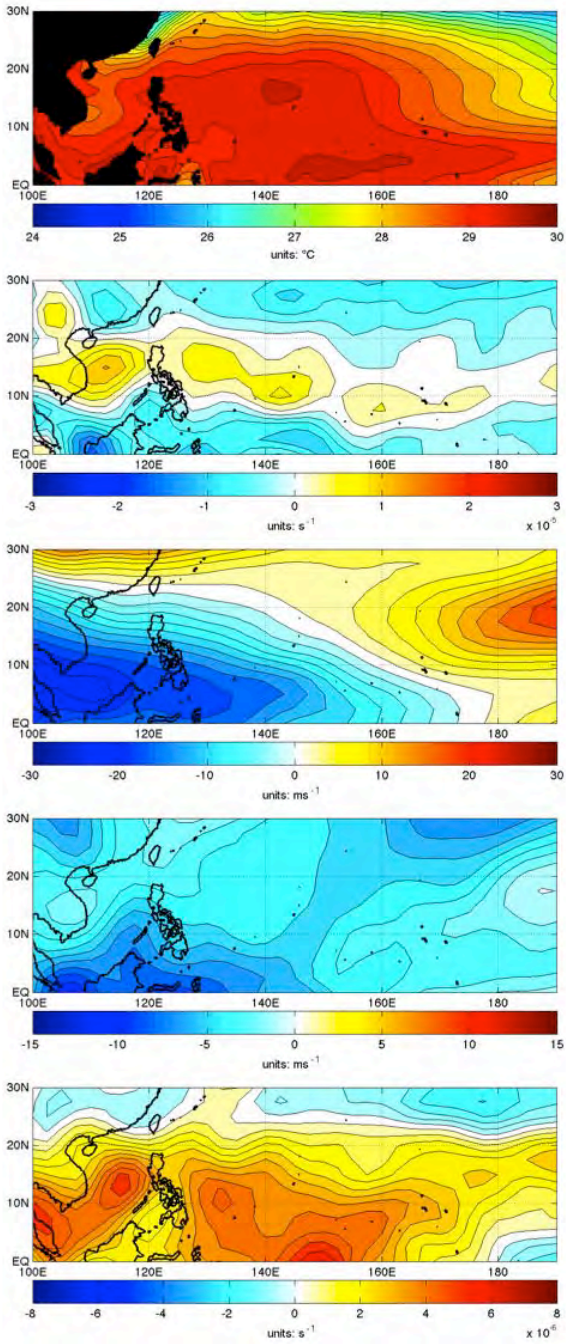

Figure 8. LTM composite LSEFs for JASO 1981—2010, in the WNP study region (contours and shading): SST (in °C, top panel); 850 hPa relative vorticity (in s^{-1}, second panel from top); zonal vertical wind shear (in ms^{-1}, third panel from top); meridional vertical wind shear (in ms^{-1}, fourth panel from top); 200 hPa divergence (in s^{-1}, bottom panel).

3. TC Formation Probabilities

Figure 9 shows the LTM TC formation probabilities based on forcing the NPS statistical model with the LTM LSEFs (Figure 8). Note that the highest probabilities are generally co-located with the areas in which the LSEFs are most favorable—for example, the areas of most positive low level relative vorticity and low vertical wind shear in the South China Sea and extending southeastward from the Luzon Strait (compare Figures 8 and 9).

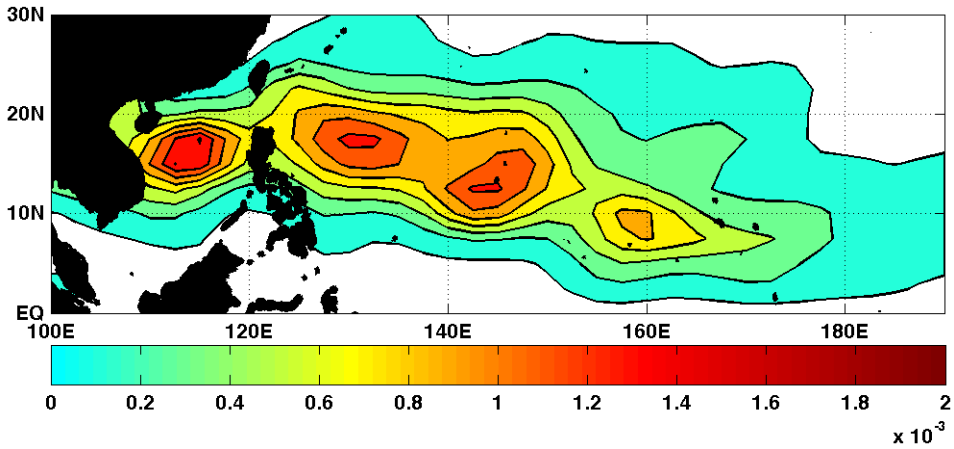

Figure 9. LTM TC formation probabilities (contours and color shading) for JASO in the WNP study region. Probabilities based on JASO 1981—2010 LTM LSEFs used to force the NPS logistic regression model. Note the high probability in the northern South China Sea and in a region extending southeastward from the Luzon Strait.

Figure 10 is the same as Figure 9 but with the LTM TC formations overlaid on the LTM probabilities. Note that most of the formations occur within the minimum contour, and that higher formation concentrations occur in the regions of higher probabilities. These results indicate that the NPS statistical model provides an accurate relative estimation of TC formation probabilities. These results, when combined with the results shown in Figure 8 indicate that the concentration of formations in the high probability areas are strongly determined by the favorable low level relative vorticity and zonal vertical wind shear

conditions in these areas. If so, then intraseasonal and interannual variations in these two LSEFs may be especially important in causing TC formation variations in the WNP.

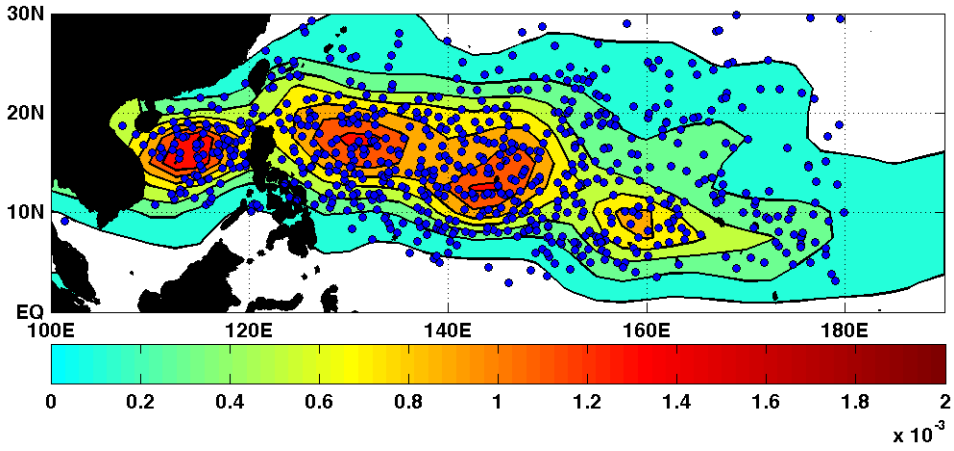

Figure 10. LTM composite TC formation probabilities (contours and color shading) and corresponding TC formations (blue dots) for JASO in the WNP study region. Probabilities based on JASO 1981—2010 LTM LSEFs used to force the NPS logistic regression model. Formation locations from JTWC WNP best track data. Note the general agreement between higher probabilities and higher formation concentrations.

B. ENLN

1. TC Formations

Figure 11 shows the TC formation locations for the composite EN (top panel) and LN (bottom panel) JASO periods. For the EN and LN composites, the numbers of formations are similar—168 for EN and 166 for LN. However, the EN and LN formation locations are shifted with respect to each other—to the southeast for EN and to the northwest for LN. Note, for example: (a) the greater number of formations in the South China Sea and north of 20°N during LN compared to EN; and (b) the greater number of formations south of 15^{o}N and east of 160^{o}E during EN compared to LN.

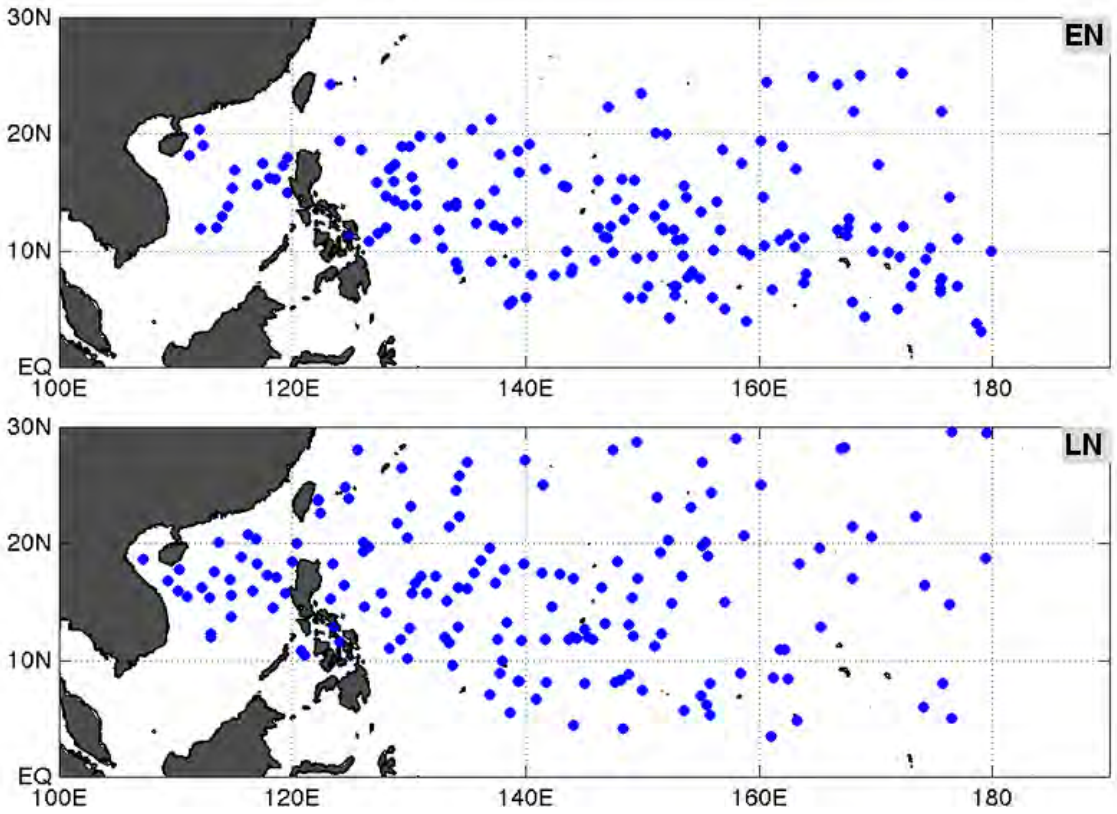

Figure 11. TC formations (blue dots) for EN composite years (upper panel) and LN composite years (lower panel) for JASO in the WNP study region. EN years: 1982, 1986, 1987, 1991, 1993, 1994, 1997, 2009. LN years: 1988, 1995, 1996, 1998, 2007, 1999, 2007, 2010. Formation locations from JTWC WNP best track data.

Figure 12 (13) shows the distribution of formations for the eight years used in the composites for EN (LN). The average number of formations for an EN (LN) JASO period is 21 (20.75). These results are consistent with prior studies that found EN and LN years have similar average number of formations but shifts in formation locations (e.g., Ford 2000).

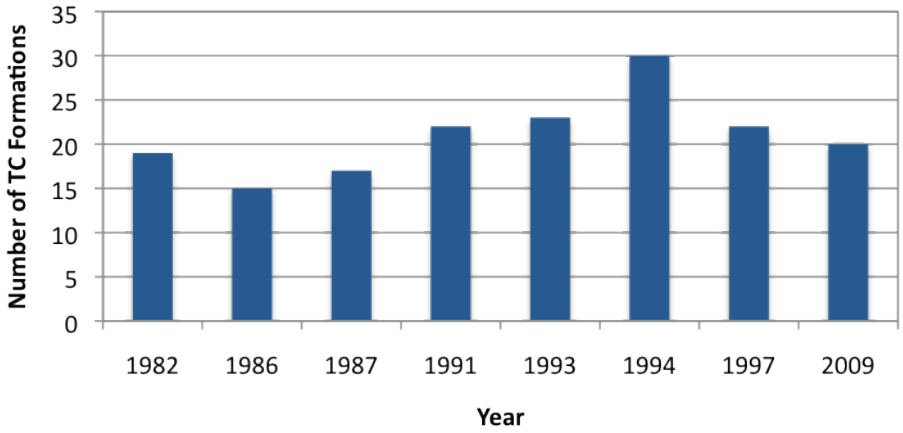

Figure 12. Number of TC formations during JASO in the WNP study region for the eight years used in the EN composites. Constructed from JTWC WNP best track data.

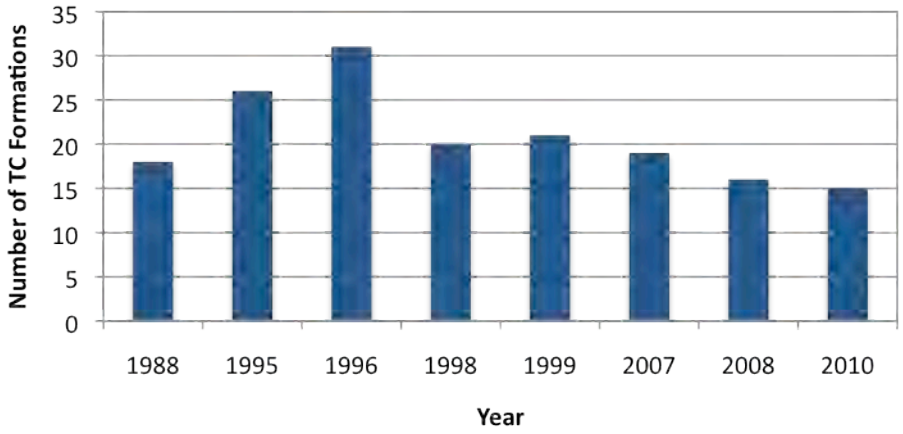

Figure 13. Number of TC formations during JASO in the WNP study region for the eight years used in the LN composites. Constructed from JTWC WNP best track data.

2. LSEFs

a. Sea Surface Temperature

Figure 14 shows the EN and LN composite SSTs. In the EN (LN) composite, the warmest SSTs occur approximately east of 170°E and from 5°N to the equator (west of 150°E and from 18°N to the equator).

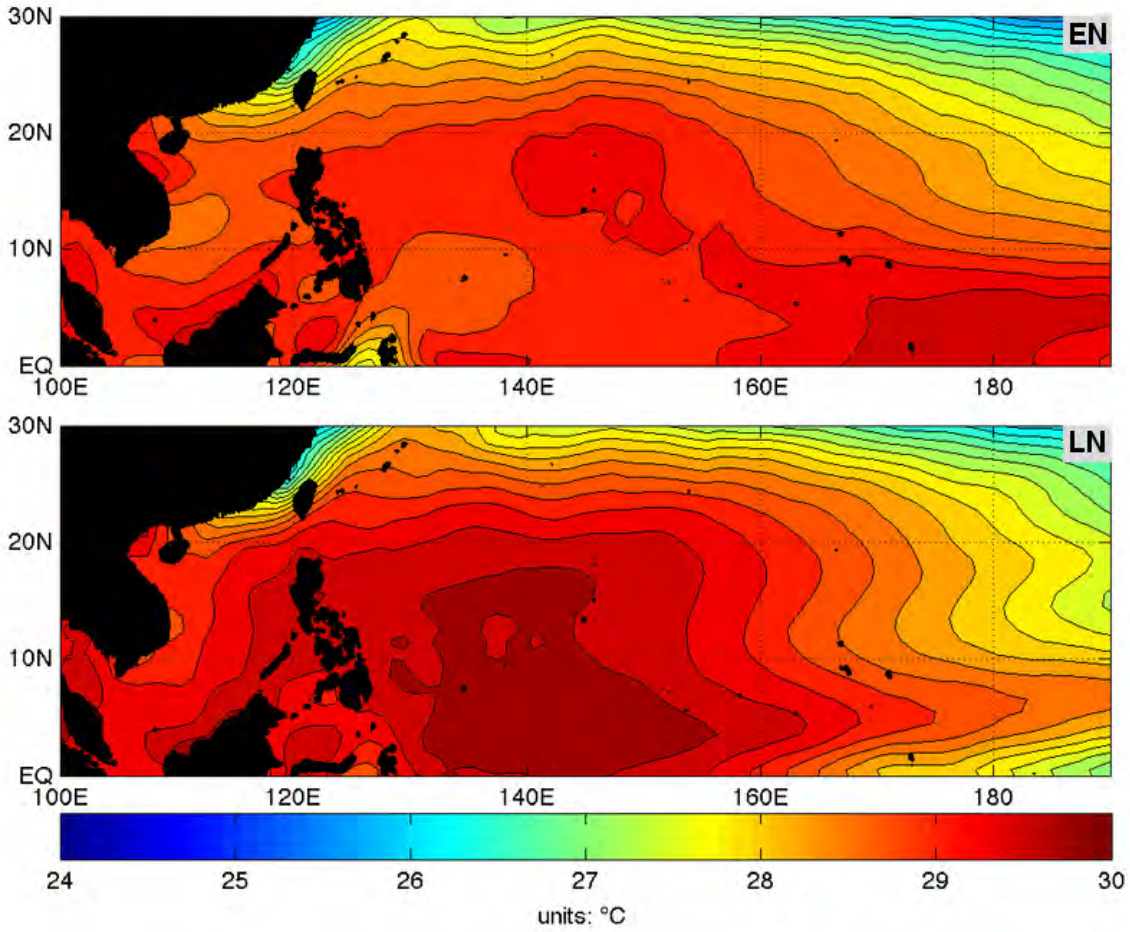

Figure 14. EN and LN composite SST (in °C) for JASO in the WNP study region (contours and color shading). Composites are for the strongest eight EN events (top panel) and LN events (bottom panel) during 1982—2010. EN years: 1982, 1986, 1987, 1991, 1993, 1994, 1997, 2009. LN years: 1988, 1995, 1996, 1998, 2007, 1999, 2007, 2010. Note in the EN (LN) composite the higher (lower) SSTs in the southeastern portion of the WNP, and the lower (higher) SSTs in the southwestern portion of the WNP.

Figure 15 shows the EN and LN composite SST anomalies. The anomaly plots highlight the EN-LN differences shown in Figure 14. In particular: (a) in the eastern equatorial portion of the WNP there is a region of anomalously warm (cool) water during EN (LN); and (b) in the western-central WNP, there is a large region of anomalously cool (warm) water during EN (LN). Note that these EN and LN composite SST and SST anomaly patterns shown in Figures 13–14 are broadly consistent with the EN-LN TC formation shifts shown in Figure 11.

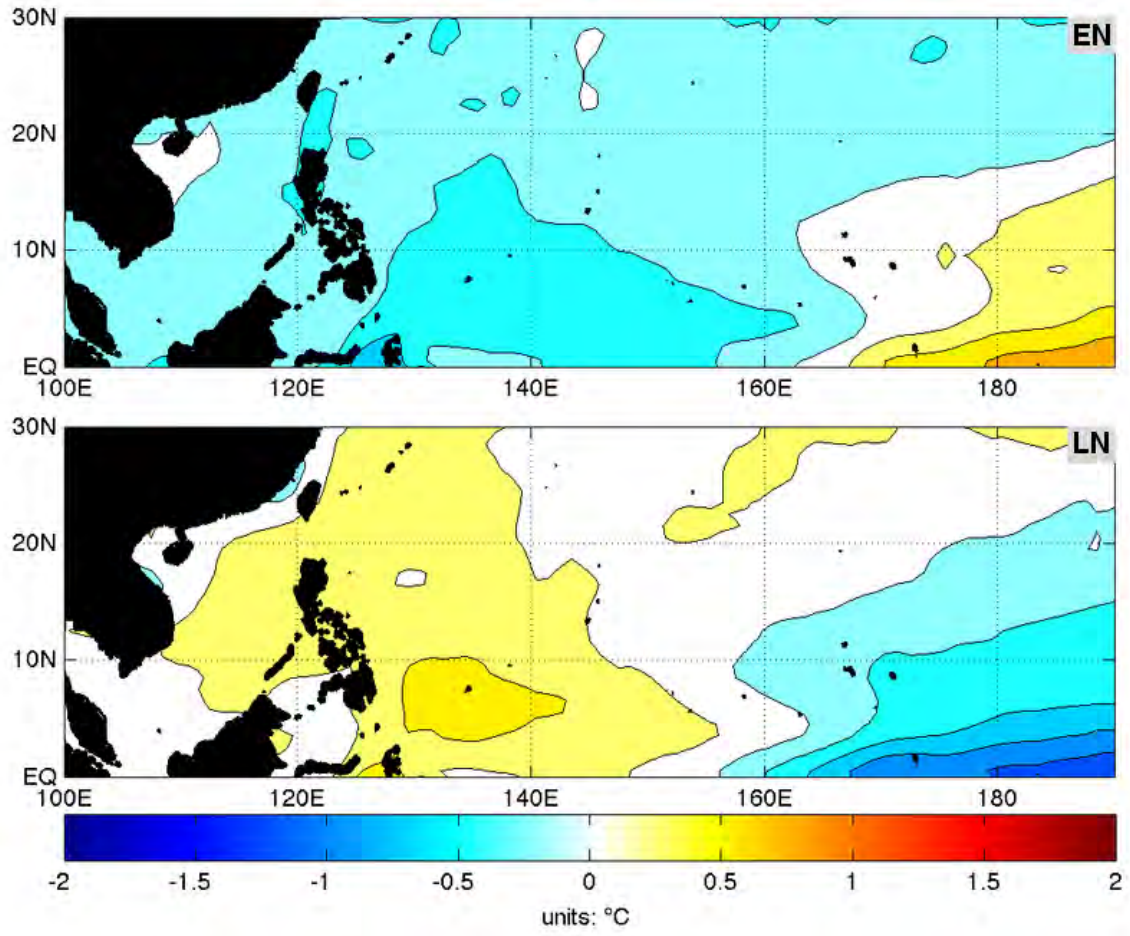

Figure 15. EN and LN composite anomalies of SST (in °C) for JASO in the WNP study region (contours and color shading). Composites are for the strongest eight EN events (top panel) and LN events (bottom panel) during 1982—2010. EN years: 1982, 1986, 1987, 1991, 1993, 1994, 1997, 2009. LN years: 1988, 1995, 1996, 1998, 2007, 1999, 2007, 2010. Note in the EN (LN) composite the anomalously high (low) SSTs in the southeastern portion of the WNP, and the anomalously low (high) SSTs in the western portion of the WNP.

b. Low Level Relative Vorticity

Figure 16 shows the EN and LN composite 850 hPa relative vorticity. The EN composite has a region of strong positive values extending across the entire central WNP, with negative values to the north and south. In contrast, the LN composite has much weaker positive values extending across the central WNP, and weaker negative values to the north and south.

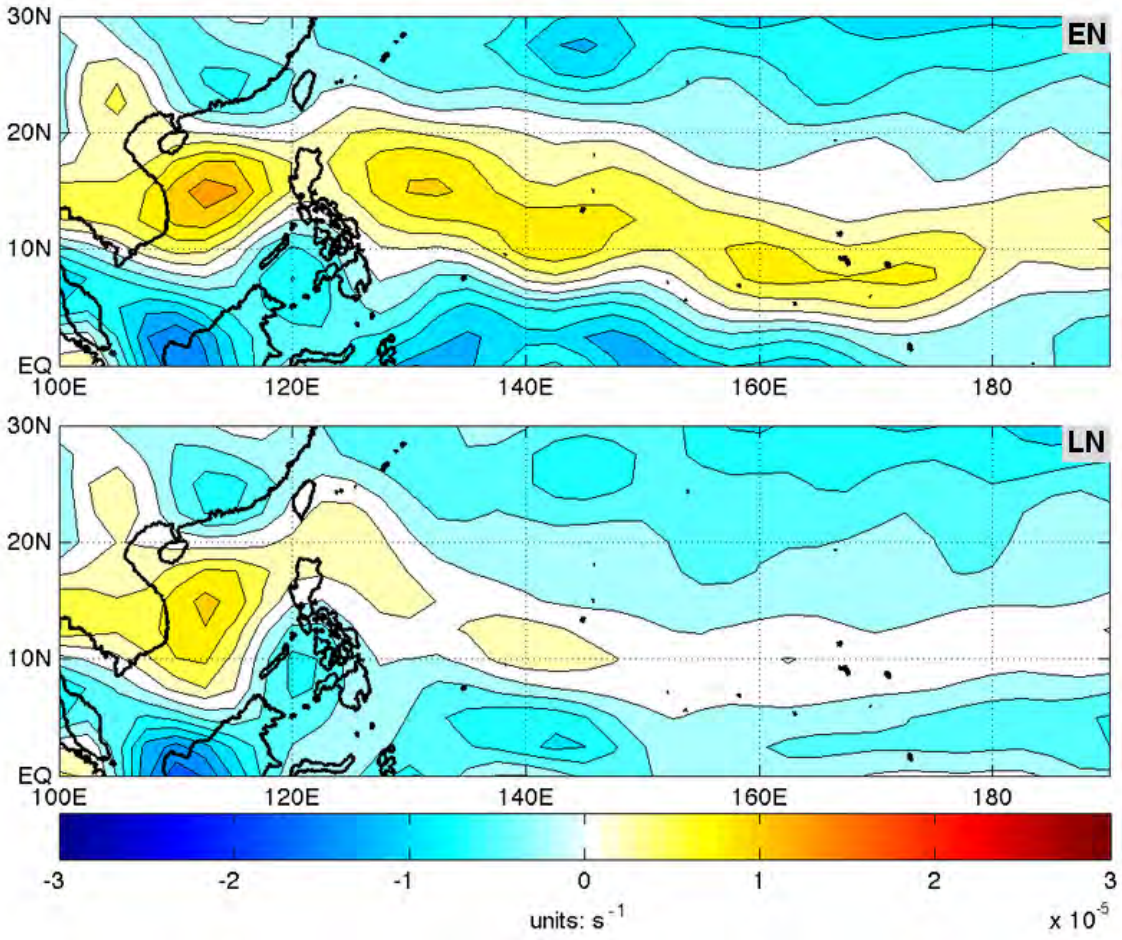

Figure 16. EN and LN composite 850 hPa relative vorticity (in s^{-1}) for JASO in the WNP study region (contours and color shading). Composites are for the strongest eight EN events (top panel) and LN events (bottom panel) during 1982—2010. EN years: 1982, 1986, 1987, 1991, 1993, 1994, 1997, 2009. LN years: 1988, 1995, 1996, 1998, 2007, 1999, 2007, 2010. Note in the EN (LN) composite stronger (weaker) positive relative vorticity region over the South China Sea and extending southeastward from the Luzon Strait over much of the WNP.

Figure 17 shows the EN and LN composite 850 hPa relative vorticity anomalies. In the EN composite anomaly, the low level relative vorticity anomalies are positive in the central South China Sea and in a band extending southeastward from the Luzon Strait. In contrast, the LN composite reveals negative anomalies in the previously identified areas where the EN anomalies are positive, with small regions of positive anomalies near the equator to the southwest, south, and southeast of the Philippines, to the southeast of Taiwan, and in a band extending northeastward from Taiwan. Note that these anomaly patterns are consistent with the EN-LN formation location shifts shown in Figure 11.

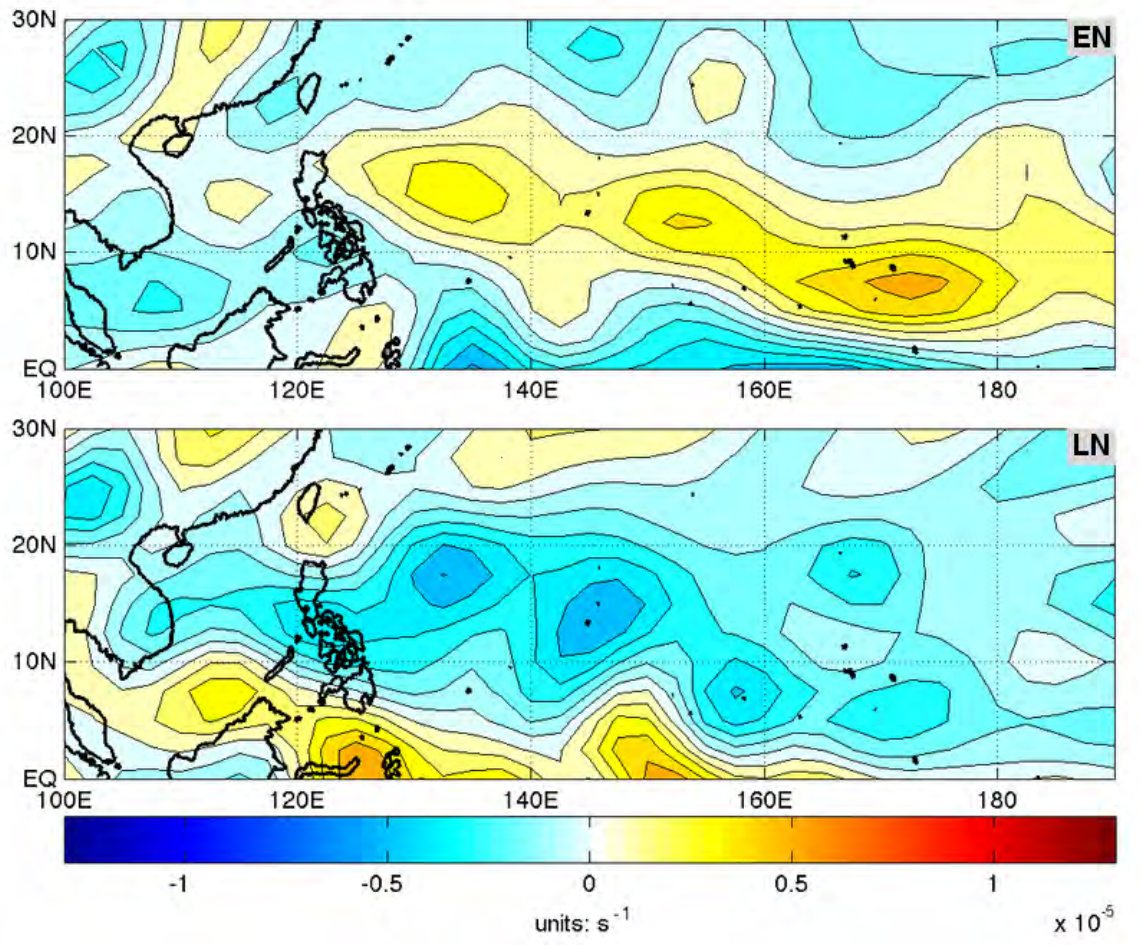

Figure 17. EN and LN composite anomalies of 850 hPa relative vorticity (in s^{-1}) for JASO in the WNP study region (contours and color shading). Composites are for the strongest eight EN events (top panel) and LN events (bottom panel) during 1982—2010. EN years: 1982, 1986, 1987, 1991, 1993, 1994, 1997, 2009. LN years: 1988, 1995, 1996, 1998, 2007, 1999, 2007, 2010. Note in the EN (LN) composite the positive (negative) relative vorticity anomalies in the central and southeastern part of the WNP (near Taiwan-Luzon, and in the southern South China Sea, central equatorial, and northern parts of the WNP).

c. Zonal Vertical Wind Shear

Figure 18 shows the EN and LN composite zonal vertical wind shear anomalies. In the EN composite, the easterly shear region and the zero shear region extend much further to the east south of about 10^{o}N than in the

LTM (Figure 8) and the LN composite. In the LN composite, the easterly shear region and the zero shear region extend much further to the northeast north of about 20^{o}N than in the LTM (Figure 8) and the EN composite. These results are consistent with prior studies (e.g., Ford 2000) and with the EN-LN TC formation location shifts shown in Figure 11.

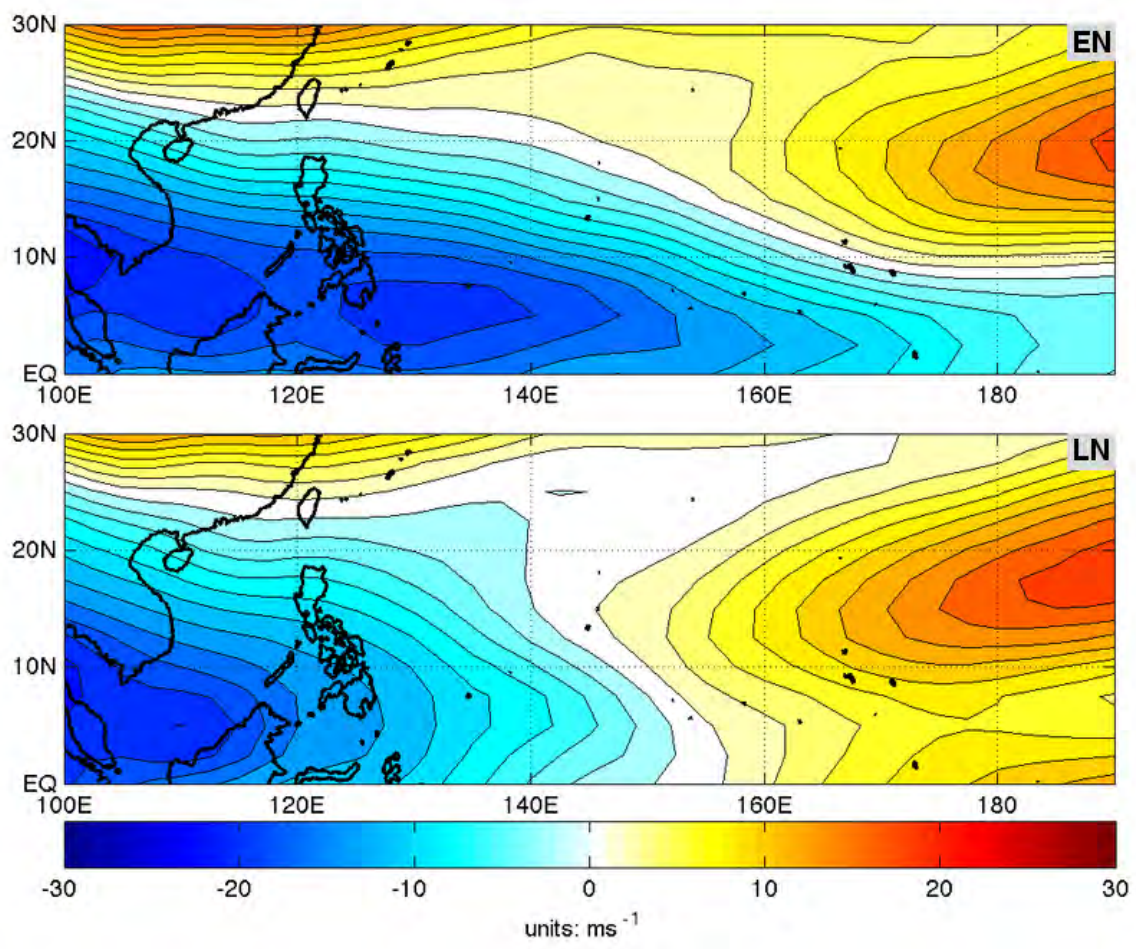

Figure 18. EN and LN composite zonal vertical wind shear (in ms^{-1}) for JASO in the WNP study region (contours and color shading). Composites are for the strongest eight EN events (top panel) and LN events (bottom panel) during 1982—2010. EN years: 1982, 1986, 1987, 1991, 1993, 1994, 1997, 2009. LN years: 1988, 1995, 1996, 1998, 2007, 1999, 2007, 2010. Note in the EN (LN) composite stronger (weaker) easterly vertical shear region extending from west to east across much of the WNP.

Figure 19 shows the EN and LN composite zonal vertical wind shear anomalies. The EN and LN composite anomalies are nearly opposite of each other. In the EN (LN) composite anomaly easterly (westerly) shear anomalies dominate most of the southern two-thirds of the WNP, while westerly (easterly) shear anomalies dominate most of the north third of the WNP. These plots help us better understand the very different positions of the zero shear lines for EN and LN shown in Figure 18. The net effects are clear shift in the location and orientation of the low vertical wind shear areas during EN and LN that are consistent with the EN-LN shifts in TC formation locations shown in Figure 11.

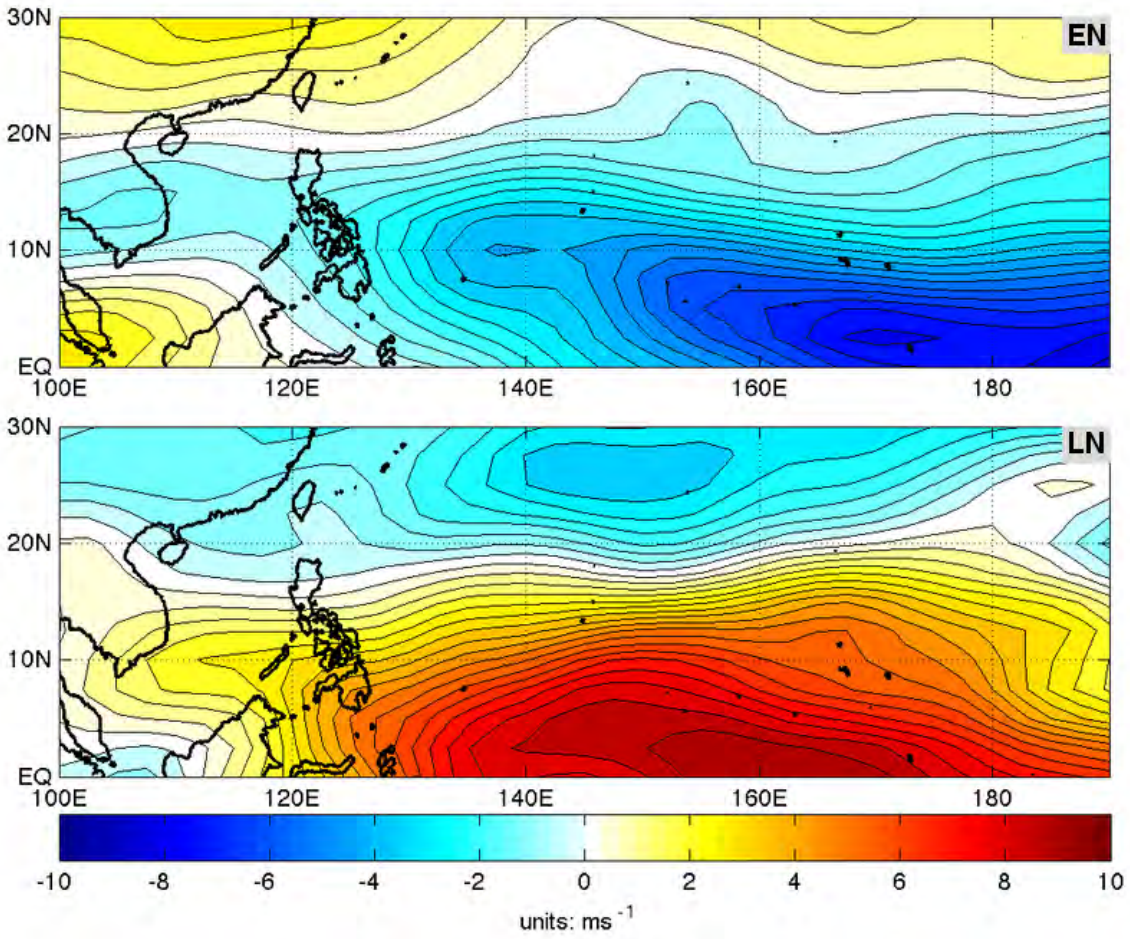

Figure 19. EN and LN composite anomalies of zonal vertical wind shear (in ms^{-1}) for JASO in the WNP study region (contours and color shading). Composites are for the strongest eight EN events (top panel) and LN events (bottom panel) during 1982–2010. EN years: 1982, 1986, 1987, 1991, 1993, 1994, 1997, 2009. LN years: 1988, 1995, 1996, 1998, 2007, 1999, 2007, 2010. Note in the EN (LN) composite the negative (positive) vertical shear anomalies in the central and southeastern part of the WNP.

d. Meridional Vertical Wind Shear

Figure 20 shows the EN and LN composite meridional vertical wind shear. The WNP is dominated by negative or northerly shear in both the EN and LN composites. The overall patterns are similar for EN and LN, but with less

negative or northerly meridional vertical shear during LN, consistent with the circulation anomalies associated with EN and LN.

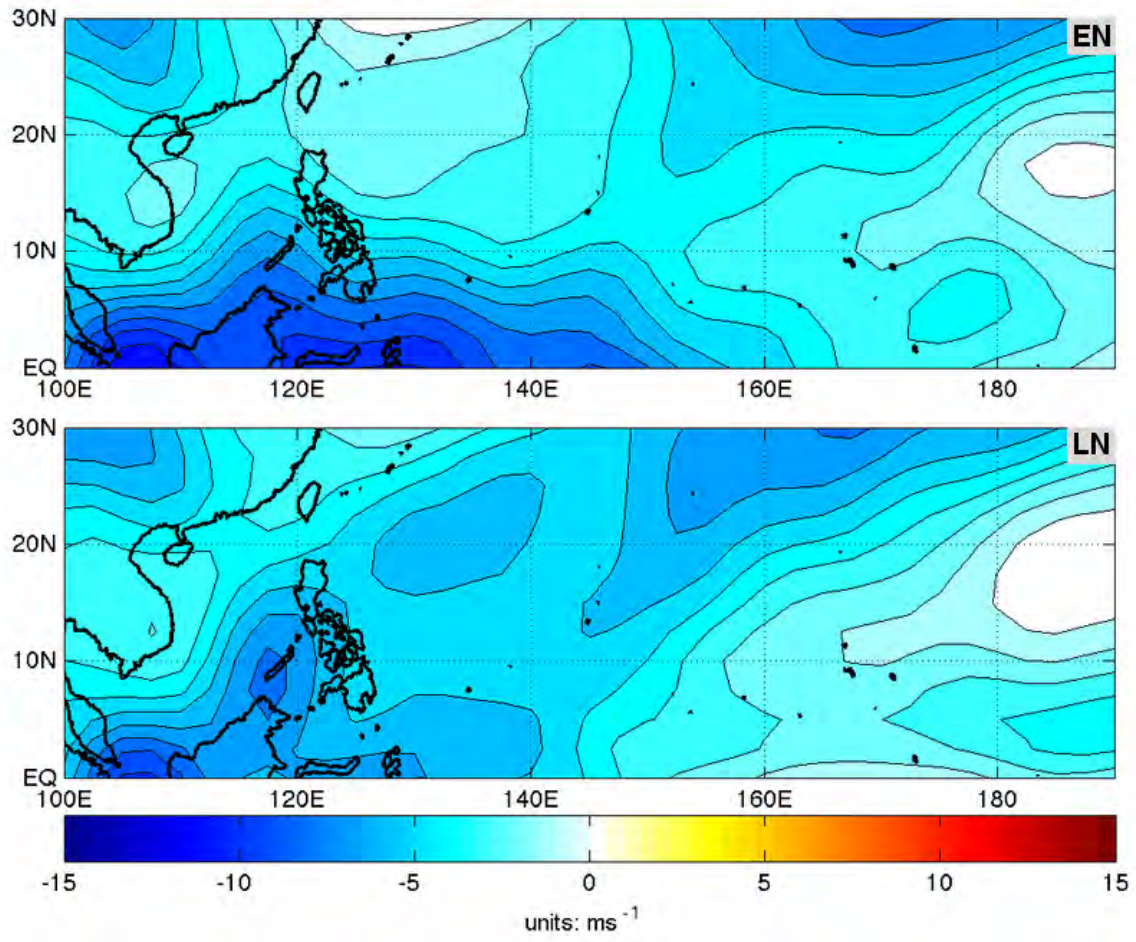

Figure 20. EN and LN composite meridional vertical wind shear (in ms^{-1}) for JASO in the WNP study region (contours and color shading). Composites are for the strongest eight EN events (top panel) and LN events (bottom panel) during 1982–2010. EN years: 1982, 1986, 1987, 1991, 1993, 1994, 1997, 2009. LN years: 1988, 1995, 1996, 1998, 2007, 1999, 2007, 2010.

Figure 21 shows the EN and LN composite meridional vertical wind shear anomalies. In the EN composite anomaly, there is a region of slightly positive anomaly northeast of the Philippines and a negative anomaly near the equator across much of the WNP. In the LN there are negative anomalies over the Philippines and to the northeast, and positive anomalies near the equator and

in the northeast WNP. These anomalies are consistent with the EN-LN TC formation location shifts shown in Figure 11 (compare with the LTM meridional vertical wind shear patterns shown in Figure 8).

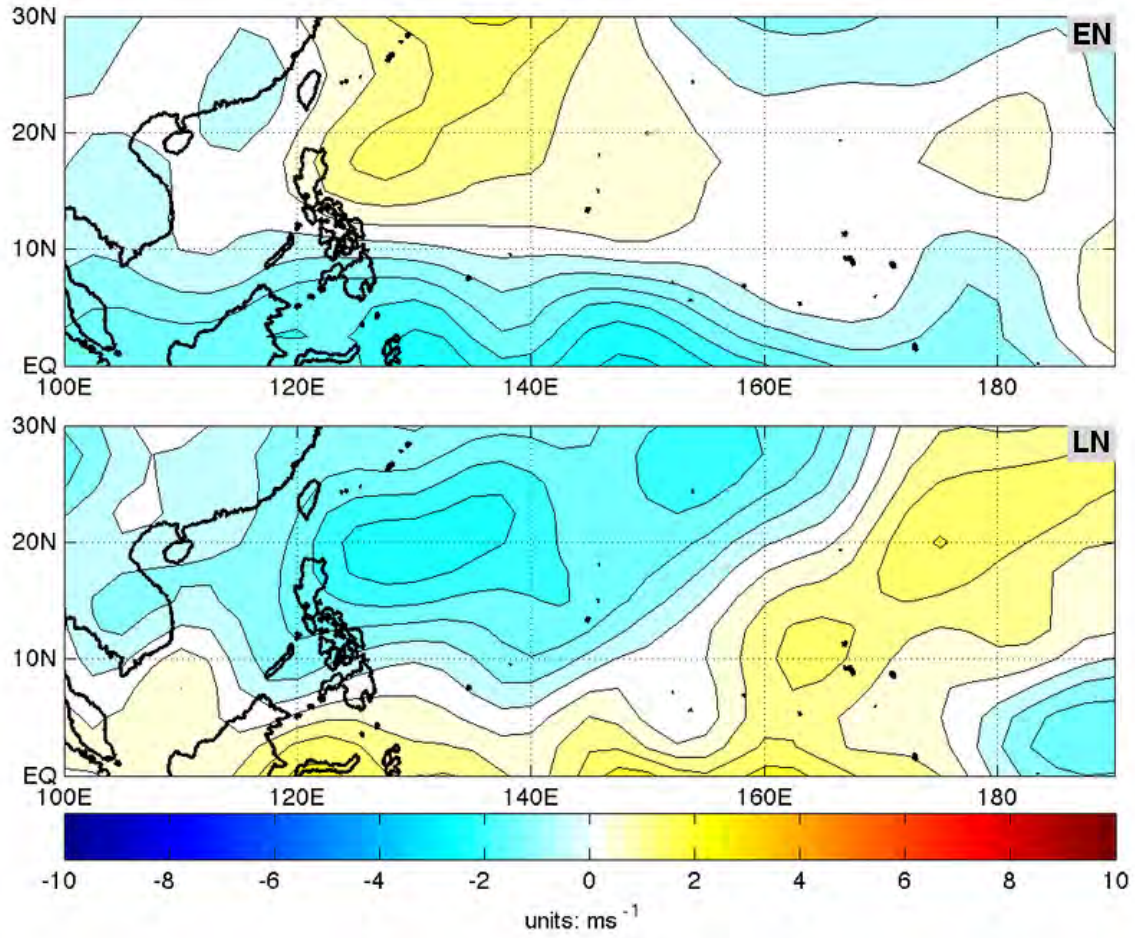

Figure 21. EN and LN composite anomalies of meridional vertical wind shear (in ms^{-1}) for JASO in the WNP study region (contours and color shading). Composites are for the strongest eight EN events (top panel) and LN events (bottom panel) during 1982–2010. EN years: 1982, 1986, 1987, 1991, 1993, 1994, 1997, 2009. LN years: 1988, 1995, 1996, 1998, 2007, 1999, 2007, 2010.

e. Upper Level Divergence

Figure 22 shows the EN and LN composite 200 hPa divergence, and Figure 23 shows the corresponding anomalies. Figure 22 shows that the EN and LN patterns are similar, but both figures show stronger divergence: (a) in the

EN composite in the South China Sea, in a band centered along approximately 10–20^{o}N, and in the southeastern part of the WNP; and (b) in the LN composite south of the Philippines, and over and to the northeast of Taiwan. These upper level divergence patterns are consistent with the EN-LN TC formation locations shifts shown in Figure 11.

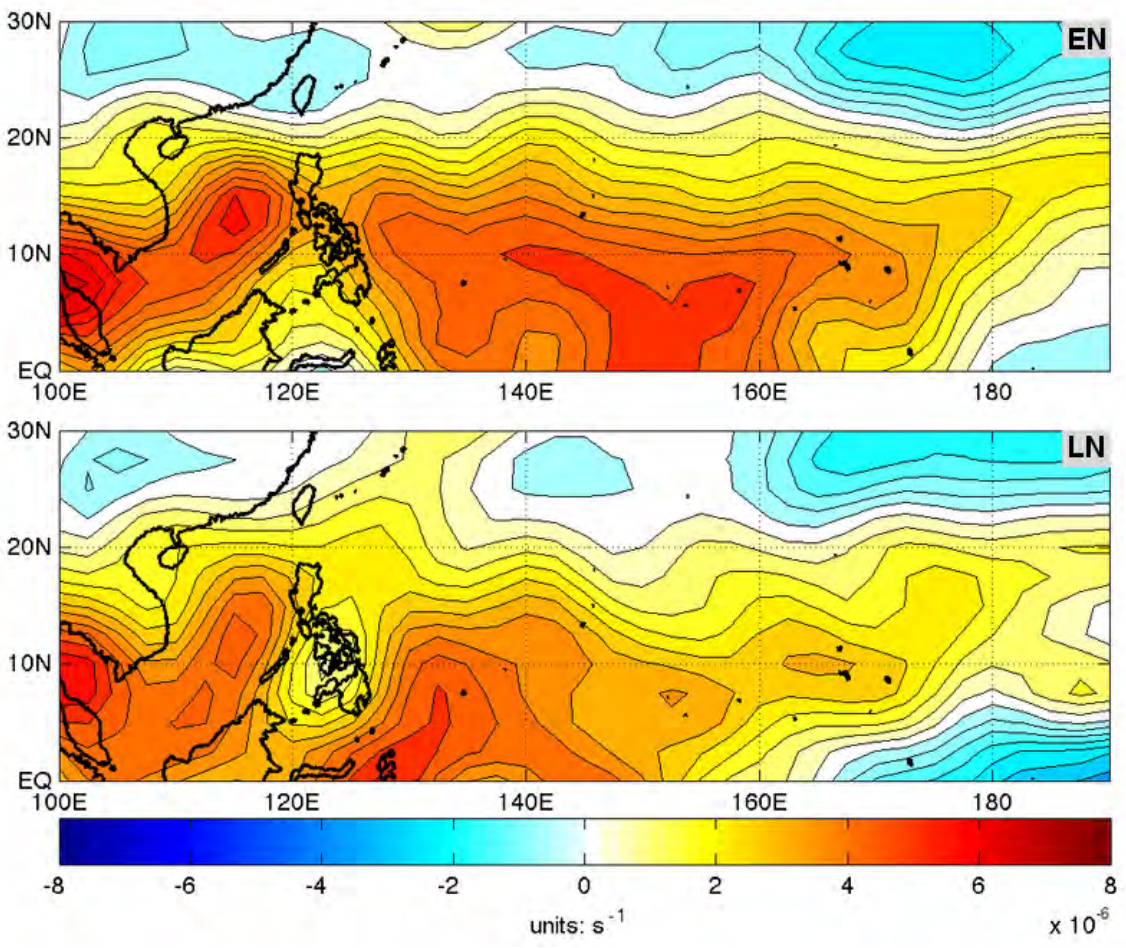

Figure 22. EN and LN composite 200 hPa divergence (in s^{-1}) for JASO in the WNP study region (contours and color shading). Composites are for the strongest eight EN events (top panel) and LN events (bottom panel) during 1982–2010. EN years: 1982, 1986, 1987, 1991, 1993, 1994, 1997, 2009. LN years: 1988, 1995, 1996, 1998, 2007, 1999, 2007, 2010. Note in the EN (LN) composite stronger (weaker) positive divergence region across much of the WNP.

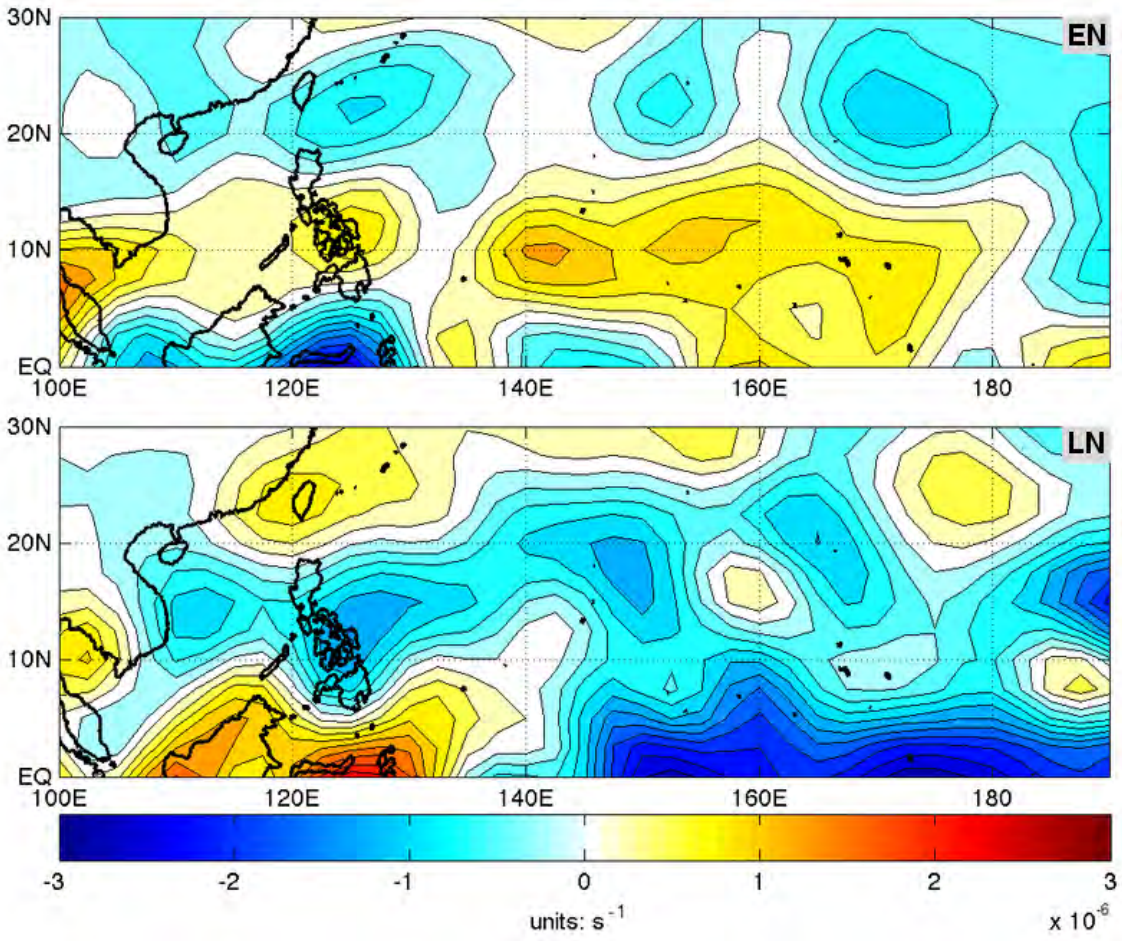

Figure 23. EN and LN composite anomalies of 200 hPa divergence (in s^{-1}) for JASO in the WNP study region (contours and color shading). Composites are for the strongest eight EN events (top panel) and LN events (bottom panel) during 1982–2010. EN years: 1982, 1986, 1987, 1991, 1993, 1994, 1997, 2009. LN years: 1988, 1995, 1996, 1998, 2007, 1999, 2007, 2010. Note in the EN (LN) composite the negative (positive) anomalies over and to the east of Taiwan, and the positive (negative) anomalies in a zonal band centered between about 10–20^{o}N and in the southeastern WNP.

3. TC Formation Probabilities

The EN and LN LSEFs were used to force the NPS statistical model and generate the EN and LN TC formation probability results shown in Figure 24. The EN and LN probability patterns are clearly different, especially in: (a) a band extending southeastward from Taiwan, where the EN probabilities are higher

than the LN probabilities; and (b) in the northern WNP east of Taiwan, where LN probabilities are higher than EN probabilities. There are striking similarities between the overall probability patterns and several of the LSEF patterns for both EN and LN. For example, the zero shear line for the EN composite extends across much of the WNP on a northwest-southeast axis (Figure 18), which is very similar to the EN axis of high probabilities (Figure 24). Similarly, the highest LN probabilities do not extend much further east than 160°E (Figure 24), which corresponds to where the zero shear line occurs in the LN composite (Figure 18).

There is also a strong connection between the EN and LN probability patterns and the corresponding SSTs, low level relative vorticity, and upper level divergence patterns. SSTs, low level relative vorticity, upper level divergence conditions are all more favorable near the IDL in the EN composite compared to the LN composite, consistent with the higher EN probabilities in that area. In contrast, the LN probabilities are higher than the EN probabilities west of 160^{o}E and within about 10^{o} of the equator, and north of about 20°N and west of 180^{o}E, especially over and just to the southeast of Taiwan. These LN probability patterns are consistent with the LN LSEF anomalies (e.g., the SST, low level relative vorticity, meridional vertical wind shear, and upper level divergence anomalies during LN).

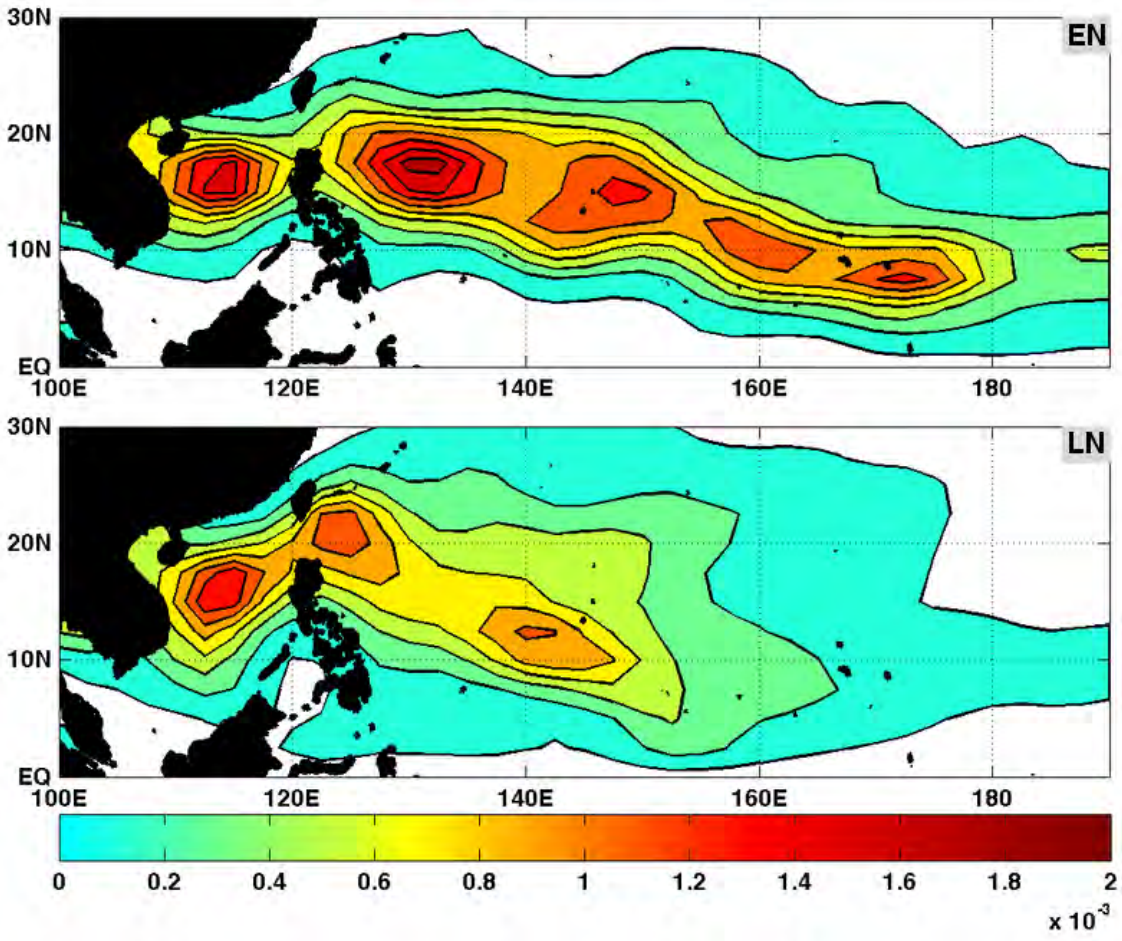

Figure 24. EN and LN composite TC formation probabilities for JASO in the WNP study region (contours and color shading). Probabilities based on JASO 1981–2010 EN and LN composite LSEFs used to force the NPS logistic regression model. Note in the EN (LN) composite the higher (lower) probabilities in the central and southeastern part of the WNP and the lower (higher) probabilities in the northern part of the WNP.

Figure 25 is the same plot as Figure 24 but with the corresponding EN and LN TC formation locations (blue dots and Figure 11) overlaid on the probabilities. Note the overall agreement between the probabilities and the formation numbers and locations—for example, the higher (lower) probabilities and number of formations in the southeastern WNP during EN (LN), and the lower (higher)

probabilities and number of formations east and southeast of Taiwan, and in much of the area north of 20°N, during LN (EN).

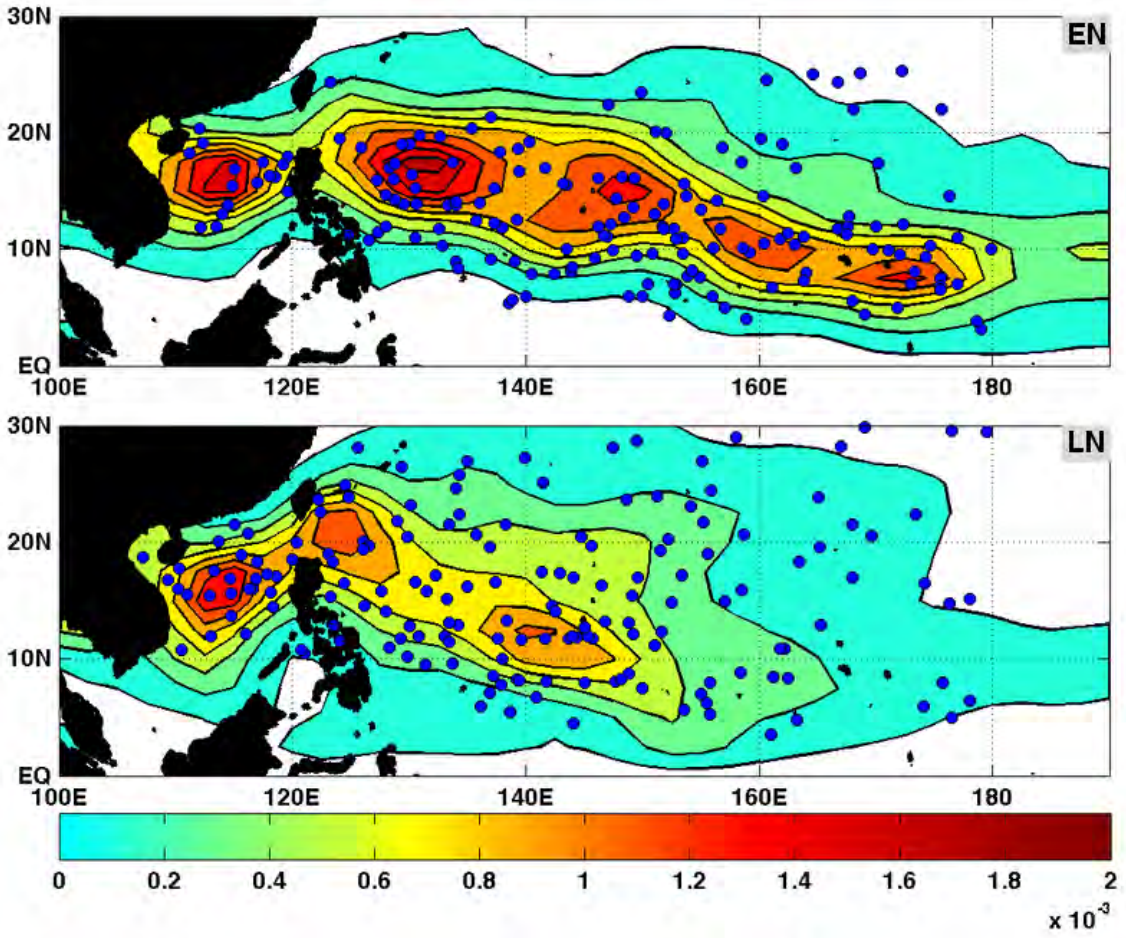

Figure 25. EN and LN composite TC formation probabilities (contours and color shading) and corresponding TC formations (blue dots) for JASO in the WNP study region. Probabilities based on JASO 1981–2010 EN and LN composite LSEFs used to force the NPS logistic regression model. Formation locations from JTWC WNP best track data. Note for both the EN and LN composites the general correspondence between the formation probability regions and the actual formations. In particular, note in the EN (LN) composite the higher (lower) probabilities and formations in the central and southeastern part of the WNP and the lower (higher) probabilities and formations in the northern part of the WNP.

To highlight the EN-LN probability differences, we calculated the EN and LN probability anomalies (Figure 26). These show for EN, a strong positive anomaly just east of the Philippines and extending east-southeastward across the WNP, negative anomalies to the north and south of this positive anomaly area, and a negative anomaly south and east of Taiwan. The LN anomaly is almost the opposite of the EN anomaly. The EN and LN anomalies are of course directly related to the LSEF anomalies, as indicated by the LSEF results shown in the prior sections, and by the use of the EN and LN LSEFs to force the NPS statistical model from which the EN and LN probabilities and probability anomalies are derived.

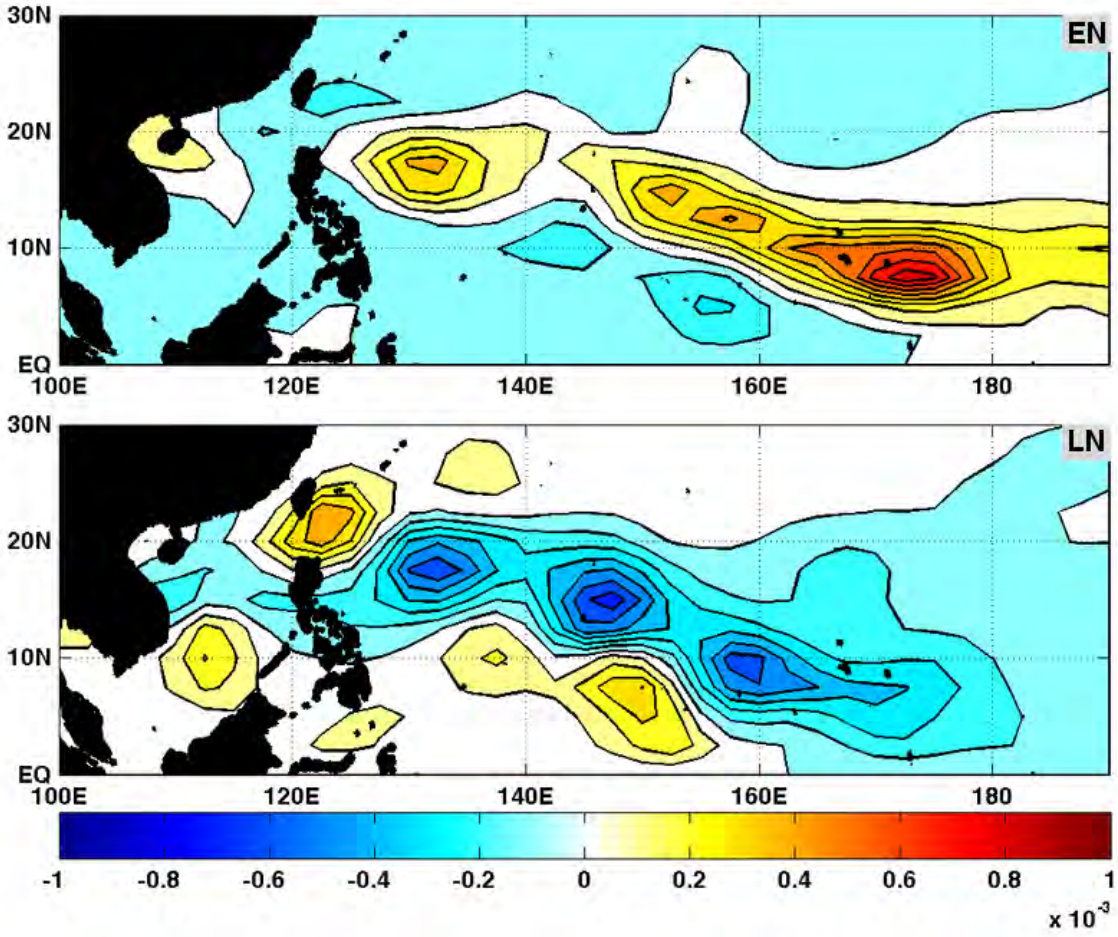

Figure 26. EN and LN composite anomalies of TC formation probabilities for JASO in the WNP study region (contours and color shading). Probabilities based on JASO 1981–2010 EN and LN composite LSEFs used to force the NPS logistic regression model. Base period for anomaly calculations was 1981–2010. Note in the EN (LN) composite the anomalously high (low) probabilities in the central and southeastern part of the WNP and the lower (higher) probabilities near Taiwan-Luzon, and in the southern South China Sea, central equatorial, and northern parts of the WNP.

C. MJO

1. TC Formations

Our MJO analyses revealed that TC formation numbers are related to MJO phase, MJO amplitude, and the number of days in each phase (see Tables 2–3). We adjusted for the differences in formations numbers per phase that were due to differences in the number of days per phase by calculating, for each phase: (a) the percentage of all the WNP TC formations that occurred in JASO during MJO days with amplitudes greater than 1.25 (Figure 27); and (b) the number of WNP TC formations normalized by the number of days in the phase (Figure 28). Figure 27 shows that phases 5 and 6 have the highest percentage of the WNP TC formations when MJO amplitude during JASO is greater than 1.25, and that phase 3 has the least. Figure 28 shows that the number of WNP TC formations per day, for JASO days with MJO amplitudes greater than 1.25, is greatest for phases 5 and 6, and lowest for phases 1–3. Thus, from both percentage and daily rate perspectives, WNP TC formations are most (least) likely during phases 5 and 6 (phase 3), when the WNP is occupied by the convective (subsidence) component—for MJO amplitudes greater than 1.25 during JASO. Prior studies have drawn similar conclusions but without making clear the need to account for MJO amplitude, and for the differing number of days in each phase, before this conclusion can be well supported (e.g., Kim et al. 2008; Camargo et al. 2009).

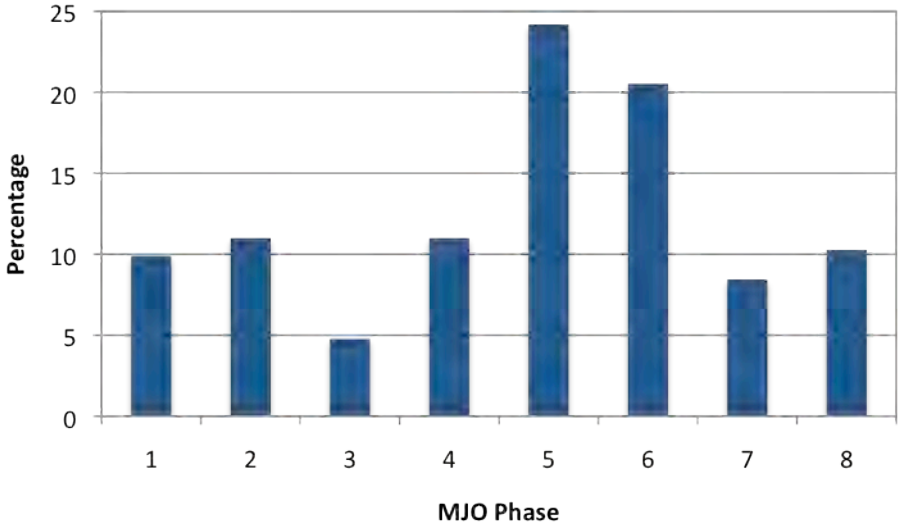

Figure 27. Percentage TC formations in each MJO phase for all MJO days with amplitude > 1.25. Percentage is equal to the number of TC formations in each MJO phase divided by the total number of TC formations in all phases (273), for formation days with MJO amplitudes > 1.25, for JASO 1975–2010, in the WNP study region. Constructed from JTWC WNP best track data and BOM MJO phase and amplitude data.

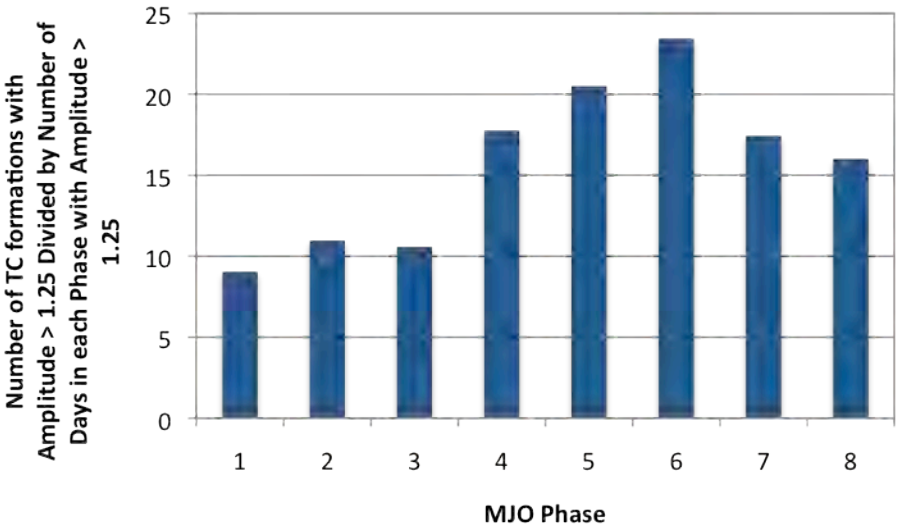

Figure 28. Number of TC formations divided by total number of days in the phase for formations days with MJO amplitudes > 1.25, for JASO 1975—2010, in the WNP study region. Constructed from JTWC WNP best track data and BOM MJO phase and amplitude data.

Figure 29 shows the TC formations that occurred when the MJO amplitude was greater than 1.25 for JASO 1975—2010 in the WNP study region, based on the MJO composite days for each phase (Table 2), and without adjusting for the different number of days in each phase composite. The differences in TC formation numbers are of course consistent with the differences shown in Table 3 (e.g., largest (smallest) formation numbers for phases 5–6 (3)). But Figure 29 provides additional information about differences in formation locations—for example: (a) phases 5 and 6 (1, 2, and 8) have the most (least) formations in the South China Sea; (b) phase 8 (3) has the most (least) formations east of 160°E; and (c) phases 3 and 4 have the least number of formations at or north of 20^{o}N.

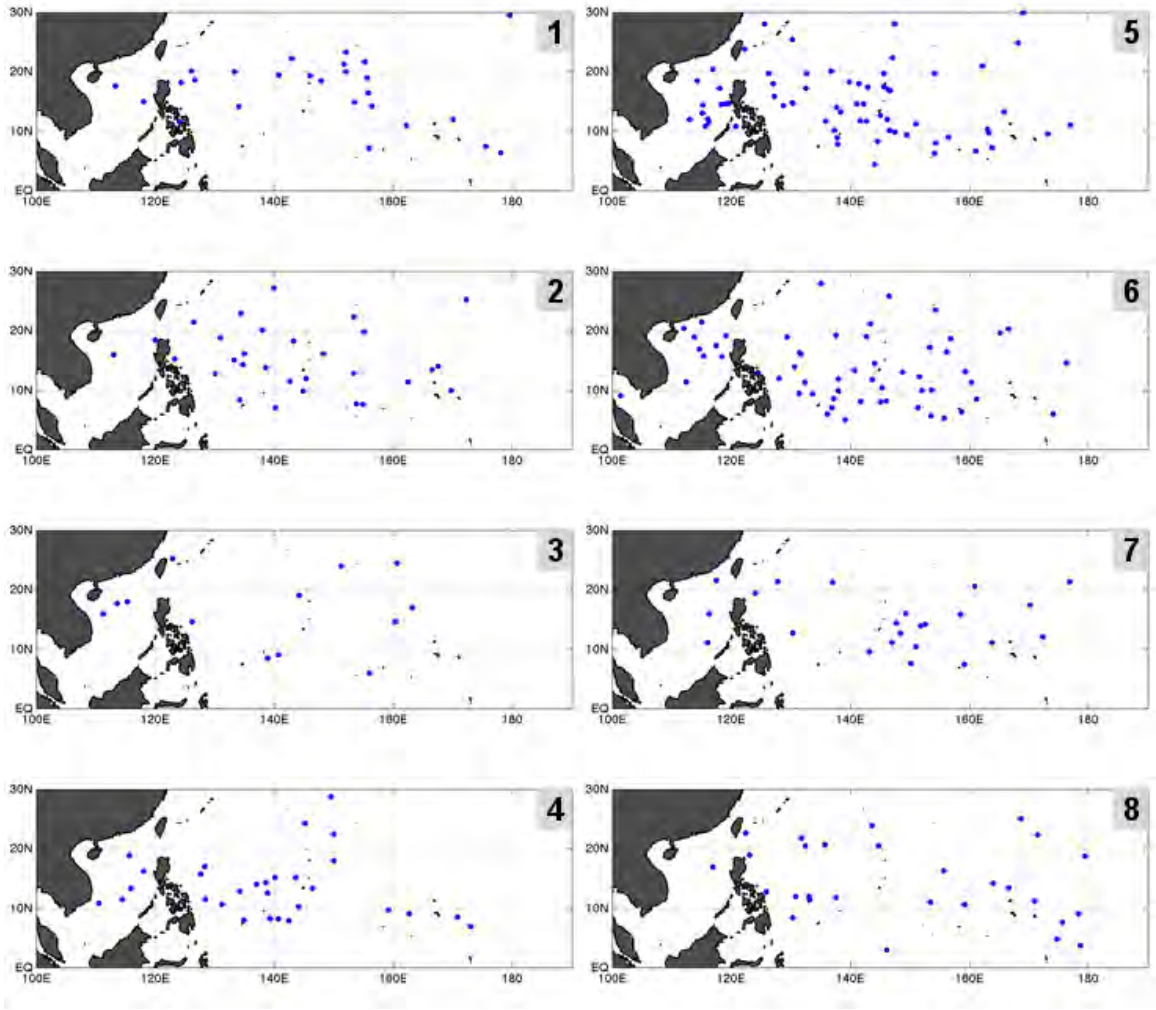

Figure 29. TC formations by phase for MJO events with amplitude > 1.25 (blue dots; phase number shown in upper right), for JASO 1975–2010, in the WNP study region. MJO phase and amplitude data from BOM. Formation locations from JTWC WNP best track data. Note the different TC formations numbers and locations for the different phases.

2. LSEFs

In this section, we summarize the LSEF results for the eight MJO phases. We found only very small differences in SST between the phases, and so we excluded the SST results from this section. However, we did include SST in the calculation of the TC formation probabilities for each phase, since SST is one of the LSEFs in the NPS statistical model.

a. Low Level Relative Vorticity

Figure 30 shows the MJO composite 850 hPa relative vorticity for the eight phases of MJO. Phases 1–3 and 8 have significantly weaker positive low level relative vorticity across the central WNP than phases 4–7. One of the most striking features is the region of strong positive low level relative vorticity in the South China Sea and extending across the central WNP during phases 4–7. That same region is significantly weaker, and in some cases negative, during phases 1–3 and 8. Phases 4–7 also show relatively strong negative relative vorticity near the equator and west of about 150^{o}E.

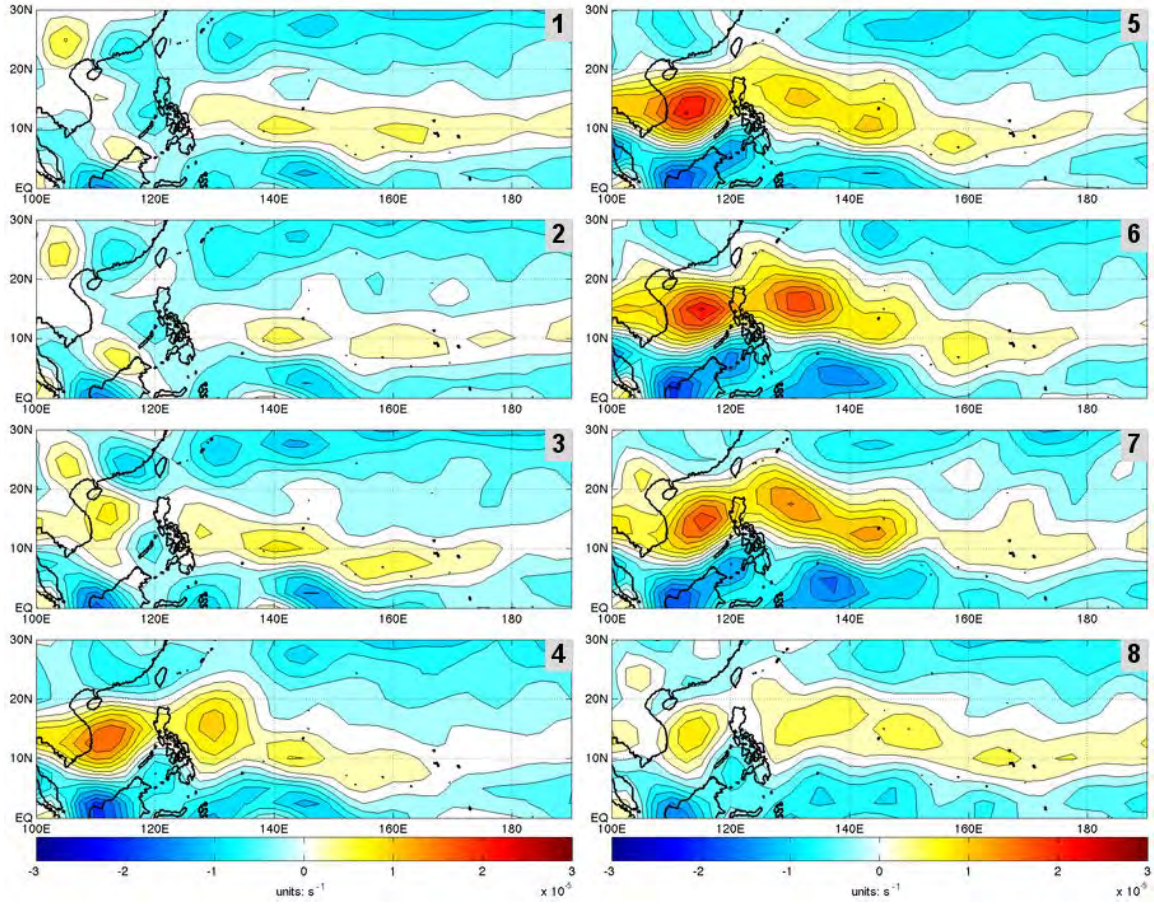

Figure 30. MJO composite 850 hPa relative vorticity (in s^{-1}), for MJO phases 1–8 with amplitude > 1.25, for JASO 1975–2010, in the WNP study region (contours and color shading; phase number shown in upper right of each panel). Note the relatively stronger (weaker) relative vorticity over the South China Sea and extending across the central part of much of WNP during phases 4–7 (1–3 and 8).

Figure 31 shows the composite 850 hPa relative vorticity anomalies for the eight phases of MJO. Phases 1–3 and 8 (4–7) have negative (positive) anomalies in the South China Sea and extending across the central WNP. Note the relatively opposite positive/negative patterns between phases 1–3, and 8, and phases 4–7 in much of the WNP. For example, comparing phase 1 to phase 5, we see that where there are negative anomalies in phase 1 there tend to be positive anomalies in phase 5, and likewise for phases 2 and 6, phases 3 and 7, and phases 8 and 4. The eastern portion of the WNP shows no distinct

differences between the phases, just relatively weak positive and negative anomalies throughout the area. However, there is a weak positive anomaly that extends past the IDL in phase 8 that does not occur in the other phases that may explain why phase 8 has a relatively large number of formations near the IDL (Figure 29).

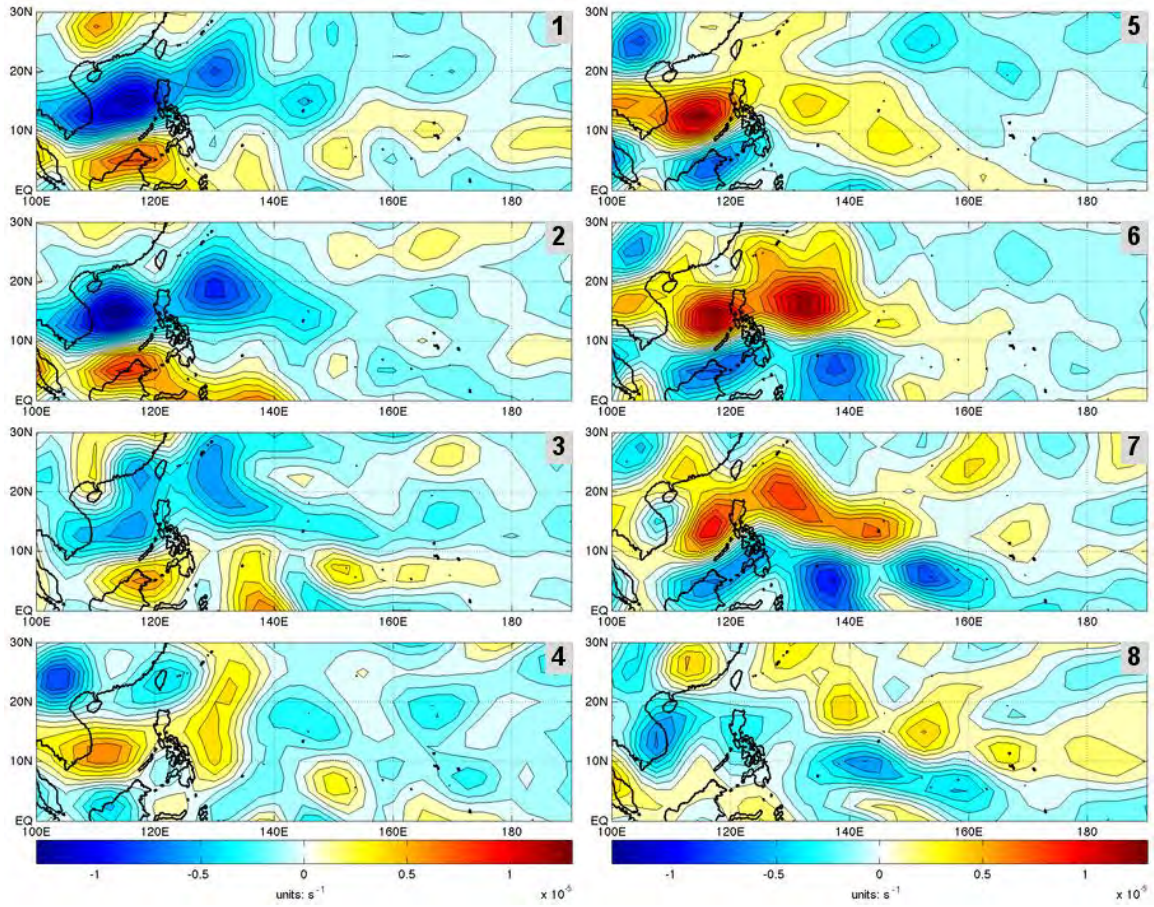

Figure 31. MJO composite anomalies of 850 hPa relative vorticity (in s^{-1}), for MJO phases 1–8 with amplitude > 1.25, for JASO 1975–2010, in the WNP study region (contours and color shading; phase number shown in upper right of each panel). Note the positive (negative) relative vorticity anomalies over the South China Sea and just east of the Philippines and Taiwan-Luzon during phases 4–7 (1–3 and 8).

b. Zonal Vertical Wind Shear

Figure 32 shows the composite zonal vertical wind shear for the eight phases of MJO. In the eight composites, easterly wind shear dominates the eastern region of the WNP, and westerly wind shear dominates the western region of the WNP. Phases 2–4 have a very similar overall pattern and no significant shifts in the zero wind shear line. Phase 4 has a slightly stronger easterly wind shear in the western WNP than the prior phases, and this shear is stronger still in phases 5–7, and similar in strength in phase 8. The eastward extent of this easterly shear region is greatest (least) in phase 8 (phase 4). The position of the zero wind shear line changes little from phase 2 to phase 4, in part because the easterly and westerly shear regions intensify simultaneously. The zero wind shear location extends east of 170°W during phases 1, 7, and 8, which is likely a result of the weakening of the westerly wind shear in the east as the convective component moves into the central tropical Pacific (cf. Figure 2).

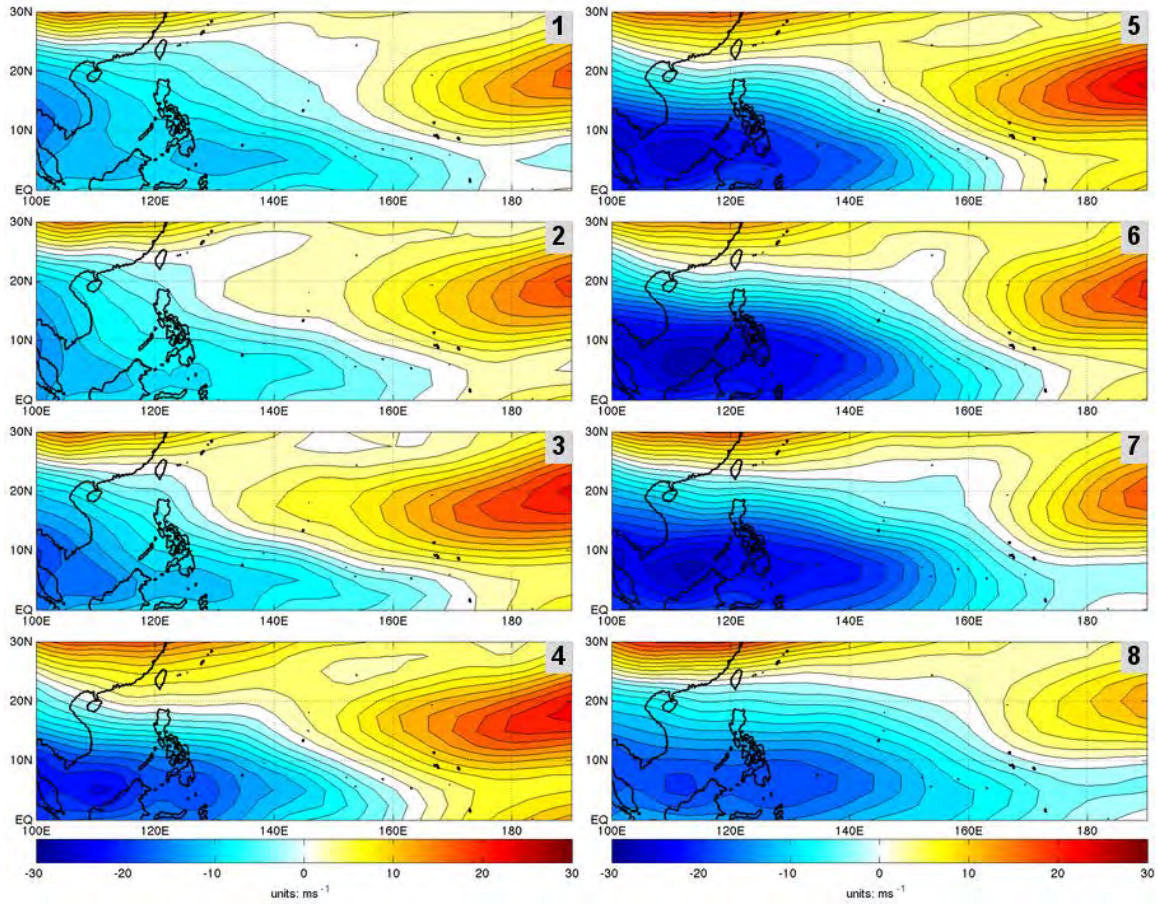

Figure 32. MJO composite zonal wind vertical shear (in ms^{-1}), for MJO phases 1–8 with amplitude > 1.25, for JASO 1975–2010, in the WNP study region (contours and color shading; phase number shown in upper right of each panel). Note the relatively strong (weak) easterly vertical shear over the west-central equatorial regions of the WNP, and the eastward (westward) shift in the zero shear location, during phases 5–8 (1–4).

Figure 33 shows the composite anomaly for zonal vertical wind shear for the eight phases of MJO. In phases 1–4 (5–8), much of the lower latitude WNP is dominated by an eastward propagating positive (negative) anomaly, consistent with the anomalous upper and lower level winds associated with each phase (cf. Figure 2) and with the results in Figure 30.

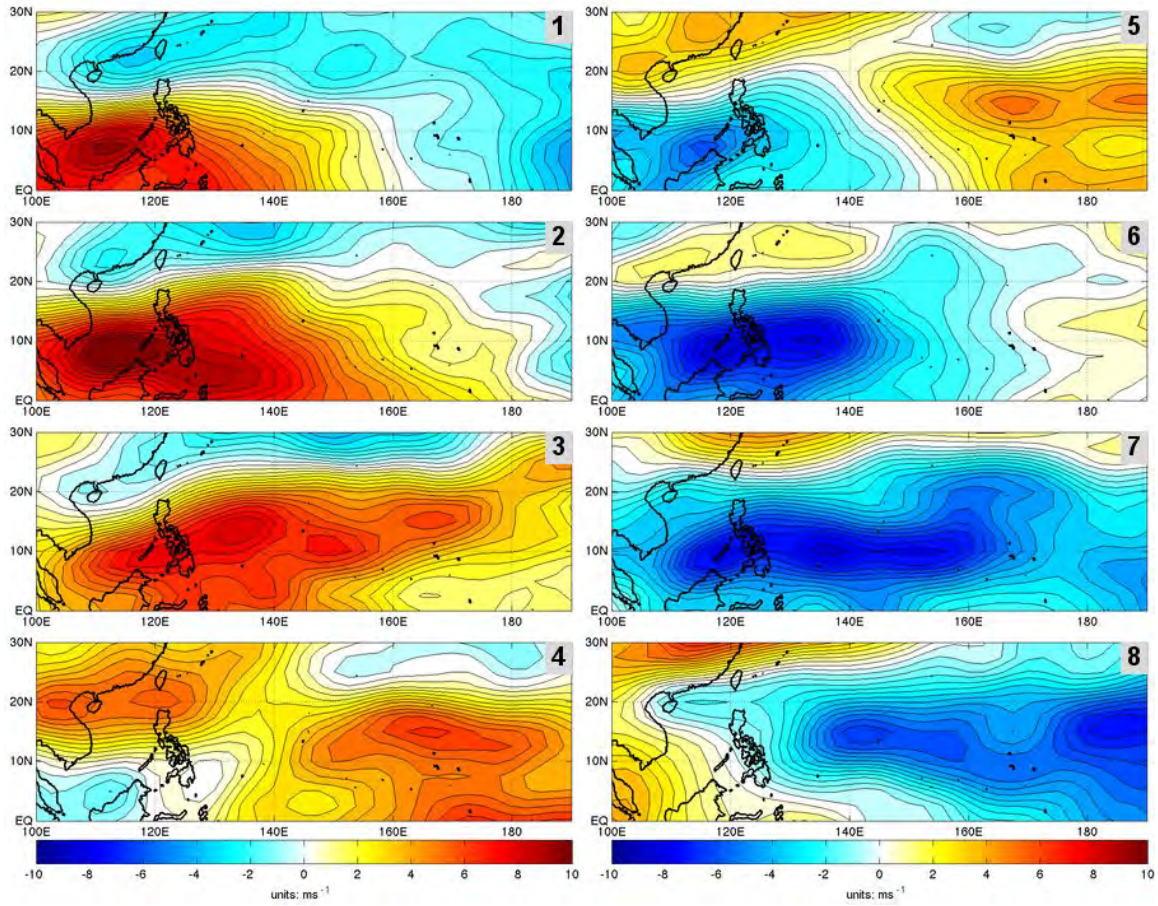

Figure 33. MJO composite anomalies of zonal wind vertical shear (in ms^{-1}), for MJO phases 1–8 with amplitude > 1.25, for JASO 1975–2010, in the WNP study region (contours and color shading; phase number shown in upper right of each panel). Note the positive (negative) vertical shear anomalies over much of the WNP during phases 1–4 (5–8).

c. Meridional Vertical Wind Shear

Figure 34 shows the composite meridional vertical wind shear for the eight phases of MJO. The region is dominated by negative or northerly shear in all phases, but with slightly stronger northerly shear on a southwest-northeast axis during phases 4–7, consistent with the circulation anomalies associated with MJO (see Figure 2).

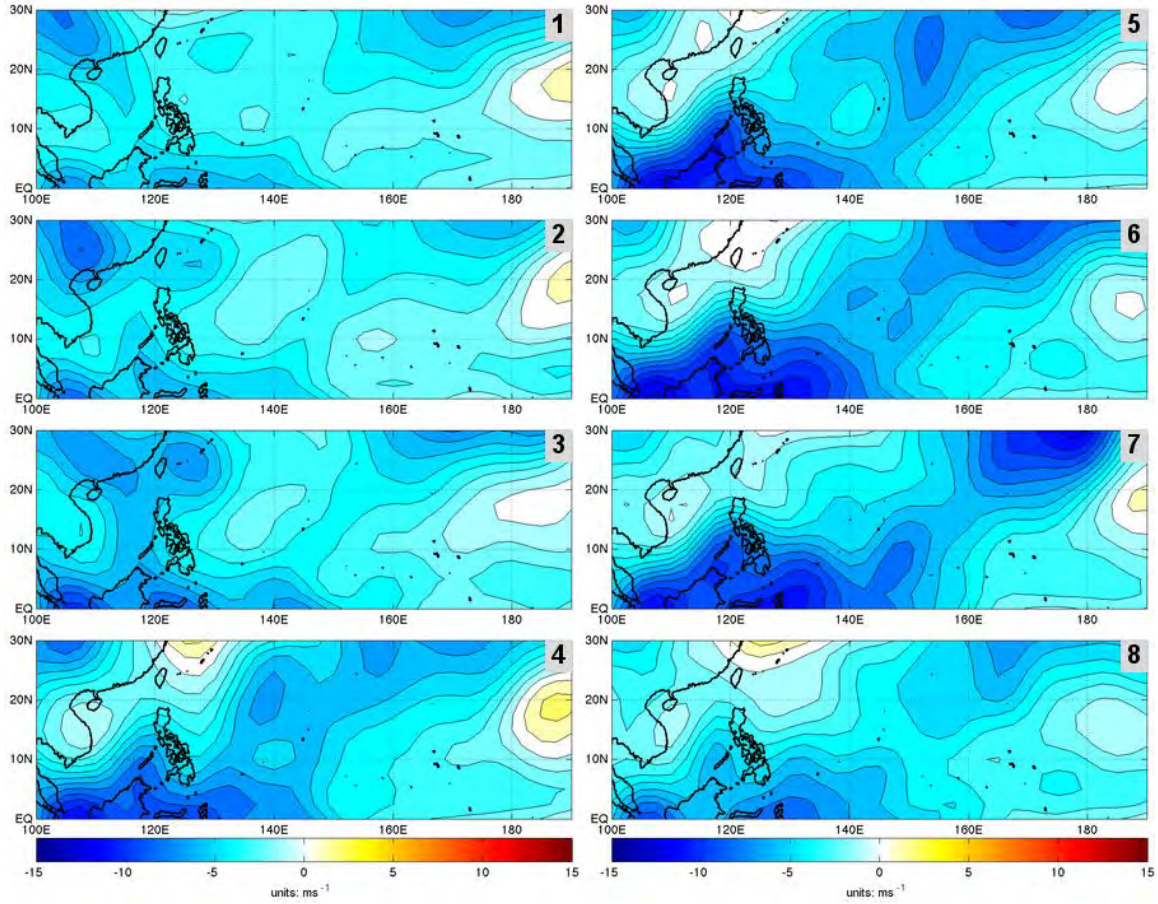

Figure 34. MJO composite meridional wind vertical shear (in ms^{-1}), for MJO phases 1–8 with amplitude > 1.25, for JASO 1975–2010, in the WNP study region (contours and color shading; phase number shown in upper right of each panel).

Figure 35 shows the composite anomaly for meridional vertical wind shear for the eight phases of MJO. These anomalies clarify those indicated in Figure 34, especially an eastward propagating northerly shear anomaly that is especially pronounced during phases 1–8.

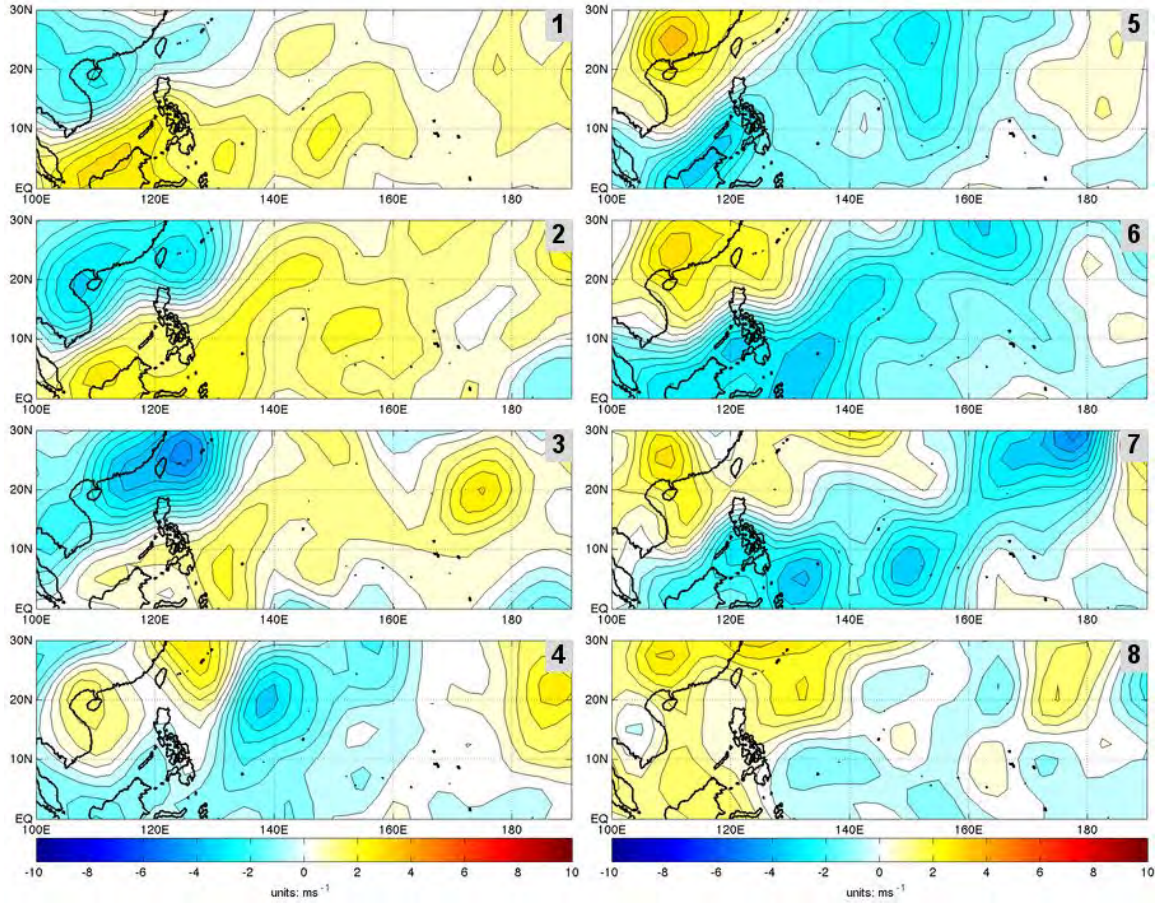

Figure 35. MJO composite anomalies of meridional wind vertical shear (in ms^{-1}), for MJO phases 1–8 with amplitude > 1.25, for JASO 1975–2010, in the WNP study region (contours and color shading; phase number shown in upper right of each panel).

d. Upper Level Divergence

Figure 36 is the composite 200 hPa divergence for the eight phases of MJO. Upper level divergence is typically positive through all MJO phases in the WNP. We observe very similar patterns in phases 1–3 and 8. In phase 4 we begin to see an increase in upper level divergence in the South China Sea extending into the central WNP, near the equator. Divergence continues to increase in phases 5 and 6. In phase 7, divergence is still relatively strong compared to phases 1–3 and 8, but it does begin to weaken compared to phases 5 and 6.

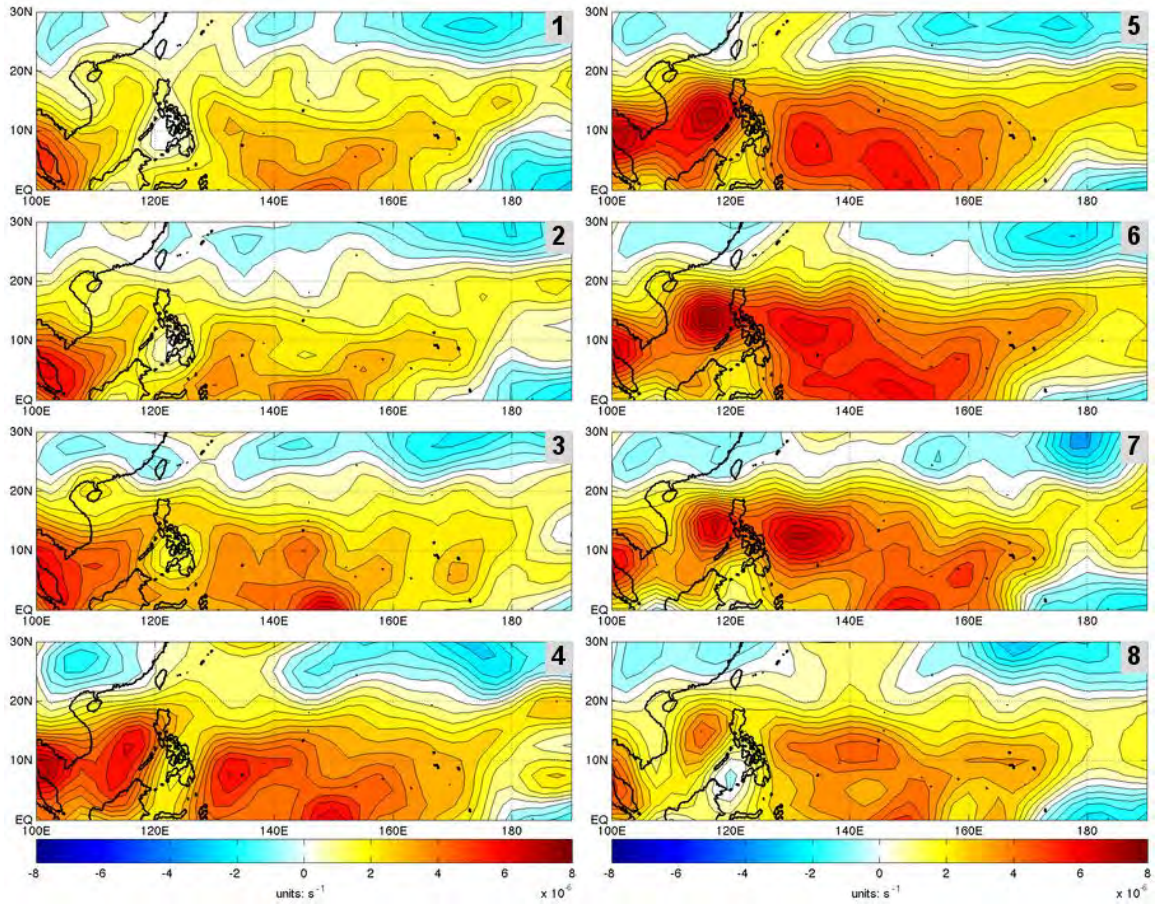

Figure 36. MJO composite 200 hPa divergence (in s^{-1}), for MJO phases 1–8 with amplitude > 1.25, for JASO 1975–2010, in the WNP study region (contours and color shading; phase number shown in upper right of each panel). Note the relatively strong (weak) divergence over much of WNP during phases 4–7 (1–3 and 8).

Figure 37 shows the composite anomaly for 200 hPa divergence for the eight phases of MJO. This figure reinforces the results shown in Figure 36, especially the results indicating eastward propagation and strengthening (weakening) of the positive divergence region from phase 2 to 6 (6 to 1). The anomalies are especially strong in the South China Sea and east of the Philippines.

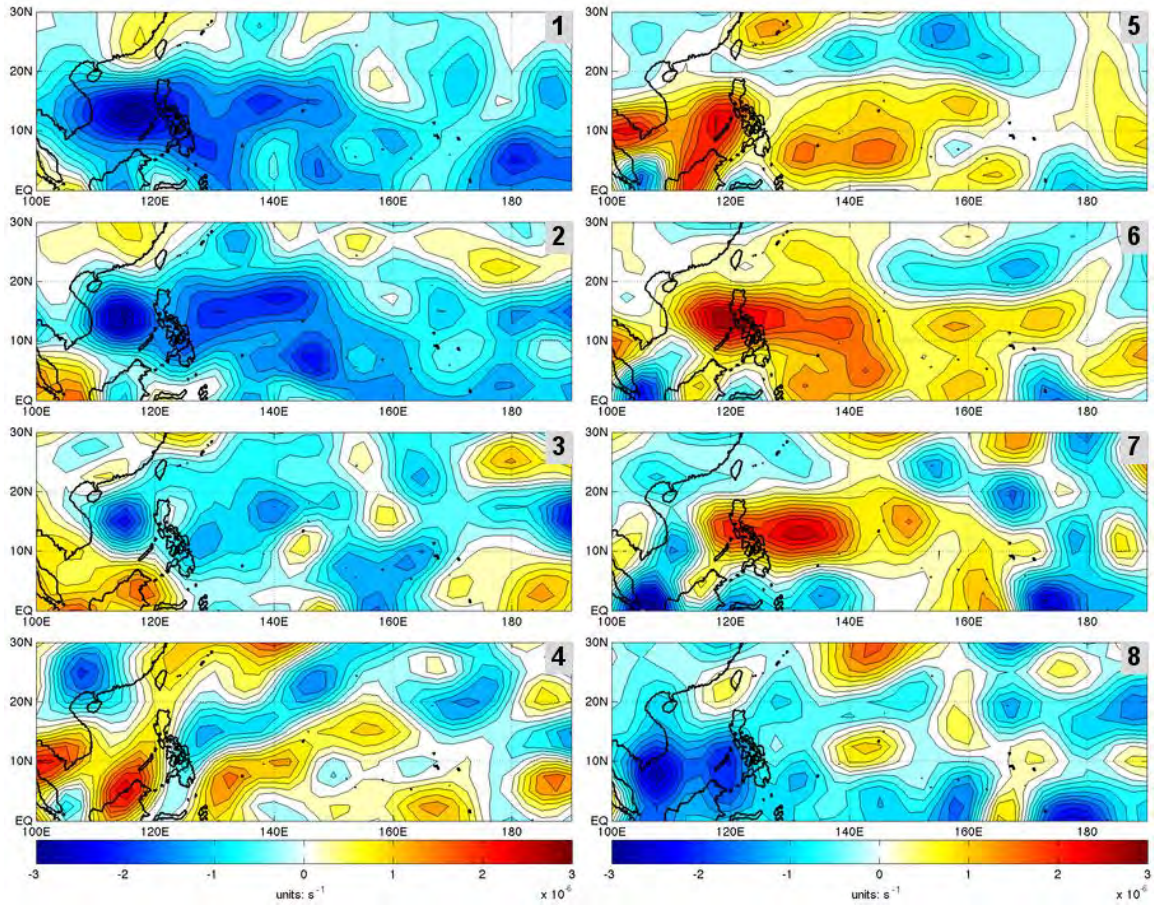

Figure 37. MJO composite anomalies of 200 hPa divergence (in s^{-1}), for MJO phases 1–8 with amplitude > 1.25, for JASO 1975–2010, in the WNP study region (contours and color shading; phase number shown in upper right of each panel). Note the positive (negative) relative vorticity anomalies over the South China Sea and just east of the Philippines and Taiwan-Luzon during phases 4–7 (1–3 and 8).

3. TC Formation Probabilities

We forced the NPS statistical model with the LSEFs for each phase of the MJO to produce TC formation probabilities for each phase (Figure 38). Note the relatively high (low) probabilities over much of WNP during phases 4–7 (1–3, 8), and the similarities in the probabilities for phases 1–3 and 8, and for phases 4–7. The increase in probabilities, and the eastward propagation of the high probabilities, is especially clear in the transition from phase 3 to phase 8. From

phase 3 to phase 4, there is an increase in probabilities in the South China Sea and just east of the Philippines. From phase 4 to phase 5, the probabilities in the South China Sea increase further, while the probabilities just due east of the Philippines slightly weaken. From phase 5 to phase 6, the high probabilities in the South China Sea weaken slightly, and the probabilities east of the Philippines increase. From phase 6 to phase 7, the probabilities in the South China Sea and east of the Philippines weaken, but are still relatively strong compared to phases 8 and 1–3.

The probabilities extend zonally across all or most of the WNP (similar to the LTM) in phases 7–8 and 1–2 but are more zonally constrained in phases 3–6, extending only to the IDL. The zonal vertical wind shear might help explain these differences in the spatial distribution of the probabilities. Recall that for phases 1, 7, and 8, the zero vertical wind shear line extends east of the IDL (Figure 32), consistent with the greater eastward extent of the probabilities in these phases (Figure 38). Comparisons of Figure 38 with the corresponding LSEF figures indicates that for the MJO, the LSEF variations that appear to have the most direct impact on the TC formation probability variations are those in low level relative vorticity, the zonal component of vertical wind shear, and upper level divergence.

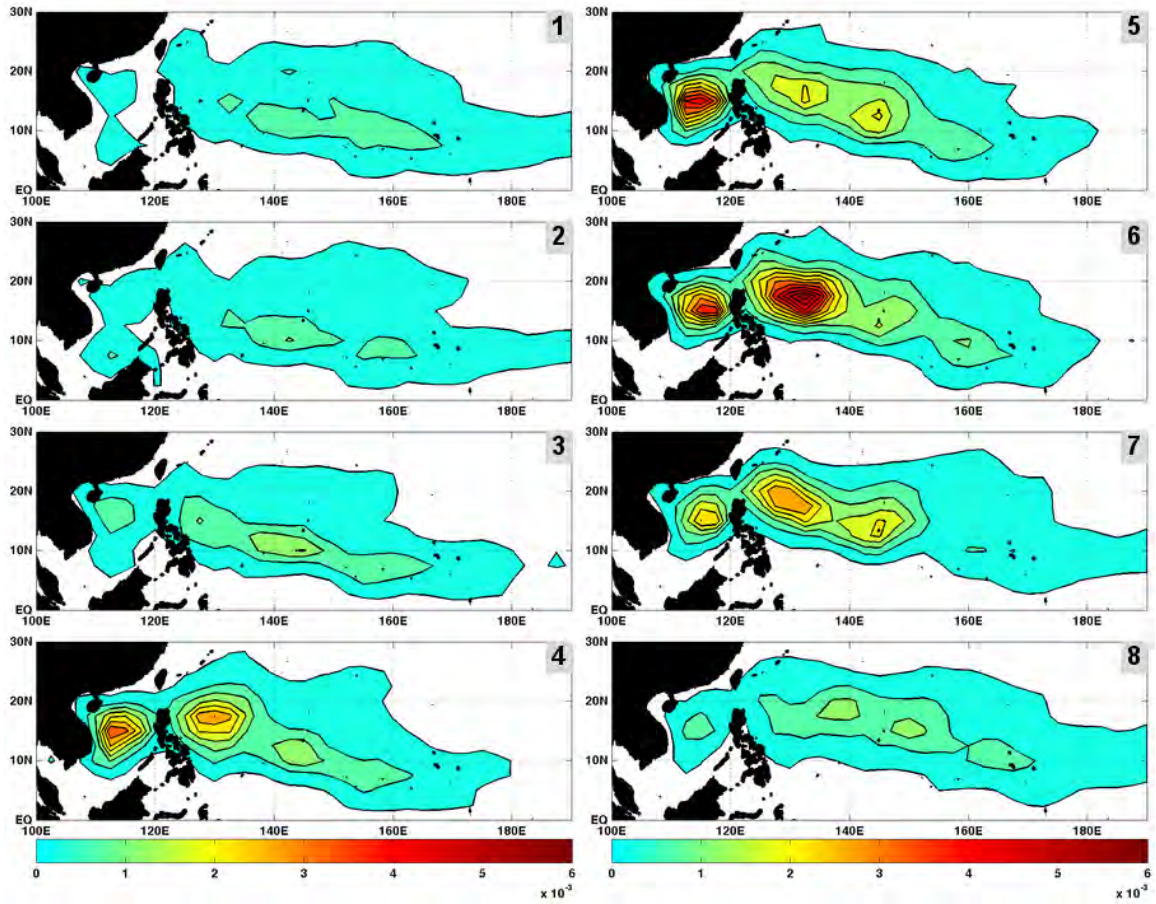

Figure 38. TC formation probabilities for MJO phases 1–8, during JASO, in the WNP study region (contours and color shading; phase number shown in upper right of each panel). Probabilities calculated based on composite LSEFs for all MJO events with amplitude > 1.25 during JASO 1975–2010, with the LSEFs used to force the NPS logistic regression model. Note the relatively high (low) probabilities over much of WNP during phases 4–7 (1–3 and 8).

Figure 39 is the same figure as Figure 38 but with corresponding TC formation locations (blue dots) overlaid on the probabilities. Recall that the formations here are based on a random selection of 123 days for each phase (Chapter II.F). Note the general correspondence between the formation probability regions and the actual formations in the eight phase composites. Phases 1–3 have the fewest number of randomly selected formations and the lowest formation probabilities, while phases 5 and 6 have the most randomly

selected formations and the highest formation probabilities. This provides qualitative verification that the NPS statistical model is skillful in describing MJO related variations in TC formation probabilities.

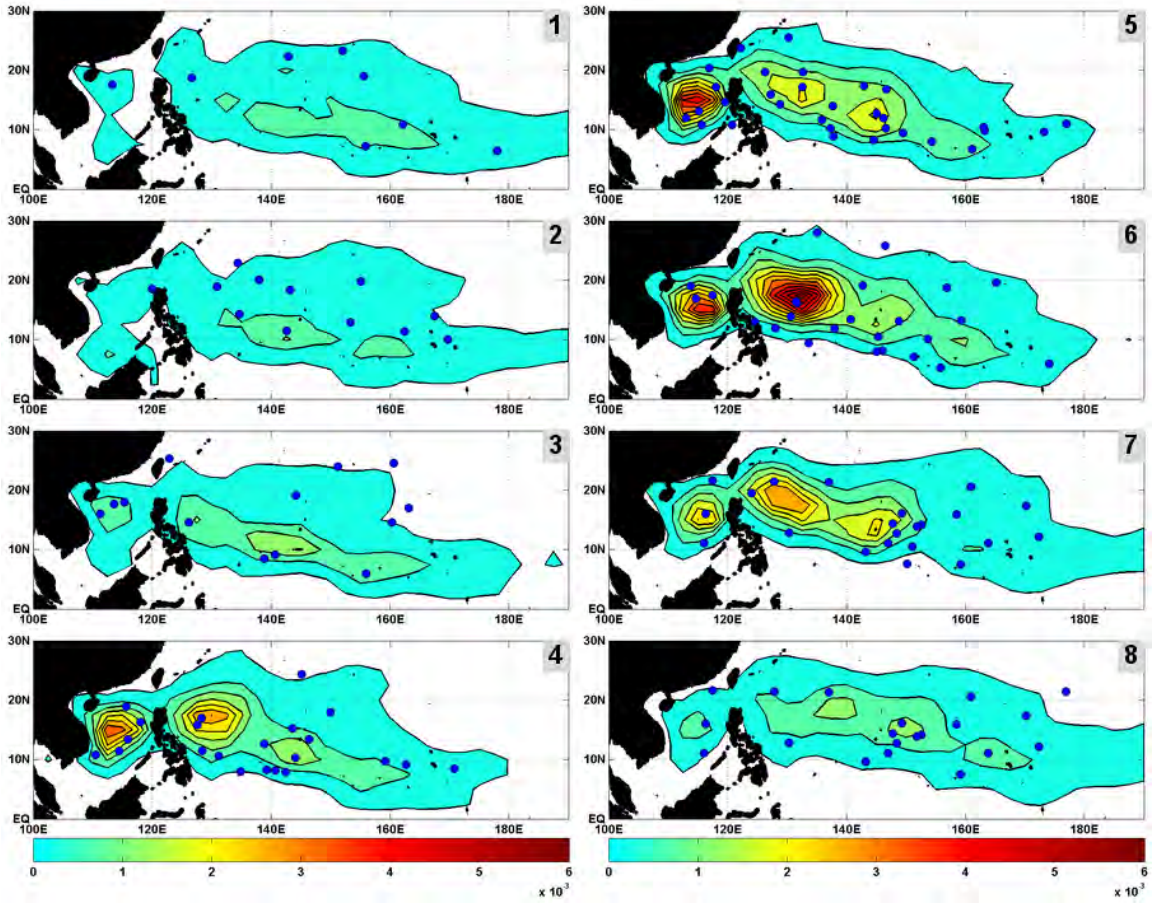

Figure 39. TC formation probabilities for MJO phases 1–8 and actual TC formation locations (blue dots), during JASO, in the WNP study region (contours and color shading; phase number shown in upper right of each panel). Probabilities calculated based on composite LSEFs for all MJO events with amplitude > 1.25 during JASO 1975–2010, with the LSEFs used to force the NPS logistic regression model. Formation locations from JTWC WNP best track data. The formations for each phase are those that occurred in a random selection of 123 days from the total number of days in the phase (see Chapter II, Section F for details). Note the relatively high (low) probability anomalies and formation numbers over much of WNP during phases 4–7 (1–3 and 8).

To highlight the regions of higher or lower probabilities between the eight MJO phases we calculated the TC formation probability anomalies for each phase (Figure 40). Note the positive (negative) probability anomalies west and east of the Philippines during phases 4–7 (1–3, 8). These results indicate that phases 1–3 and 8 tend to suppress TC formations in most of the WNP, especially in the South China Sea, southeast of Taiwan, and east of the Philippines, while phases 4–7 tend to do the reverse.

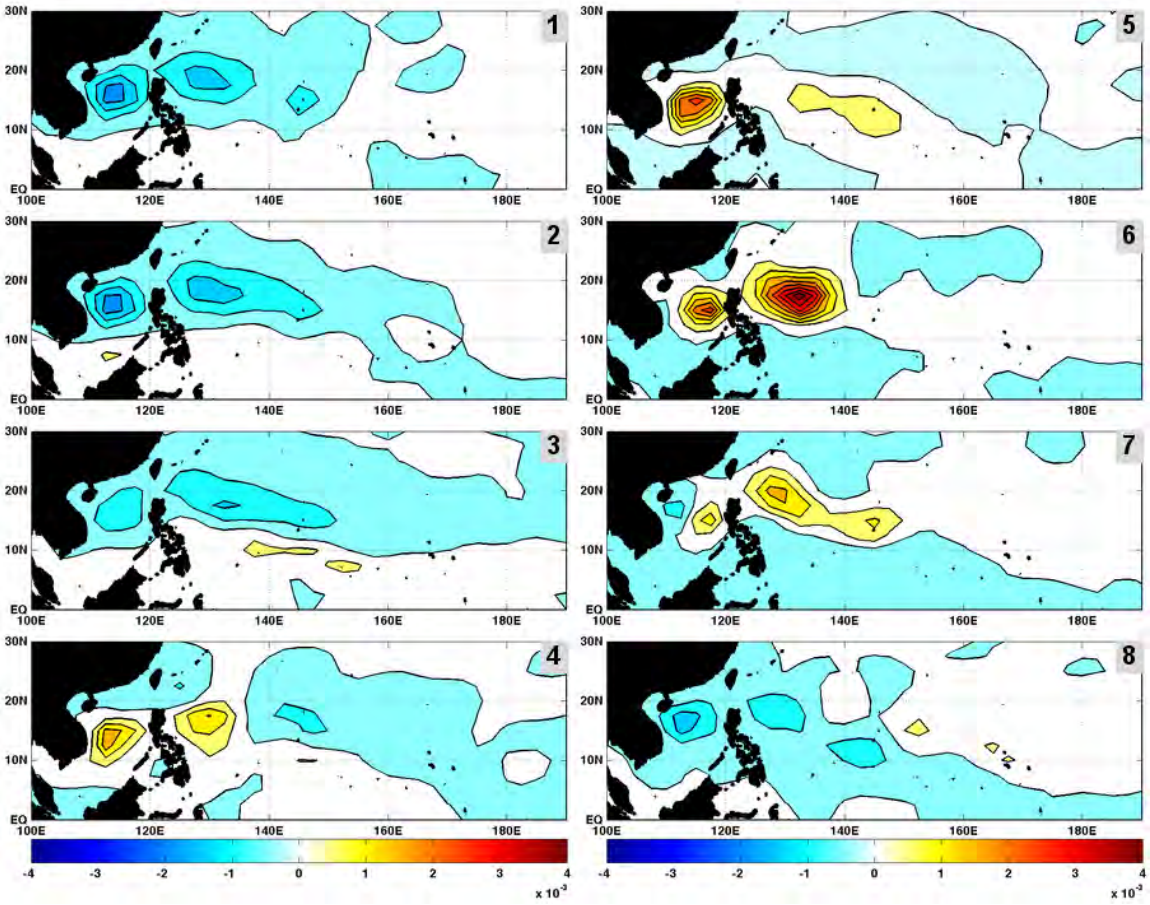

Figure 40. TC formation probability anomalies for MJO phases 1–8, during JASO, in the WNP study region (contours and color shading, phase number shown in upper right of each panel). Probability anomalies calculated using LTM probabilities (Figure 9) and actual probabilities (Figure 39). Note the positive (negative) probability anomalies west and east of the Philippines during phases 4–7 (1–3 and 8).

These ENLN and MJO results are broadly consistent with prior studies, but go well beyond those studies to objectively quantify the probabilistic impacts of EN, LN, and each MJO phase by sub-regions within the WNP. The verification of these results via direct comparison with observed formations also indicates that the NPS statistical model has skill in depicting the impacts on WNP TC formations. This skill can be used to improve the analysis and forecasting of TC formations by forcing the NPS statistical model with: (a) observed and analyzed LSEFs; and (b) forecasted LSEFs.

THIS PAGE INTENTIONALLY LEFT BLANK

IV. SUMMARY, CONCLUSIONS, AND RECOMMENDATIONS

A. KEY RESULTS AND CONCLUSIONS

We have analyzed the modulation of TC formations in the WNP during JASO by EN, LN, and the MJO. This analysis was conducted from the perspective of several LSEFs that strongly influence TC formation: SST, low level relative vorticity, vertical wind shear, and upper level divergence. We examined the variations in each LSEF associated with EN, LN, and MJO.

We found the following variations in the LSEFs during EN (LN): (1) a shift in the SST warm pool to the east (west); (2) relatively stronger (weaker) low level relative vorticity in the South China Sea and extending east of the Philippines across the central WNP; (3) relatively stronger (weaker) easterly zonal vertical wind shear across much of the WNP; and (4) relatively stronger (weaker) upper level divergence over the Maritime Continent and the central WNP.

We found the following variations in LSEFs during the eight phases of MJO: (1) relatively stronger (weaker) relative vorticity over the South China Sea and extending across the central part of much of WNP during phases 4–7 (1–3 and 8); (2) relatively stronger (weaker) easterly vertical shear over the south and central equatorial regions of the WNP during phases 4–7 (1–3 and 8); and (3) relatively stronger (weaker) divergence over much of WNP during phases 4–7 (1–3 and 8).

We then used the composite LSEFs for EN, LN, and each of the eight MJO phases to force the NPS statistical model for calculating TC formation probabilities. We then compared the resulting probabilities to actual formations to determine how accurately the model represented ENLN and MJO related variations in TC formations. We observed for EN, LN and the eight phases of MJO composites a clear correspondence between the formation probability regions and the actual formations. This visual verification demonstrates the skill

of NPS statistical model as it accurately models the shift in probabilities and corresponding TC formations associated with ENLN and the MJO.

Thus, the model based probabilities provide a realistic quantitative representation of how ENLN and MJO make TC formations more and less likely in the WNP. In particular, the model accurately represents: (1) the southeastward (northwestward) shift in conditions favorable for TC formation during EN (LN); and (2) the enhancement (suppression) of formation favorable conditions to the west and east of the Philippines during phases 4–7 (1–3, 8) of the MJO. For ENLN, the LSEF variations that appear to have the most direct impacts on the TC formation probability variations are those in SST, low level relative vorticity, and the zonal component of vertical wind shear. For MJO, the LSEF variations that appear to have the most direct impacts on the TC formation probability variations are those in low level relative vorticity, the zonal component of vertical wind shear, and upper level divergence.

These results provide additional insights on which LSEFs lead to intraseasonal to interannual variations in TC formations in the WNP, and the mechanisms by which they do so. Our results also indicate that the NPS model has the potential to improve operational forecasting of TC formations in the WNP, if forced by skillful forecasts of the LSEFs. If so, the resulting forecasts would be useful in improving the planning of DoD and other operations in the WNP.

In summary, our results show the follow:

(1) By comparing LSEF plots to the probability plots generated by the NPS statistical model, we gain insight as to how the LSEFs influence TC formation.

(2) We can aid forecasters by using information about the status of ENLN, or the phase of the MJO, to determine where TC formation is more and less likely to occur, and thus where to focus their attention and the attention of their customers.

(3) By overlaying actual TC formations on TC formation probabilities, we have developed at least qualitative validation of the performance of the NPS statistical model. This indicates that the model has the potential to improve both TC analysis and TC forecasting.

B. AREAS FOR FURTHER RESEARCH

We have developed some compelling results, but have also identified several potential improvements in our data sets and methods that should be considered in extending our study. Thus, we recommend the following future research.

(1) Repeat our analyses using more up to date reanalysis data sets, especially the Climate Forecast System Reanalysis (CFSR; Saha et al. 2010) and TC reanalysis data sets, as they become available.

(2) Conduct sensitivity analyses to more quantitatively determine the most influential LSEF variations during ENLN and MJO.

(3) Analyze ENLN impacts on TC activity separately from MJO impacts (e.g., composite only days that represent ENLN *or* MJO but not *both* ENLN and MJO).

(4) Apply the statistical model to analyze TC activity in other months and in other TC basins. Then modify or rebuild the statistical model, if results indicate that is needed.

(5) Apply the statistical model to analyze TC variations that occur at:

a) Decadal and longer scales

b) Global warming scales (e.g., 1971—1985 versus 1996—2010)

(6) Force the statistical model with forecasted LSEFs to produce forecasts of TC formation probabilities (statistical-dynamical forecasting; on-going research by NPS researchers).

THIS PAGE INTENTIONALLY LEFT BLANK

APPENDIX. LIST OF DATES USED IN MJO COMPOSITES

For each MJO phase, we composited a different number of days (see Chapter II.C.3). Table 4 lists the dates we used for each MJO phase composite. These dates are for JASO 1975–2010, and for when the MJO amplitude was greater than 1.25.

Table 4. List of dates during JASO 1975–2010 when MJO amplitude was greater than 1.25 by MJO phase. Constructed from BOM phase and amplitude data. These dates were used to develop the MJO phase composites used in this study.

Phase 1	Phase 2	Phase 3	Phase 4	Phase 5	Phase 6	Phase 7	Phase 8
7/8/75	7/12/75	7/26/75	7/28/75	7/29/75	8/6/76	9/16/76	7/1/75
7/9/75	7/14/75	7/27/75	8/28/76	7/30/75	8/7/76	9/17/76	7/2/75
7/10/75	7/17/75	8/23/76	8/29/76	7/31/75	9/6/76	9/18/76	7/3/75
7/11/75	7/19/75	8/24/76	10/14/76	8/1/75	9/7/76	9/19/76	7/4/75
8/13/76	7/20/75	8/25/76	10/15/76	8/2/75	9/8/76	9/20/76	7/5/75
9/25/76	7/21/75	8/26/76	10/16/76	8/3/75	9/9/76	9/21/76	7/6/75
9/26/76	7/22/75	8/27/76	10/17/76	8/4/75	9/10/76	9/14/77	7/7/75
9/27/76	7/23/75	7/4/77	10/18/76	8/5/75	9/11/76	9/16/77	9/22/76
9/29/76	7/24/75	7/5/77	7/8/77	8/8/75	9/12/76	9/17/77	9/23/76
9/30/76	7/25/75	7/6/77	7/9/77	8/9/75	9/13/76	9/18/77	9/24/76
10/1/76	8/27/75	7/7/77	7/10/77	9/30/75	9/14/76	9/19/77	9/20/77
10/2/76	8/28/75	9/20/79	9/22/79	10/1/75	9/15/76	8/12/79	9/21/77
10/3/76	8/29/75	9/21/79	9/23/79	10/2/75	9/7/77	8/13/79	9/22/77
10/4/76	8/30/75	8/20/80	9/24/79	10/3/75	9/8/77	8/14/79	7/7/79
10/5/76	8/31/75	10/14/80	9/25/79	10/4/75	9/9/77	8/15/79	7/8/79
8/8/77	8/14/76	10/15/80	8/21/80	10/5/75	9/10/77	8/16/79	7/9/79
8/9/77	8/15/76	7/9/81	8/22/80	10/6/75	9/11/77	8/17/79	7/10/79
8/10/77	8/16/76	7/10/81	8/23/80	8/5/76	9/12/77	10/15/79	7/11/79
8/11/77	8/17/76	7/11/81	7/27/81	8/30/76	9/13/77	10/16/79	7/17/79
9/23/77	10/6/76	7/22/81	7/28/81	8/31/76	9/15/77	10/17/79	7/18/79
9/24/77	10/7/76	7/23/81	9/17/81	9/1/76	7/1/79	8/11/81	8/18/79
9/25/77	10/8/76	7/24/81	9/18/81	9/2/76	7/2/79	8/12/81	8/19/79
9/26/77	10/9/76	7/25/81	8/11/83	9/3/76	8/8/79	10/2/81	8/20/79
9/27/77	9/8/79	7/26/81	8/12/83	9/4/76	8/9/79	10/3/81	8/21/79
9/28/77	9/9/79	9/14/81	8/13/83	9/5/76	8/10/79	7/1/82	10/18/79
9/29/77	9/12/79	9/15/81	8/14/83	10/19/76	8/11/79	7/21/82	10/19/79
9/30/77	9/17/79	8/6/82	8/15/83	10/20/76	10/6/79	7/22/82	10/20/79
10/1/77	9/18/79	7/13/83	8/16/83	10/21/76	10/7/79	7/23/82	10/21/79
10/2/77	7/16/81	7/14/83	8/17/83	10/22/76	10/8/79	7/2/84	10/22/79
10/3/77	7/17/81	7/15/83	8/18/83	10/23/76	10/9/79	7/27/84	7/24/82

7/12/79	7/18/81	7/16/83	9/18/83	7/28/77	10/10/79	9/14/84	9/10/84
7/13/79	7/19/81	7/17/83	9/19/83	7/29/77	10/11/79	9/15/84	9/11/84
7/16/79	7/20/81	7/18/83	9/20/83	8/1/77	10/12/79	9/16/84	9/12/84
7/19/79	7/21/81	7/19/83	9/21/83	9/2/77	10/13/79	10/15/84	9/13/84
7/20/79	8/31/81	7/20/83	9/22/83	9/3/77	10/14/79	10/16/84	9/17/84
7/21/79	9/1/81	8/4/83	9/23/83	9/4/77	9/11/80	10/20/84	9/18/84
7/22/79	9/2/81	8/5/83	9/24/83	9/5/77	9/12/80	10/21/84	9/19/84
7/23/79	9/3/81	8/6/83	7/12/86	9/6/77	9/13/80	10/22/84	9/20/84
8/22/79	9/4/81	8/7/83	7/14/86	8/1/79	10/27/80	10/23/84	10/24/84
8/23/79	9/5/81	8/8/83	9/9/86	8/2/79	10/28/80	10/25/84	10/27/84
8/24/79	9/6/81	8/9/83	9/10/86	8/3/79	8/2/81	10/26/84	10/28/84
8/25/79	9/7/81	8/10/83	9/11/86	8/4/79	8/3/81	10/19/85	10/29/84
8/26/79	9/8/81	9/17/83	8/19/87	8/5/79	8/4/81	10/20/85	10/30/84
8/27/79	9/9/81	9/6/86	8/20/87	8/6/79	8/5/81	10/21/85	10/31/84
8/28/79	9/10/81	9/7/86	8/21/87	8/7/79	8/6/81	10/22/85	9/22/85
8/29/79	9/11/81	9/8/86	8/22/87	9/26/79	8/7/81	7/1/86	10/23/85
8/30/79	9/12/81	10/27/86	8/23/87	9/27/79	8/8/81	7/2/86	10/24/85
8/31/79	9/13/81	10/28/86	8/24/87	9/28/79	8/9/81	7/3/86	10/25/85
9/1/79	8/3/82	10/29/86	8/25/87	9/29/79	8/10/81	7/4/86	10/26/85
9/2/79	8/7/82	10/30/86	8/26/87	9/30/79	9/29/81	8/17/86	10/27/85
9/3/79	8/8/82	10/31/86	8/27/87	10/1/79	9/30/81	8/18/86	10/28/85
9/4/79	10/25/82	8/12/87	9/10/87	10/2/79	10/1/81	8/19/86	10/29/85
9/5/79	10/26/82	8/13/87	9/11/87	10/3/79	10/10/83	8/20/86	7/26/89
9/6/79	10/27/82	8/14/87	9/12/87	10/4/79	10/11/83	8/21/86	7/27/89
9/7/79	10/28/82	8/15/87	9/13/87	10/5/79	10/27/83	8/22/86	7/28/89
10/23/79	10/29/82	8/16/87	9/14/87	7/3/80	10/28/83	8/23/86	7/29/89
10/24/79	10/30/82	8/17/87	9/19/88	7/4/80	7/24/84	10/21/88	7/1/90
10/26/79	10/31/82	8/18/87	9/20/88	8/24/80	7/25/84	10/22/88	9/17/91
10/27/79	8/3/83	9/23/87	9/21/88	8/25/80	7/26/84	10/23/88	9/18/91
10/28/79	9/2/83	9/24/87	9/22/88	8/26/80	7/28/84	10/24/88	9/19/91
10/29/79	9/6/83	9/26/87	9/23/88	8/27/80	8/3/84	7/24/89	10/2/91
8/1/80	9/7/83	9/27/87	9/24/88	8/28/80	8/4/84	7/25/89	9/14/92
8/11/80	9/8/83	9/17/88	9/25/88	9/8/80	8/5/84	8/18/89	9/15/92
9/20/80	9/9/83	9/18/88	9/26/88	9/9/80	8/6/84	10/29/89	9/17/92
9/21/80	9/10/83	9/25/90	10/10/89	9/10/80	8/7/84	8/24/90	9/18/92
9/22/80	9/11/83	10/31/90	10/11/89	10/19/80	8/8/84	9/11/91	9/19/92
9/23/80	9/29/86	10/12/91	10/12/89	10/20/80	8/9/84	9/12/91	10/25/93
9/24/80	9/30/86	10/13/91	10/13/89	10/21/80	8/10/84	9/13/91	10/26/93
8/26/81	10/1/86	10/14/91	10/14/89	10/22/80	8/11/84	9/14/91	10/27/93
8/27/81	10/24/86	10/15/91	10/15/89	10/23/80	8/12/84	9/15/91	10/28/93
8/28/81	10/25/86	10/16/91	8/22/91	10/24/80	8/13/84	9/16/91	10/29/93
8/29/81	10/26/86	7/15/92	10/9/92	10/25/80	8/14/84	9/10/92	9/23/94
8/30/81	8/5/87	10/25/94	10/10/92	10/26/80	8/15/84	9/11/92	9/24/94
9/19/82	8/6/87	10/26/94	10/11/92	7/29/81	8/16/84	9/16/92	9/25/94
9/20/82	8/7/87	7/5/95	10/12/92	7/30/81	8/17/84	8/8/93	9/26/94
10/24/82	8/8/87	7/6/95	10/13/92	7/31/81	8/18/84	10/24/93	9/27/94

9/3/83	8/9/87	7/7/95	10/14/92	8/1/81	8/22/84	7/23/94	9/28/94
9/4/83	8/10/87	8/27/95	10/15/92	9/19/81	8/23/84	7/24/94	9/29/94
9/5/83	8/11/87	8/28/95	10/16/92	9/20/81	8/24/84	9/18/94	9/30/94
7/18/85	9/19/87	8/26/96	8/29/95	9/21/81	8/25/84	9/19/94	10/1/94
7/19/85	9/20/87	7/1/97	8/30/95	9/22/81	8/26/84	9/20/94	10/2/94
7/20/85	9/21/87	7/2/97	8/31/95	9/23/81	8/27/84	9/21/94	10/9/96
7/21/85	9/22/87	7/3/97	9/1/95	9/24/81	10/17/85	9/22/94	10/11/97
10/30/85	9/25/87	7/4/97	10/31/95	9/25/81	10/18/85	10/8/95	10/12/97
10/31/85	10/30/87	7/5/97	7/9/97	9/26/81	8/6/86	10/9/95	8/28/98
9/25/86	10/31/87	7/6/97	7/10/97	9/27/81	8/7/86	10/10/95	8/29/98
9/26/86	8/15/88	7/7/97	7/11/97	9/28/81	8/8/86	9/25/96	8/30/98
9/27/86	8/16/88	7/8/97	7/12/97	9/25/83	8/9/86	7/12/00	8/31/98
9/28/86	8/17/88	7/13/97	7/15/97	9/26/83	8/10/86	7/13/00	9/1/98
7/23/87	9/16/89	7/14/97	7/16/97	9/27/83	8/11/86	7/14/00	9/2/98
7/26/87	9/17/89	9/19/98	7/22/97	9/28/83	8/12/86	7/15/00	9/3/98
7/27/87	9/18/89	10/3/00	9/20/98	9/29/83	8/13/86	7/16/00	9/4/98
7/28/87	9/19/89	10/4/00	9/21/98	9/30/83	8/14/86	8/31/00	9/5/98
7/29/87	9/20/89	10/5/00	9/22/98	10/1/83	8/15/86	9/1/00	9/6/98
7/30/87	9/21/89	8/5/01	9/23/98	10/2/83	8/16/86	7/4/01	9/7/98
7/31/87	9/22/89	9/29/01	9/24/98	10/3/83	9/16/86	7/5/01	9/8/98
8/1/87	9/23/89	9/30/01	9/25/98	10/4/83	9/17/86	7/6/01	9/9/98
8/2/87	9/24/89	10/1/01	9/26/98	10/5/83	9/18/86	7/7/01	7/17/00
8/3/87	9/25/89	10/2/01	9/27/98	10/6/83	10/6/88	7/8/01	7/18/00
8/4/87	9/26/89	9/24/04	9/28/98	10/7/83	10/7/88	7/9/01	7/19/00
7/1/88	9/27/89	9/25/04	7/21/99	10/26/83	10/8/88	7/10/01	7/20/00
7/2/88	9/20/90	9/26/04	7/22/99	7/19/84	10/9/88	8/20/01	7/21/00
7/3/88	9/23/90	10/30/04	10/29/99	7/20/84	10/10/88	8/21/01	7/24/00
7/4/88	9/24/90	10/31/04	10/30/99	7/21/84	10/16/88	8/22/01	7/25/00
7/5/88	10/18/90	9/10/06	8/17/00	7/22/84	10/17/88	8/23/01	9/2/00
8/25/88	10/19/90	9/11/06	10/6/00	7/23/84	10/18/88	8/24/01	9/3/00
8/26/88	10/20/90	9/12/06	10/7/00	10/11/84	10/19/88	8/25/01	9/4/00
8/27/88	10/21/90	9/13/06	8/6/01	8/1/86	10/20/88	10/13/01	9/5/00
8/28/88	10/25/90	9/14/06	10/3/01	8/2/86	7/18/89	10/14/01	9/6/00
8/29/88	10/26/90	9/15/06	10/4/01	8/3/86	7/19/89	7/6/02	9/7/00
8/30/88	10/27/90	7/19/08	10/5/01	8/4/86	7/20/89	7/7/02	9/8/00
8/31/88	10/28/90	7/20/08	10/6/01	8/5/86	7/21/89	7/8/02	9/9/00
9/1/88	10/29/90	9/5/08	8/9/02	9/12/86	10/26/89	7/9/02	7/11/01
7/2/90	10/30/90	10/18/08	8/10/02	9/13/86	10/27/89	7/10/02	7/12/01
7/3/90	10/8/91	10/19/08	7/21/03	9/15/86	10/28/89	7/11/02	7/13/01
7/4/90	10/9/91	10/20/08	9/10/03	8/28/87	8/20/90	7/12/02	7/14/01
7/10/90	10/10/91	9/15/09	10/1/04	8/29/87	8/21/90	7/13/02	7/15/01
10/14/90	10/11/91	9/16/09	10/2/04	8/30/87	8/22/90	10/25/03	9/7/01
10/15/90	7/10/92	7/22/10	10/3/04	8/31/87	8/23/90	10/26/03	10/23/01
10/16/90	7/11/92	7/23/10	7/30/05	9/1/87	9/2/91	10/16/04	10/24/01
10/17/90	7/12/92	7/24/10	9/3/05	9/2/87	9/7/91	10/17/04	7/14/02
10/22/90	7/13/92	7/25/10	9/4/05	9/3/87	9/8/91	7/5/06	7/15/02

10/23/90	7/14/92	7/28/10	9/5/05	9/4/87	9/9/91	7/6/06	7/16/02
10/24/90	9/26/92		9/6/05	10/17/87	9/10/91	7/7/06	7/17/02
10/4/91	10/21/94		9/7/05	10/18/87	10/24/92	7/8/06	7/18/02
10/5/91	7/1/95		9/8/05	9/27/88	10/25/92	7/12/06	7/19/02
10/6/91	7/2/95		10/29/05	9/28/88	10/26/92	10/9/06	7/20/02
10/7/91	7/3/95		10/30/05	9/29/88	8/4/93	10/10/06	8/22/02
7/4/92	7/4/95		10/31/05	9/30/88	8/5/93	7/9/07	8/23/02
7/5/92	7/25/95		9/21/06	10/1/88	8/6/93	7/10/07	8/24/02
7/6/92	7/26/95		9/22/06	10/2/88	8/7/93	7/11/07	8/25/02
7/8/92	7/27/95		9/23/06	10/3/88	7/25/94	7/12/07	8/26/02
7/9/92	7/29/95		9/24/06	10/4/88	7/26/94		8/27/02
7/1/93	7/30/95		9/25/06	10/5/88	7/27/94		8/28/02
7/2/93	7/31/95		9/26/06	7/15/89	7/28/94		8/29/02
10/30/93	8/1/95		9/27/06	7/16/89	9/9/94		10/27/03
10/31/93	8/2/95		9/28/06	7/17/89	9/10/94		10/28/03
8/8/94	8/3/95		9/6/08	10/20/89	9/15/94		10/29/03
8/9/94	8/4/95		9/7/08	10/21/89	9/16/94		10/30/03
8/10/94	8/5/95		9/8/08	10/22/89	9/17/94		7/1/04
8/11/94	8/6/95		9/9/08	10/23/89	9/7/95		7/2/04
8/12/94	8/14/95		9/10/08	10/24/89	9/8/95		7/3/04
10/3/94	8/15/95		10/21/08	10/25/89	9/9/95		7/4/04
10/4/94	7/5/96		10/22/08	8/15/90	9/21/95		7/5/04
10/5/94	7/6/96		10/23/08	8/16/90	9/22/95		8/21/04
10/6/94	8/16/96		10/24/08	8/17/90	9/23/95		8/22/04
10/7/94	7/16/98		10/25/08	8/18/90	7/15/96		8/23/04
10/9/94	7/17/98		10/26/08	8/19/90	7/16/96		8/24/04
10/10/94	8/15/98		10/27/08	8/14/91	7/17/96		10/18/04
10/11/94	8/16/98		9/1/09	8/15/91	7/18/96		10/19/04
10/12/94	8/18/98		9/2/09	8/16/91	7/19/96		10/20/04
10/13/94	8/19/98		9/3/09	8/17/91	7/20/96		9/21/05
10/14/94	8/22/99		9/4/09	8/18/91	7/21/96		9/22/05
10/15/94	8/23/99		9/5/09	8/19/91	7/22/96		7/13/06
10/16/94	8/24/99		9/6/09	8/20/91	7/23/96		7/14/06
10/17/94	8/25/99		9/7/09	8/21/91	7/24/96		7/15/06
10/18/94	8/26/99		9/8/09	8/23/91	7/25/96		10/11/06
10/19/94	9/28/99		9/10/09	8/24/91	7/26/96		10/12/06
10/20/94	9/29/99		9/17/09	8/25/91	7/27/96		10/13/06
7/18/95	9/30/99		9/18/09	8/26/91	7/28/96		10/14/06
7/19/95	10/1/99		9/19/09	8/27/91	7/29/96		10/15/06
7/20/95	10/2/99		9/21/09	8/28/91	7/30/96		10/16/06
7/21/95	10/3/99		9/23/09	8/29/91	7/31/96		10/17/06
7/22/95	10/4/99		9/30/09	8/30/91	8/1/96		10/9/07
7/23/95	10/5/99		10/1/09	9/3/91	9/20/96		10/10/07
7/24/95	10/6/99		10/2/09	9/4/91	9/21/96		10/11/07
8/9/95	10/8/99		10/3/09	9/5/91	9/22/96		10/12/07
8/10/95	9/19/00		10/6/10	9/6/91	10/9/98		10/13/07

8/11/95	9/20/00		10/7/10	8/29/92	10/10/98		10/14/07
8/12/95	9/29/00			8/30/92	10/15/98		10/15/07
8/13/95	9/30/00			8/31/92	10/16/98		10/16/07
8/16/95	10/1/00			10/17/92	10/17/98		10/17/07
7/1/96	10/2/00			10/18/92	7/8/00		10/28/09
7/2/96	7/24/01			10/19/92	7/10/00		7/10/10
7/3/96	7/25/01			10/20/92	7/11/00		7/11/10
7/4/96	7/26/01			10/21/92	8/26/00		
8/15/96	9/12/01			10/22/92	8/27/00		
10/7/96	9/13/01			10/23/92	8/28/00		
10/8/96	9/14/01			7/27/93	8/29/00		
10/13/97	9/16/01			7/28/93	8/30/00		
10/14/97	9/17/01			7/29/93	10/24/00		
10/15/97	9/18/01			7/30/93	10/25/00		
10/16/97	9/26/01			7/31/93	10/26/00		
10/17/97	9/27/01			8/1/93	10/27/00		
7/1/99	9/28/01			8/2/93	10/28/00		
7/2/99	10/28/01			8/3/93	10/29/00		
7/3/99	10/29/01			9/2/95	10/30/00		
7/4/99	10/30/01			9/3/95	10/31/00		
8/18/99	10/31/01			9/4/95	7/1/01		
8/19/99	9/26/02			9/5/95	7/2/01		
8/20/99	10/29/02			9/6/95	7/3/01		
8/21/99	10/30/02			7/14/96	8/16/01		
9/19/99	10/31/02			9/9/96	8/17/01		
9/20/99	7/1/03			9/10/96	8/18/01		
9/21/99	7/2/03			9/11/96	8/19/01		
9/22/99	7/4/03			9/12/96	10/10/01		
9/23/99	7/7/03			9/13/96	10/11/01		
9/24/99	7/8/03			9/14/96	10/12/01		
9/25/99	9/5/04			10/31/96	7/1/02		
9/26/99	9/6/04			7/23/97	7/2/02		
9/27/99	9/11/04			9/29/98	7/3/02		
7/26/00	9/12/04			9/30/98	7/4/02		
7/27/00	9/13/04			10/1/98	7/5/02		
7/28/00	9/14/04			10/2/98	8/15/02		
7/29/00	9/15/04			10/3/98	8/16/02		
7/30/00	9/16/04			10/4/98	8/17/02		
7/31/00	9/17/04			10/5/98	8/18/02		
8/1/00	9/18/04			10/6/98	10/20/03		
8/2/00	9/19/04			10/7/98	10/21/03		
8/3/00	9/20/04			10/8/98	10/22/03		
9/13/00	9/21/04			10/31/99	10/23/03		
9/17/00	9/22/04			7/6/00	10/24/03		
9/18/00	9/23/04			7/7/00	8/3/04		
7/16/01	10/26/04			7/9/00	8/4/04		

7/17/01	10/27/04			8/15/00	8/5/04		
7/18/01	10/28/04			8/16/00	8/6/04		
7/19/01	10/29/04			8/18/00	8/8/04		
7/20/01	7/1/05			8/19/00	8/10/04		
7/21/01	7/2/05			8/20/00	8/11/04		
7/22/01	7/3/05			8/21/00	8/12/04		
7/23/01	7/4/05			8/22/00	8/13/04		
9/15/01	7/5/05			8/23/00	8/14/04		
10/27/02	7/6/05			8/24/00	8/15/04		
10/28/02	10/10/05			8/25/00	10/15/04		
7/3/03	10/11/05			10/8/00	8/3/05		
7/6/04	9/7/06			10/9/00	8/4/05		
7/7/04	9/8/06			10/10/00	8/5/05		
7/8/04	9/9/06			10/11/00	8/6/05		
7/9/04	10/23/06			10/12/00	10/5/06		
7/10/04	10/25/06			10/13/00	10/6/06		
7/11/04	7/22/07			10/14/00	10/7/06		
7/12/04	7/23/07			10/15/00	10/8/06		
7/13/04	7/24/07			10/16/00	10/12/10		
7/14/04	7/25/07			10/17/00	10/13/10		
7/15/04	7/26/07			10/18/00	10/14/10		
7/16/04	8/27/07			10/21/00	10/15/10		
7/17/04	8/28/07			10/22/00	10/16/10		
7/18/04	8/29/07			10/23/00	10/17/10		
7/19/04	8/30/07			8/11/01	10/18/10		
9/3/04	8/31/07			8/12/01			
9/4/04	9/1/07			8/13/01			
10/21/04	9/2/07			8/14/01			
10/22/04	7/16/08			8/15/01			
10/23/04	7/17/08			10/7/01			
10/24/04	7/18/08			10/8/01			
10/25/04	8/19/08			10/9/01			
7/14/05	8/20/08			8/11/02			
8/13/05	8/21/08			8/12/02			
8/14/05	8/22/08			8/13/02			
8/15/05	8/23/08			8/14/02			
8/24/06	8/24/08			10/7/02			
8/25/06	8/25/08			7/22/03			
8/26/06	8/26/08			10/16/03			
10/18/06	8/27/08			10/17/03			
10/19/06	8/28/08			10/18/03			
10/20/06	8/29/08			10/19/03			
10/21/06	8/30/08			8/7/04			
10/22/06	8/31/08			10/4/04			
10/24/06	9/1/08			10/5/04			
7/15/07	9/2/08			10/6/04			

7/16/07	8/15/09			10/7/04			
7/17/07	8/16/09			10/8/04			
7/18/07	8/17/09			10/9/04			
7/19/07	8/18/09			7/26/05			
7/20/07	7/17/10			8/2/05			
7/21/07	7/18/10			9/9/05			
10/18/07	7/19/10			9/10/05			
10/19/07	7/20/10			9/11/05			
10/20/07	7/21/10			9/12/05			
7/1/08	7/26/10			9/13/05			
7/2/08	7/27/10			9/14/05			
7/3/08	8/17/10			9/15/05			
7/4/08	9/3/10			9/16/05			
7/5/08	9/4/10			10/19/05			
7/6/08				8/10/06			
7/9/08				8/11/06			
7/10/08				9/29/06			
7/11/08				9/30/06			
7/13/08				10/1/06			
7/14/08				10/2/06			
8/12/09				10/3/06			
8/13/09				10/4/06			
8/14/09				9/9/07			
8/19/09				9/10/07			
8/20/09				9/11/07			
10/29/09				9/12/07			
10/30/09				9/15/07			
10/31/09				9/16/07			
7/1/10				9/17/07			
7/2/10				9/18/07			
7/3/10				9/19/07			
7/4/10				9/20/07			
7/5/10				9/21/07			
7/12/10				9/22/07			
7/13/10				9/23/07			
7/14/10				9/11/08			
7/15/10				9/12/08			
7/16/10				9/13/08			
9/22/10				9/14/08			
				9/15/08			
				9/16/08			
				9/17/08			
				9/22/08			
				10/28/08			
				10/29/08			
				10/30/08			

				10/31/08			
				9/9/09			
				9/20/09			
				9/22/09			
				9/24/09			
				9/25/09			
				9/26/09			
				9/27/09			
				9/28/09			
				9/29/09			
				8/26/10			
				8/27/10			
				10/8/10			
				10/9/10			
				10/10/10			
				10/11/10			

LIST OF REFERENCES

Camargo, S. J., A.G. Barnston, P.J. Klotzbach and C.W. Landsea, 2007a: Seasonal tropical cyclone forecasts, *WMO Bull.*, **56**, 297–309.

———, K. A. Emanuel, and A. H. Sobel, 2007b: Use of a genesis potential index to diagnose ENSO effects of tropical cyclone genesis. *J. Climate,* **20,** 4819–4834.

———, A. H. Sobel, A. G. Barnston, and K. A. Emanuel, 2007c: Tropical cyclone genesis potential index in climate models. *Tellus*, **59A**, 428–443.

———, M.C. Wheeler, and A.H. Sobel, 2009: Diagnosis of the MJO modulation of tropical cyclogenesis using an empirical index, *J. Atmos. Sci.*, **66**, 3061–3074.

———, A. H. Sobel, A. G. Barnston, and P. J. Klotzbach, 2010. The influence of natural climate variability, and seasonal forecasts of tropical cyclone activity. *Global Perspectives on Tropical Cyclones: from Science to Mitigation*, 2nd ed., J.C.L. Chan and J.D. Kepert, Eds., World Scientific Series on Earth Systems Science in Asia, Vol. 4, World Scientific Publishing Co., 325–360.

Chan, J. C. L., 1985 Tropical cyclone activity in the northwest Pacific in relation to the El Niño/Southern Oscillation phenomenon. *Mon. Wea. Rev.,* **113**, 599–606.

———, 2000: Tropical cyclone activity over the western North Pacific associated with El Niño and La Niña events. *J. Climate*, **13,** 2960–2972.

———, J. E. Shi, and C. M. Lam, 2001: Improvements in the seasonal forecasting of tropical cyclone activity over the western North Pacific, *Wea. Forecasting,* **16**, 997–1004.

Chu, J.-H., C. R. Sampson, A. S. Levine, and E. Fukada, 2002: The Joint Typhoon Warning Center tropical cyclone best-tracks, 1945–2000. Tech Rep. NRL/MR/7540–02–16, 26 pp.

Ford, B. W., 2000: El Niño and La Niña effects on tropical cyclones: the mechanisms. M.S. thesis, Dept. of Meteorology, Naval Postgraduate School, 190 pp.

Frank, W. M., 2006: External influences on formations. Proc. *The Sixth WMO International Workshop on Tropical Cyclones*, San Jose, Costa Rica, World Meteo. Org., 261–265

———, and P. E. Roundy, 2006: The role of tropical waves in tropical cyclogenesis. *Mon. Wea. Rev*., **134**, 2397–2417.

Gray, W. M., 1975: Tropical cyclone genesis in the western North Pacific. U.S. Navy Tech. Rep. NEPRF TP 16–75, 66 pp.

———, 1984a: Atlantic seasonal hurricane frequency. Part I: El Niño and 30 mb quasi-biennial oscillation influences. *Mon. Wea. Rev.,* **112**, 1649–1668.

———, 1984b: Atlantic seasonal hurricane frequency. Part II: Forecasting its variability. *Mon. Wea. Rev.,* **112**, 1669–1683.

Hartmann, D. L., and E. D. Maloney, 2001: The Madden–Julian Oscillation, barotropic dynamics, and North Pacific tropical cyclone formation. Part II: Stochastic barotropic modeling. *J. Atmos. Sci.,* **58**, 2559–2570.

Kalnay, E. M. Kanamitsu, R. Kistler, W. Collins, D. Deaven, L. Gandin, M. Iredell, S. Saha, G. White, J. Woollen, Y. Zhu, A. Leetmaa, R. Reynolds, M. Chelliah, W. Ebisuzaki, W. Higgins, J. Janowiak, K. Mo, C. Ropelewski, J. Wang, R. Jenne, and D. Joseph, 1996: The NCEP/NCAR 40-Year reanalysis project. *Bull. Amer. Meteor. Soc.,* **77**, 437–471.

Kanamitsu, M., W. Ebisuzaki, J, Woollen, S.-K. Yang, J. J. Hnilo, M. Fiorino, and G. L. Potter, 2002: NCEP-DOE AMIP-II Reanalysis (R-2). *Bull. Amer. Meteor. Soc.,* **83**, 1631–1643.

Kim, J. H., Ho, C.-H., Kim, H.-S., Sui, C.-H., Park, S. K., 2008: Systematic variation of summertime tropical cyclone activity in the western North Pacific in relation to the Madden–Julian Oscillation. *J. Climate*, **21**, 1171–1191.

Knaff, J., S. Seseke, M. DeMaria, J. Demuth, 2004: On the influences of vertical wind shear on symmetric tropical cyclone structure as derived from AMSU. *Mon. Wea. Rev.* **132**, 2503–2510.

Liebmann, B., H. H. Hendon, and J. D. Glick, 1994: The relationship between tropical cyclones of the western Pacific and Indian Oceans and the Madden–Julian oscillation. *J. Meteor. Soc. Japan*, **72**, 401–411.

Madden, R., and P. Julian, 1994: Observations of the 40–50 day tropical oscillation – a review. Mon, Wea. Rev., 122, 814–837.

Maloney, E. D., and D. L. Hartmann, 2011: The Madden–Julian Oscillation, barotropic dynamics, and North Pacific tropical cyclone formation. Part I: Observations. *J. Atmos. Sci*., **58**, 2545–2558.

McBride, J. L., 1995: Tropical Cyclone Formation, *Global Perspectives on Tropical Cyclones*, R. L. Elsberry, Ed., WMO/TD-No. **693**, 63–105.

Mundhenk, B. D., 2009: A statistical-dynamical approach to intraseasonal prediction of tropical cyclogenesis in the western North Pacific. M.S. thesis, Dept. of Meteorology, Naval Postgraduate School, 190 pp.

Murphree, T., 2010: *Modern Climatology.* Naval Postgraduate School, lecture notes for MR3610.

Murphree, T., and D. Meyer, 2011: Statistical-dynamical prediction of tropical cyclone formation probability at intraseasonal to seasonal lead times: A statistical-dynamical approach. Manuscript in preparation.

Nakazawa, T., 1986: Intraseasonal variations of OLR in the Tropics during the FGGE year. *J. Meteor. Soc. Japan*, **64**, 17–34.National Research Council (NRC), 2010: *Assessment of Intraseasonal to Interannual Climate Prediction and Predictability.* National Academies Press, Washington, DC, 192 pp.

Reynolds, R. W., N. A. Rayner, T. M. Smith, D. C. Stokes, and W. Wang, 2002: An improved in situ and satellite SST analysis for climate. *J. Climate*, **15**, 1609–1625.

Rui. H., and B. Wang, 1990: Development characteristics and dynamic structure of tropical intraseasonal convection anomalies. *J. Atmos. Sci.,* **47**, 357–379.

Saha, S., and Co-Authors, 2006: The NCEP Climate Forecast System. *J. Climate*, 19, 3483–3517.

Saha, S., and Co-authors, 2010: The NCEP Climate Forecast System Reanalysis. *Bull. Amer. Meteor. Soc*., 91, 1015–1057.

van den Dool, H., 2007: *Empirical Methods in Short-Term Climate Prediction*. Oxford University Press, 215 pp.

Wang, B. and J. C. L. Chan, 2002: How ENSO regulates tropical storm activity over the western North Pacific. *J. Climate*, **15,** 1643–1658.

Wheeler, M. C., and H. H. Hendon, 2004: An all-season real-time multivariate MJO index: Development of an index for monitoring and prediction. *Mon. Wea. Rev.*, **132**, 1917–1932.

Wilks, D. S., 2006: *Statistical Methods in the Atmospheric Sciences*. 2nd ed. Academic Press, 627 pp.

Wolter, K., and M. S. Timlin, 2011: El Niño/Southern Oscillation behaviour since 1871 as diagnosed in an extended multivariate ENSO index (MEI.ext). *Intl. J. Climatology*, **31**, 14 pp., in press.

INITIAL DISTRIBUTION LIST

1. Defense Technical Information Center
   Ft. Belvoir, Virginia

2. Dudley Knox Library
   Naval Postgraduate School
   Monterey, California

3. Prof. Tom Murphree
   Naval Postgraduate School
   Monterey, California

4. Mr. David W. Meyer
   Naval Postgraduate School
   Monterey, California